THE ROLE FOR THE P85 SUBUNIT OF PI3KINASE IN THE REGULATION OF RAB PROTEINS

A Thesis Submitted to the College of

Graduate Studies and Research

in Partial Fulfillment of the Requirements

for the Degree of Masters of Science

in the Department of Biochemistry

University of Saskatchewan

Saskatoon

By

Jennifer C. King

PERMISSION TO USE

In presenting this thesis/dissertation in partial fulfillment of the requirements for a Postgraduate degree from the University of Saskatchewan, I agree that the Libraries of this University may make it freely available for inspection. I further agree that permission for copying of this thesis/dissertation in any manner, in whole or in part, for scholarly purposes may be granted by the professor or professors who supervised my thesis/dissertation work or, in their absence, by the Head of the Department or the Dean of the College in which my thesis work was done. It is understood that any copying or publication or use of this thesis/dissertation or parts thereof for financial gain shall not be allowed without my written permission. It is also understood that due recognition shall be given to me and to the University of Saskatchewan in any scholarly use which may be made of any material in my thesis/dissertation.

Requests for permission to copy or to make other uses of materials in this thesis/dissertation in whole or part should be addressed to:

Dr. D. H. Anderson

Saskatchewan Cancer Agency

Cancer Research Unit

20 Campus Drive

University of Saskatchewan

Saskatoon, Saskatchewan S7N 4H4

Canada

ABSTRACT

Upon activation by the platelet-derived growth factor receptor (PDGFR), phosphatidylinositol 3'-kinase (PI3K) converts phosphatidylinositol 4,5-bisphosphate to phosphatidylinositol 3,4,5-trisphosphate to activate the PI3K/Akt cellular survival signalling pathway within cells. The p85 subunit of PI3K has also been shown to have GTPase activating protein (GAP) activity towards Rab proteins involved in receptor endocytosis and trafficking, specifically Rab5 and Rab4. Rab5 is responsible for regulating the fusion of vesicles containing activated receptors to traffic them to intracellular early/sorting endosomes. Rab4 is responsible for regulating the exit of receptors to a recycling pathway back to the plasma membrane. The p85 RabGAP activity is responsible for deactivating Rab5 and Rab4 function by accelerating their GTPase activity, resulting in the inactive conformation of Rab5 and Rab4, and decreased vesicle fusion events during receptor trafficking. The work in this thesis was performed to understand how p85 interacts with, and regulates, Rab5 and Rab4. Glutathione S-transferase pulldown experiments showed the p85 protein was able to interact with Rab5 through its BH domain and another unidentified domain. Cells expressing a p85-R274A mutant defective for RabGAP activity displayed increased PDGFR activation and decreased degradation. To understand the mechanism of decreased PDGFR degradation, PDGFR immunoprecipitation experiments showed the PDGFR was ubiquitinated, a signal needed for multi-vesicular body sorting. Biotinylation experiments showed the PDGFR was being more rapidly endocytosed and then sequestered within the cell. Immunofluorescence experiments showed cells expressing the p85-R274A mutant clearly altered PDGFR trafficking during receptor endocytosis. These results suggest the PDGFR was not spending longer periods of time on the cell surface to continue signalling and was not lacking the modification needed to be sorted to a degradative pathway. The defective trafficking observed in p85-R274A expressing cells, over time, may block PDGFR trafficking, which prevents normal PDGFR dephosphorylation and degradation, and could be attributed to a lack of sufficient cytosolic Rab5-GDP and Rab4-GDP required to associate with new membranes and facilitate additional vesicle fusion events. The lack of lysosomal targeting allows the receptor to be sequestered in cells, but still have the ability to signal as the receptor would not be targeted to multi-vesicular bodies where signalling is abolished.

ACKNOWLEDGMENTS

I would like to thank my supervisor Dr. Deborah H. Anderson for giving me this opportunity to work in her laboratory. Her guidance, advice and patience were greatly appreciated throughout this graduate studies work. I would like to thank my advisory committee Dr. Warrington, Dr. Khandelwal, Dr. Delbaere, and Dr. Desautels for their advice and encouragement. I would also like to thank Dr. Mousseau for the use of the confocal microscope, without which the immunofluorescence studies could not have been carried out. I would also like to thank Dean Chamberlain for his assistance and friendship throughout my thesis work. Thank you to the Anderson laboratory and the Cancer Research Unit at the Saskatchewan Cancer Agency for making my stay fun and exciting and for the friendships that I have made throughout my work. Lastly, I would like to thank my family and friends for their continuous support of my studies.

TABLE OF CONTENTS

Page

LIST OF TABLES

Page

LIST OF FIGURES

Page

LIST OF ABBREVIATIONS

aa	amino acid
AP2	adapter protein 2
APS	ammonium persulfate
Arf	ADP-ribosylation factor
BH	BCR homology domain
BSA	bovine serum albumin
CFP	cyan fluorescent protein
DMEM	Dulbecco's Modified Eagle Medium
DTT	dithiothreitol
E. coli	*Escherichia coli*
EEA1	endosomal antigen 1
EDTA	ethylenediaminetetraacetic acid
EGFR	epidermal growth factor receptor
EGTA	ethyleneglycol-bis (B-aminoethylether) N,N,N,N, tetraacetic acid
Eps15	EGFR pathway substrate clone 15
ESCRT	endosomal sorting complex required for transport
FBS	fetal bovine serum
FRAP	fluorescence recovery after photobleaching
GAP	GTPase activating protein
GDF	GDI-displacement factor
GEF	guanine nucleotide exchange factor
GDI	guanine-dissociation inhibitor
GDP	guanosine diphosphate

Grb2	growth factor receptor-bound protein 2
GST	glutathione S-transferase
GTP	guanosine triphosphate
HECT	homologous to the E6-AP carboxy terminus
HEPES	N-2-hydroxyethylpiperazine-H`-2-ethanesulfonic acid
Hrs	hepatocyte growth factor-regulated tyrosine kinase substrate
IF	immunofluorescence
Ig	immunoglobulin
IP	immunoprecipitation
IPTG	isopropyl β-D-thiogalactopyranoside
LB	Luria-Bertani Broth
LBA	Luria-Bertani Broth + ampicillin
MAPK	mitogen activated protein kinase
MEK	MAPK/Erk kinase
MVB	multi-vesicular body
NaN_3	sodium azide
NaPPi	sodium pyrophosphate
Na_3VO_4	sodium orthovanadate
NP-40	nonidet P40
PDGF	platelet-derived growth factor
PDGFR	platelet-derived growth factor receptor
PH	pleckstrin homology domain
PI3K	phosphatidylinositol 3'-kinase
PI3P	phosphatidylinositol 3-phosphate
$PI3,4,5P_3$	phosphatidylinositol 3,4,5-trisphosphate

$PI4,5P_2$	phosphatidylinositol 4,5-bisphosphate
PLC-γ	phospholipase C-γ
PTB	pTyr binding domain
PTEN	phosphatase and tensin homology
PTP1D	phosphotyrosine phosphatase 1D
pTyr or pY	phosphotyrosine
RING	really interesting new gene
RTK	Receptor tyrosine kinases
S6K	p70 S6 kinase
SDS	Sodium dodecyl sulphate
SDS-PAGE	Sodium dodecyl sulphate/polyacrylamide gel electrophoresis
SH2	Src homology 2
SH3	Src homology 3
SHC	Src homologous and collagen-like
SNARE	soluble N-ethylmaleimide-sensitive factor attachment protein (SNAP) receptor proteins
SoS	Son of Sevenless
STAM	signal/transducer molecule
Rb	rabbit
TBST	tris-buffered saline plus tween-20
TKB	tyrosine kinase binding domain
TEMED	N,N,N',N'-Tetra-methylethylenediamine
Tween-20	polyoxyethylenesorbitan monolaurate
Ub	ubiquitin
UBA	ubiquitin associated domain

UIM	ubiquitin interacting motif
wt	wild type

Amino Acids

A or Ala	Alanine
C or Cys	Cysteine
D or Asp	Aspartic Acid
E or Glu	Glutamic Acid
F or Phe	Phenylalanine
G or Gly	Glycine
H or His	Histidine
I or Ile	Isoleucine
K or Lys	Lysine
L or Leu	Leucine
M or Met	Methionine
N or Asn	Asparagine
P or Pro	Proline
Q or Gln	Glutamine
R or Arg	Arginine
S or Ser	Serine
T or Thr	Threonine
V or Val	Valine
W or Trp	Tryptophan
Y or Tyr	Tyrosine

INTRODUCTION

1.1 Receptor tyrosine kinases (RTK) and signalling

Receptor tyrosine kinases (RTK) are involved in several cellular signalling pathways that regulate key cell signalling functions like proliferation, differentiation, and apoptosis (Gavi *et al*., 2006). RTK pathways are no longer considered linear pathways. They are now viewed as intricate signalling networks which contain modules of multi-protein complexes that assemble at various intracellular compartments to process, integrate and transmit information. These signals ultimately specify a particular biological response (McKay and Morrison, 2007). The receptor is at the head of these pathways and is the gateway between the extracellular matrix and the inside of the cell.

RTKs consist of an extracellular ligand binding domain, a transmembrane domain and an intracellular catalytic domain (Gavi *et al*., 2006). They are classified as such because they contain an intrinsic tyrosine kinase activity. The receptors dimerize after ligand binding and become active by autophosphorylation on tyrosine residues. These phosphotyrosine (pTyr or pY) residues generally serve two purposes: i) to regulate the kinase activity of the receptor and; ii) to create binding sites for downstream signalling molecules. Thus, through the receptor itself and adaptor proteins, numerous signalling components are recruited to the cell surface, thereby activating the repertoire of effector cascades required for a specific response within the cell (Claesson-Welsh, 1994a).

RTKs are classified into more than 16 subfamilies which are grouped by receptor structure (Alvarez *et al*., 2006). The insulin receptor, vascular endothelial growth factor receptor, epidermal growth factor receptor (EGFR) and platelet-derived growth factor (PDGF) receptor (PDGFR) are a few prototypical growth factor receptors representing four of the different RTK subfamilies. The EGFR is the most well-studied but the PDGFR has been shown to display signalling analogous to the EGFR. For the purpose of this thesis, the focus will be on the PDGFR and the pathways it regulates.

1.2 PDGF ligands and receptors

The PDGFR family consists of two receptors: PDGFRα and PDGFRβ. The PDGFRα is 170 kDa and the PDGFRβ is 180 kDa. Both receptors are structurally-related transmembrane glycoproteins that contain N-linked and O-linked glycosylations. The extent of glycosylation varies between different cell types (Heldin *et al*., 1988). Both receptors contain an extracellular region consisting of five immunoglobulin (Ig)-like domains, a single transmembrane segment, a juxtamembrane segment, a protein-tyrosine kinase domain separated by a kinase insert region, and a carboxy-terminal tail (Fig. 1.1) (Heldin and Westermark, 1999; Wang *et al*., 2004). Unique to these receptors is a 100 amino acid (aa) non-catalytic sequence dividing its protein-tyrosine kinase domain into two parts. The overall aa identity between the different parts of the α and β receptors are also indicated in Fig. 1.1 (Claesson-Welsh, 1994b). The PDGFRα and the PDGFRβ are induced to dimerize and form homo- or heterodimers: αα, αβ, and ββ. The dimers produced are dependent on the specific PDGF ligands (see below) that bind the three N-terminal Ig-like domains on the receptors (Bornfeldt *et al*., 1995; Claesson-Welsh, 1994a; Heidaran *et al*., 1990; Shih and Holland, 2006).

PDGF is synthesized in the α-granules of platelets. Upon platelet stimulation, PDGF is released and stimulates the proliferation of arterial smooth muscles, fibroblasts, and glial cells (Linder *et al*., 1979). The PDGF family consists of four ligands A-D. A and B were discovered first (Heldin *et al*., 1985) and C and D were discovered later (LaRochelle *et al*., 2001; Li *et al*., 2000). The PDGF ligands form dimers joined by disulfide bonds. There are five different PDGF dimers: AA, AB, BB, CC, and DD. AA, AB, and BB are secreted in an active form whereas CC and DD are secreted in an inactive form and must first be cleaved to become active (Tallquist and Kazlauskas, 2004). The active form of each dimer selectively binds the PDGFRα and the PDGFRβ homo- or heterodimers with different affinities (Fig. 1.2). The PDGFRαα homodimer binds PDGF-AA, PDGF-AB, PDGF-BB and PDGF-CC. The PDGFRαβ heterodimer binds PDGF-AB, PDGF-BB, PDGF-CC and PDGF-DD. The PDGFRββ homodimer binds PDGF-BB and PDGF-DD. The PDGF-BB is the universal ligand as it is able to bind to all homo- and heterodimer PDGFRs and is the only ligand used in this thesis. PDGFR activation is stimulated by ligand binding.

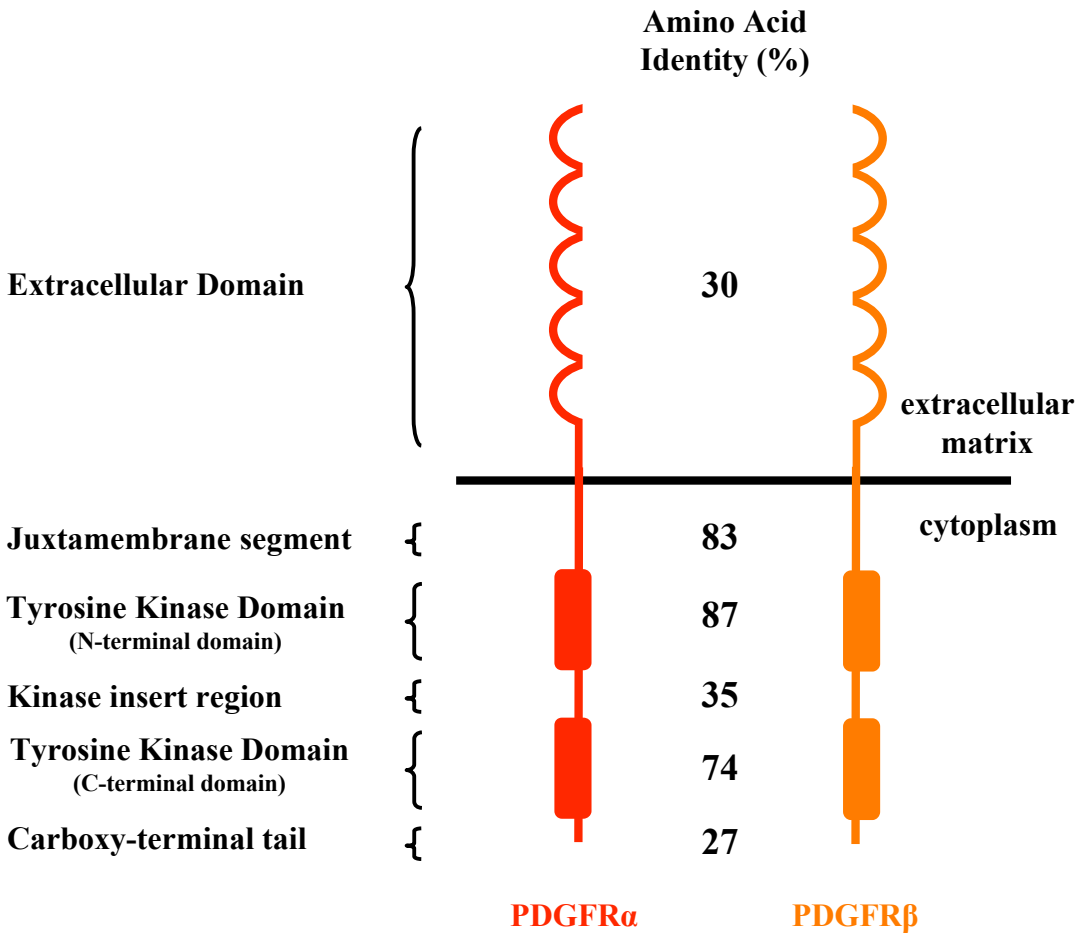

Fig. 1.1. Structure and overall amino acid identity between the different domains of the PDGFR. PDGFRα and PDGFRβ contain an extracellular region consisting of five immunoglobulin-like domains, a single transmembrane segment, a juxtamembrane segment, a protein-tyrosine kinase domain seperated by a 100 aa non-catalytic kinase insert region and a carboxy-terminal tail. (Adapted from Heldin and Westermark, 1999 and Claesson-Welsh, 1994b)

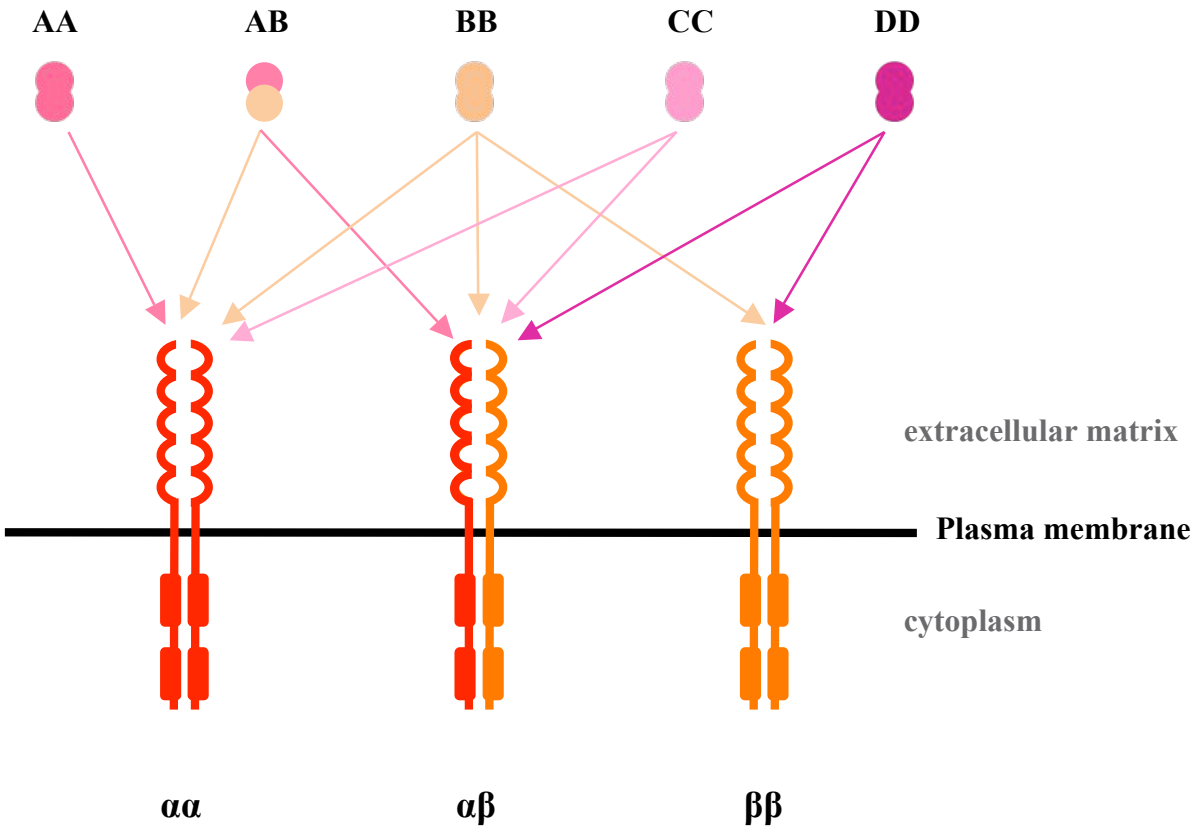

Fig. 1.2. PDGF ligand and receptor interactions. The PDGFRαα homodimer binds PDGF-AA, PDGF-AB, PDGFR-BB and PDGF-CC. The PDGFRαβ heterodimer binds PDGF-AB, PDGFR-BB, PDGF-CC and PDGF-DD. The PDGFRββ homodimer binds PDGF-BB and PDGF-DD.

Ligand binding to the PDGFR induces receptor dimerization. Dimerization activates the intrinsic kinase activity of the receptors and the receptors are able to autophosphorylate on specific tyrosine residues thereby becoming more active. This autophosphorylation is known as trans-phosphorylation. Phosphorylation of Tyr 857 of the PDGFRβ and Tyr 849 of the PDGFRα has been shown to be the key steps critical for full enzymatic activation of the receptors (Claesson-Welsh, 1994b). There are several Tyr residues that are phosphorylated. The pTyr residues act as binding sites for signal transduction molecules which contain Src homology 2 (SH2) domains and/or pTyr binding (PTB) domains and which are then able to transduce signalling information cascades to the cell.

The PDGFRα and the PDGFRβ are expressed at variable levels in different cell types (Table 1.1) and elicit similar cellular effects (Table 1.2) (Alvarez *et al*., 2006). This thesis uses NIH 3T3 mouse fibroblast cells, and although fibroblasts express both the α and β PDGFR, they generally express higher levels of PDGFRβ (Alvarez *et al*., 2006). Due to this, PDGFRβ was used in the immunoprecipitation studies. Currently there have been several pTyr residues within the PDGFRβ identified which are known binding sites for specific effector molecules (Fig. 1.3) (Claesson-Welsh, 1994a). Several effector molecules include: i) Src Tyr kinase which binds to pTyr579 and 581; ii) Src homologous and collagen-like (SHC) adaptor protein binds pTyr 579, 740, 751, and 771; iii) the adaptor protein growth factor receptor-bound protein 2 (Grb2) binds pTyr 716; iv) the adaptor protein Nck binds pTyr 751 and; v) phosphatidylinositol 3'-kinase (PI3K) which converts phosphatidylinositol 4,5-bisphosphate ($PI4,5P_2$) to phosphatidylinositol 3,4,5-trisphosphate ($PI3,4,5P_3$) and binds pTyr 740 and 751; vi) the GAP protein which stimulates the hydrolysis of Ras-coupled GTP and binds pTyr 771; vii) phosphotyrosine phosphatase 1D (PTP1D) binds pTyr 1009; and viii) phospholipase C-γ (PLC-γ) which hydrolyses $PI4,5P_2$ and binds pTyr 1009 and 1021. The binding of these effector molecules activate distinct signalling cascades throughout the cell (Claesson-Welsh, 1994a).

The PDGFR is one of many RTKs responsible for controlling numerous cellular processes such as proliferation, differentiation, and cell survival (Schlessinger, 2000). For the purpose of this thesis, there are two main pathways regulated by the PDGFR which will

Table 1.1. Types of cells that express PDGFRα and PDGFRβ

Cell Types	PDGFRα	PDGFRβ
Platelets	YES	-
Fibroblasts	YES	YES
Pericytes	YES	YES
Vascular smooth muscle cells	YES	YES
Neurons	YES	YES
Mammary epithelial cells	-	YES
Myeloid hematopoietic cells	-	YES
Macrophages	-	YES
Kidney mesangial cells	YES	YES
Liver cells	-	YES
Myoblasts	YES	-

Adapted from Alverez et al., 2006

Table 1.2. PDGFR biological responses

Biological Response	PDGFRα	PDGFRβ
Turnover of phosphatidylinositols and inositol phosphatases	YES	YES
Calcium fluxes	YES	YES
Membrane ruffles, cytoskeletal rearrangements	YES	YES
Migration	YES Cell type dependent	YES
Proliferation	YES	YES
Angiogenesis	-	YES
Timing of differentiation	YES	-

Adapted from Claesson-Welsh, 1994a

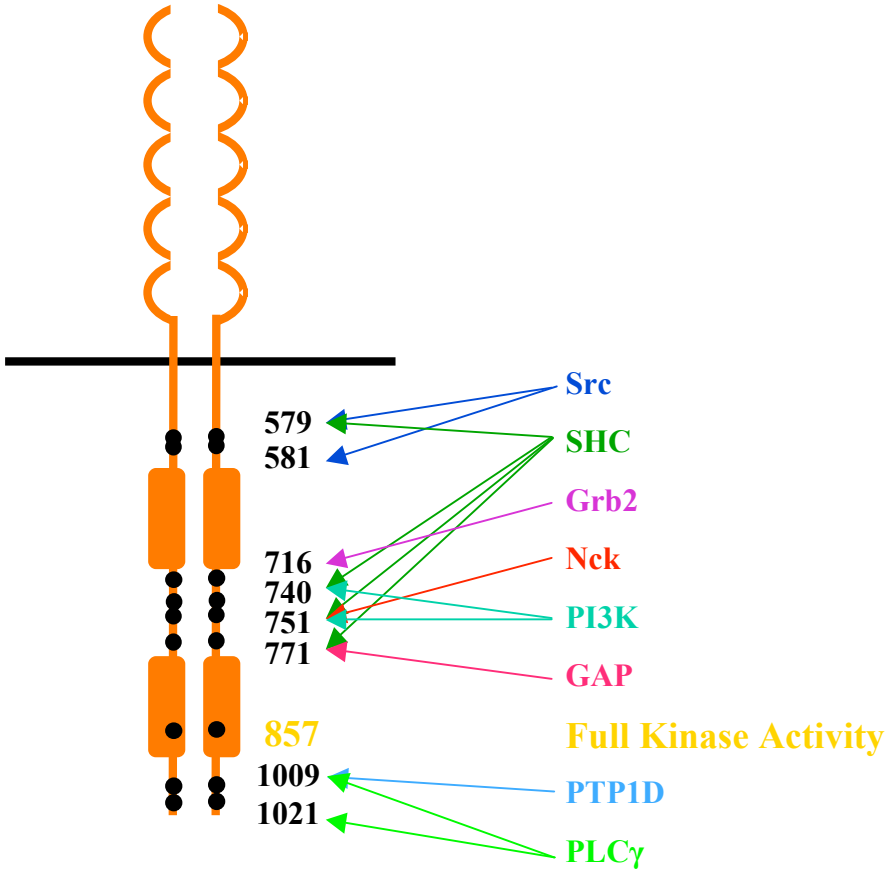

Fig. 1.3. PDGFRβ phosphotyrosine binding sites for known effector molecules. Src Tyr kinase which binds to pTyr579 and 581. Src homologous and collagen-like (SHC) adaptor protein binds pTyr 579, 740,751, and 771. The adaptor protein growth factor receptor-bound protein 2 (Grb2) binds pTyr 716. The adaptor protein Nck binds pTyr 751. Phosphatidylinositol 3'-kinase (PI3K) binds pTyr 740 and 751. The GAP protein stimulates the hydrolysis of Ras-coupled GTP and binds pTyr 771. Phosphotyrosine phosphatase 1D (PTP1D) binds pTyr 1009, and phospholipase C-γ (PLC-γ) hydrolyses $PI4,5P_2$ and binds pTyr 1009 and 1021. Phosphorylation of Tyr 857 results in full kinase activity of the PDGFRβ. (Adapted from Claesson-Welsh, 1994a)

become the focus of the next two sections: the Ras/mitogen activated protein kinase (MAPK) pathway (section 1.2.1.1) and the PI3K /Akt pathway (section 1.2.1.2) (Fig. 1.4).

1.2.1 PDGFR signalling pathways

1.2.1.1 Ras/MAPK pathway

One of the signalling cascades stimulated by PDGFR activation is the Ras/MAPK pathway (McKay and Morrison, 2007). The Ras/MAPK pathway and in particular the phosphorylated MAPK protein is important to the contents of this thesis because it is a measurement of signalling output from the PDGFR. Key proteins within this pathway are highlighted in Fig. 1.4. Upon activation and autophosphorylation of the PDGFR the SHC adaptor protein is recruited to the plasma membrane and binds the receptor via its pTyr binding domain. The PDGFR phosphorylates SHC on Tyr 317 (Heldin *et al*., 1998). Grb2 contains a SH2 domain capable of binding SHC at this phosphorylated tyrosine residue. Grb2 constitutively interacts with Son of Sevenless (Sos) and recruits this guanine nucleotide exchange factor (GEF) to the plasma membrane. Sos is brought into the same vicinity as the G-protein Ras. Interaction with Ras bound to guanosine diphosphate (GDP) activates the GEF activity of Sos (Margarit *et al*., 2003); (Freedman *et al*., 2006; Sondermann *et al*., 2004) causing Ras to exchange the bound GDP for guanosine triphosphate (GTP) to become active. RasGTP recruits and activates the serine (Ser)/threonine (Thr) protein kinase activity of Raf (Avruch *et al*., 2001). Raf phosphorylates MAPK/Erk kinase (MEK) on Ser 218 and Ser 222 (Zheng and Guan, 1994) thereby activating its dual Tyr and Ser/Thr protein kinase activity. MEK in turn phosphorylates MAPK on Thr 183 and Tyr 185 (Payne *et al*., 1991). Activated MAPK is then able to phosphorylate cytoplasmic and nuclear targets responsible for initiating cellular proliferation (McKay and Morrison, 2007).

1.2.1.2 PI3K/Akt pathway

The PI3K/Akt pathway is a signal transduction pathway that contributes to several

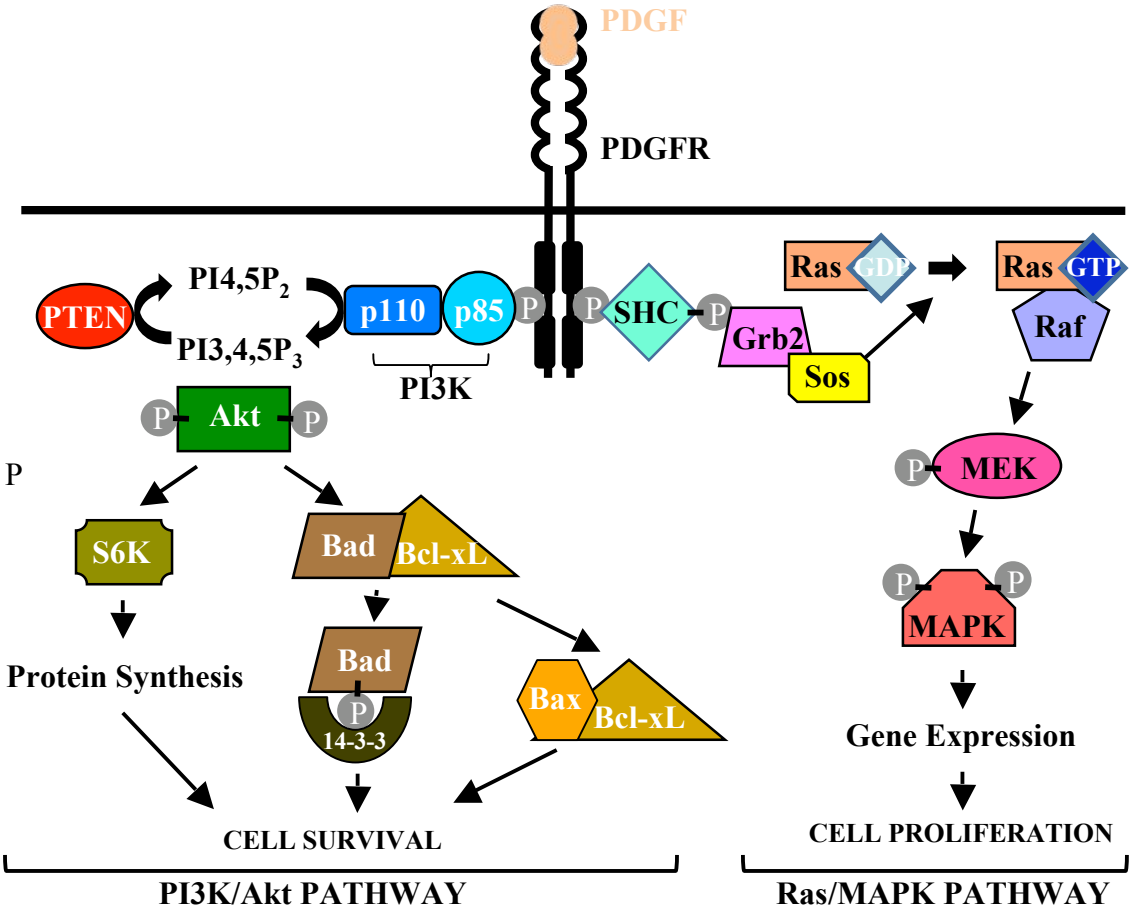

Fig. 1.4. PDGFR Signalling Pathways. The PDGFR is activated and autophosphorylates specific tyrosine residues which become binding sites for effector molecules. PI3K is activated and converts $PI4,5P_2$ into $PI3,4,5P_3$. This leads to the activation of Akt. Akt contributes to cellular survival in several ways including: 1) leading to the phosphorylation of p70 S6 kinase (S6K) resulting in the synthesis of prosurvival proteins and; 2) phosphorylating BAD causing the release the prosurvival protein Bcl-xL thereby promoting cellular survival by inhibiting apoptotic signals from Bax.. PTEN dephosphorylates $PI3,4,5P_3$ back into $PI4,5P_2$ resulting in the inactivation of the Akt pathway. The Ras/MAPK pathway is activated when Grb2 and Sos are recruited to the plasma membrane by SHC. Sos is brought into the same vicinity as the Ras and this interaction activates the GEF activity of Sos causing Ras to exchange the bound GDP for GTP to become active. RasGTP recruits and activates Raf. Raf phosphorylates and activates MEK. MEK in turn phosphorylates MAPK. Activated MAPK is then able to phosphorylate cytoplasmic and nuclear targets responsible for initiating cellular proliferation.

cellular functions ultimately resulting in cellular survival (Song *et al*., 2005); (Manning and Cantley, 2007). Key proteins within this pathway are highlighted in Fig. 1.4. This pathway is stimulated by the activation of the PDGFR. The PI3K protein (discussed in section 1.2.1.2.1) is able to bind to two pTyr residues on the PDGFR via its two SH2 domains. PI3K converts $PI4,5P_2$ to $PI3,4,5P_3$. Akt is a serine/threonine protein kinase and is recruited to $PI3,4,5P_3$ at the plasma membrane via its pleckstrin homology (PH) domain (Andjelkovic *et al*., 1997). Akt is activated by phosphorylation of two key residues: Thr 308 and Ser 473. Akt is phosphorylated on Thr 308 by phosphoinositide-dependent kinase-1 (Anderson *et al*., 1998). The protein responsible for Ser 473 phosphorylation has not yet been identified. After activation, Akt contributes to cellular survival in several ways including: 1) the phosphorylation of p70 S6 kinase (S6K) resulting in the synthesis of prosurvival proteins and; 2) directly phosphorylating Ser 136 and inhibiting the proapoptotic protein BAD (Datta *et al*., 2000). Phosphorylated BAD binds 14-3-3 releasing the pro-survival protein Bcl-xL to bind Bax, which blocks the apoptotic function of Bax. The net result is the promotion of cellular survival by inhibiting apoptotic signals. The phosphatase and tensin homology (PTEN) phosphatase regulates the PI3K/Akt pathway by dephosphorylating $PI3,4,5P_3$ back into $PI4,5P_2$ resulting in the inactivation of the downstream Akt pathway.

The PI3K/Akt pathway and in particular the phosphorylated Akt protein is important to the contents of this thesis because it is representative of signalling output from the PDGFR. The main focus of this thesis is, however, to better understand how PI3K and PI3K protein:protein interactions dictate cellular outcomes within cells. To do this, a closer look at the PI3K protein and function is needed (Section 1.2.1.2.1).

1.2.1.2.1 PI3K

PI3Ks are grouped into three classes (I-III) that are differentiated by their substrate preference and sequence homology (Engelman *et al*., 2006). The class I PI3Ks are further divided into two subfamilies known as A and B. Class IA PI3K are activated by growth factors and RTKs and the Class IB are activated by G-protein-coupled receptors (Katso *et al*., 2001).

For the purpose of this thesis, only Class IA PI3K will be discussed. Class IA PI3K are heterodimers and have a p85 regulatory subunit and a p110 catalytic subunit. The p110 catalytic subunit is a serine and lipid kinase that has a number of different isoforms: α, β, δ. Class IA PI3K phosphorylate the D3 position of the inositol ring of phosphatidylinositols (Carpenter and Cantley, 1996). The p85 protein is responsible for regulating p110 lipid kinase activity and in relocalizing p110 to the plasma membrane (Carpenter and Cantley, 1996).

There have been five isoforms of the p85 regulatory subunit identified: p85α, p85β, p55α, p50α, and $p55^{PIK}$ (Harpur *et al*., 1999). The p85α and p85β regulatory subunits are composed of five domains (Harpur *et al*., 1999). They have an N-terminal SH3 domain, a BCR homology (BH) domain flanked by two proline rich regions, two SH2 domains, and a p110 binding site between the two SH2 domains (Fig. 1.5). The p85α, p55α, and p50α isoforms are encoded by the same gene. The p55α and p50α isoforms are splice variants of p85α and lack the N-terminal SH3, BH and the first proline rich regions (Fig. 1.5). The main difference between p55α and p50α is an addition of an amino-terminal extension of 34 aa and six aa, respectively, to the sequence common with p85α. The p85β and $p55^{PIK}$ are analogous to the p85α and p55 isoforms, respectively, but are encoded by two different genes. The p85α isoform has been shown to possess intrinsic signalling functions (Harpur *et al*., 1999). For the remainder of this thesis, the p85α isoform will be referred to as p85 and a more detailed analysis of its regulatory functions will be discussed.

The p85 protein is responsible for regulating p110 lipid kinase activity and in relocalizing p110 to the plasma membrane (Fig. 1.6) (Carpenter and Cantley, 1996). In resting cells, p85 is complexed with p110 in the cytosol and inhibits its lipid kinase activity (Yu *et al*., 1998). Upon PDGFR activation, the p85:p110 complex is recruited to the plasma membrane by the binding of p85 SH2 domains to pTyr 740 and 751 of the PDGFR (Claesson-Welsh, 1994a). The p110 lipid kinase activity inhibition is relieved and the p85 subunit brings the p110 subunit in close proximity to its lipid substrates. The p110 subunit is able to produce the second messenger $PI3,4,5P_3$ (Carpenter and Cantley, 1996). This action is responsible for activating downstream signalling cascades (Section 1.2.1.2.)

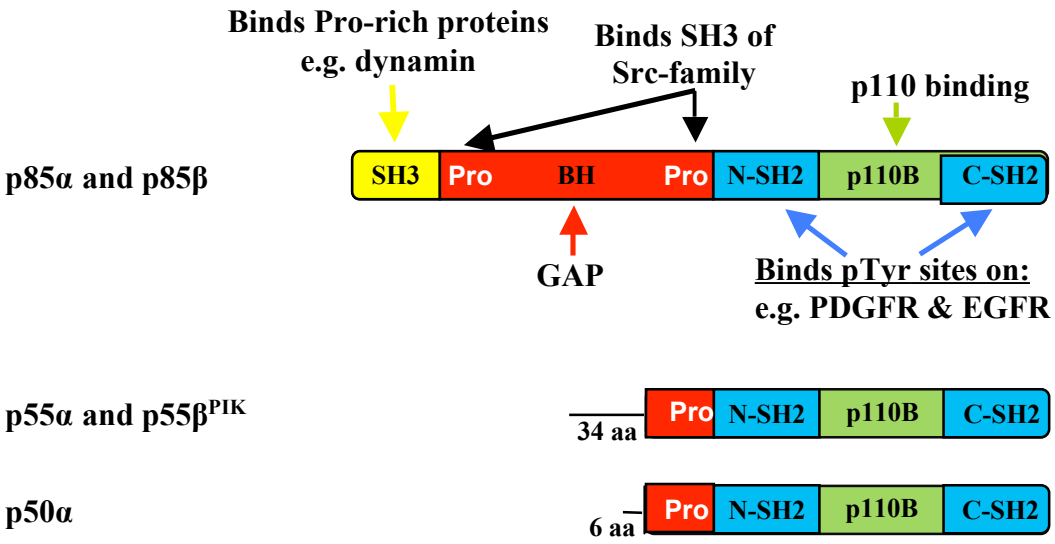

Fig. 1.5. Isoforms of the p85 regulatory subunit of PI3K. The p85α and p85β regulatory subunit are composed of an N-terminal SH3 domain, a BH domain flanked by two proline rich regions, two SH2 domains, and a p110 binding site between the two SH2 domains. The p55α and p50α isoforms lack the SH3, the BH and the first proline rich regions but contain an amino-terminal extension of 34 aa and six aa respectively. The p85β and p55β^{PIK} are analogous to the p85α and p55α isoform.

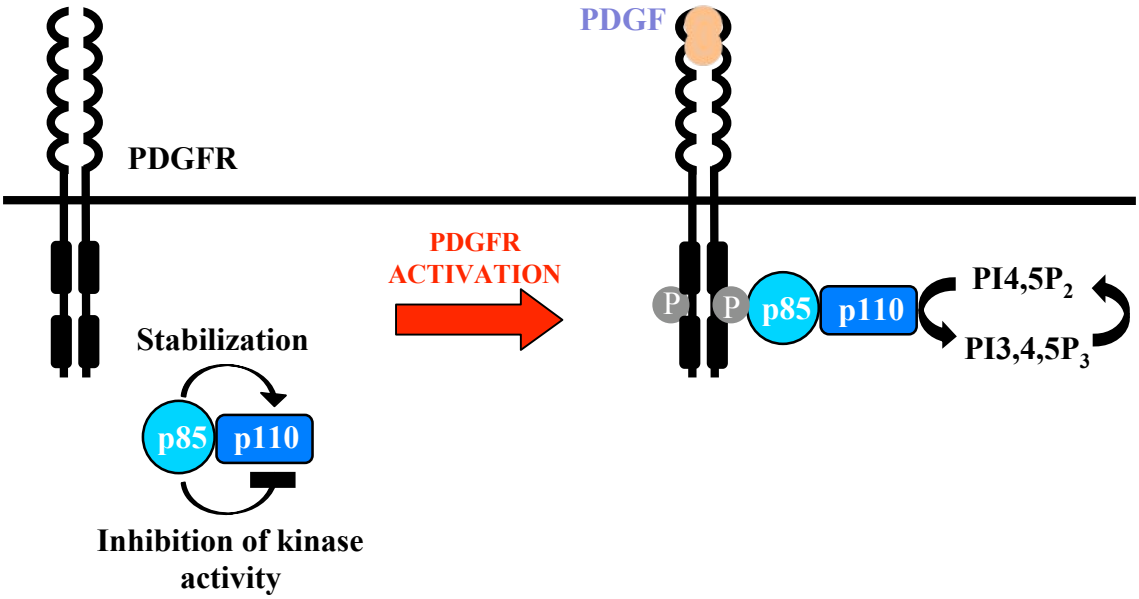

Fig. 1.6. The p85 subunit of PI3K is responsible for regulating p110 activity. In resting cells, p85 is complexed with p110 in the cytosol and inhibits its lipid kinase activity. Upon PDGFR activation, the p85:p110 complex is recruited to the plasma membrane by the binding of p85 to the PDGFR. The lipid kinase activity inhibition is relieved and p110 is able to produce the second messenger $PI3,4,5P_3$. The p85 subunit brings the p110 subunit in close proximity to its lipid substrates.

1.3 Endocytosis

The plasma membrane of a cell is a dynamic structure which functions to separate the intracellular cytoplasm from the extracellular matrix (Conner and Schmid, 2003). It coordinates the entry and exit of small and large molecules. Larger molecules known as macromolecules must be carried into the cell by the "pinching off" of the plasma membrane into vesicles, a process known as endocytosis. Endocytosis consists of phagocytosis, eating of particles, or pinocytosis, drinking of particles, (Conner and Schmid, 2003). Phagocytosis requires the use of specialized cells such as macrophages. Pinocytosis, on the other hand, is the uptake of fluids or solutes through one of four different mechanisms: macropinocytosis, clathrin-mediated uptake, caveolae-mediated uptake, or clathrin/caveolae-independent uptake (Fig. 1.7). All mechanisms of endocytosis differ with regards to the size of vesicle, the nature of the cargo (ligands, receptors, lipids) and the mechanism of vesicle formation (Conner and Schmid, 2003). Of particular interest to this thesis is the process of clathrin-mediated endocytosis which controls the levels of surface receptors and mediates the downregulation of activated signalling receptors.

1.3.1 Receptor-mediated endocytosis

Clathrin-mediated endocytosis is also known as receptor-mediated endocytosis and is initiated/facilitated by ligands binding to receptors (Fig. 1.8) (Conner and Schmid, 2003). Vesicles containing activated receptors bound to ligands are encapsulated by a polygonal clathrin coat. Clathrin is a three-legged (triskelion) structure formed by three clathrin heavy chains, each with a tightly associated clathrin light chain (Brodsky *et al*., 2001; Kirchhausen, 2000). For vesicle formation, clathrin assembles at the plasma membrane into polygonal cages. Clathrin assembly is mediated by assembly proteins, specifically EGFR pathway substrate clone 15 (Eps15), epsin, and adapter protein 2 (AP2) (Brodsky *et al*., 2001; Urbe, 2005).

AP2 consists of two large structurally related α and β2-adaptins, a medium subunit known as μ2, and a smaller subunit known as σ2. The AP2 has a barrel shaped core where μ2 and σ2 are surrounded by both the α and β2-adaptins. There are two protruding appendages

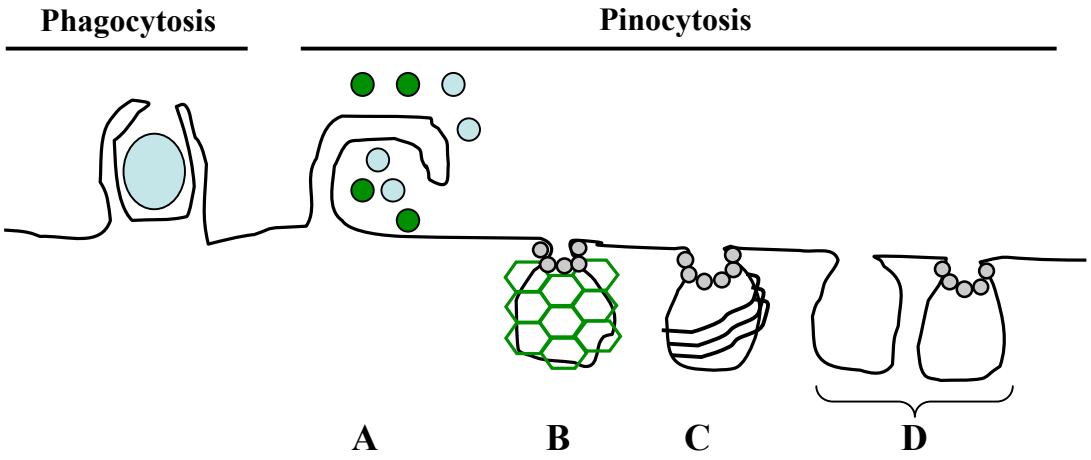

Fig. 1.7. Types of endocytosis: Phagocytosis and Pinocytosis. Phagocytois is the engulfing of larger particles by specialized cells. Pinocytosis is the uptake of fluids or solutes through one of four different mechanisms: A) macropinocytosis, B) clathrin-mediated uptake, C) caveolae-mediated uptake, or D) clathrin/caveolae-independent uptake.

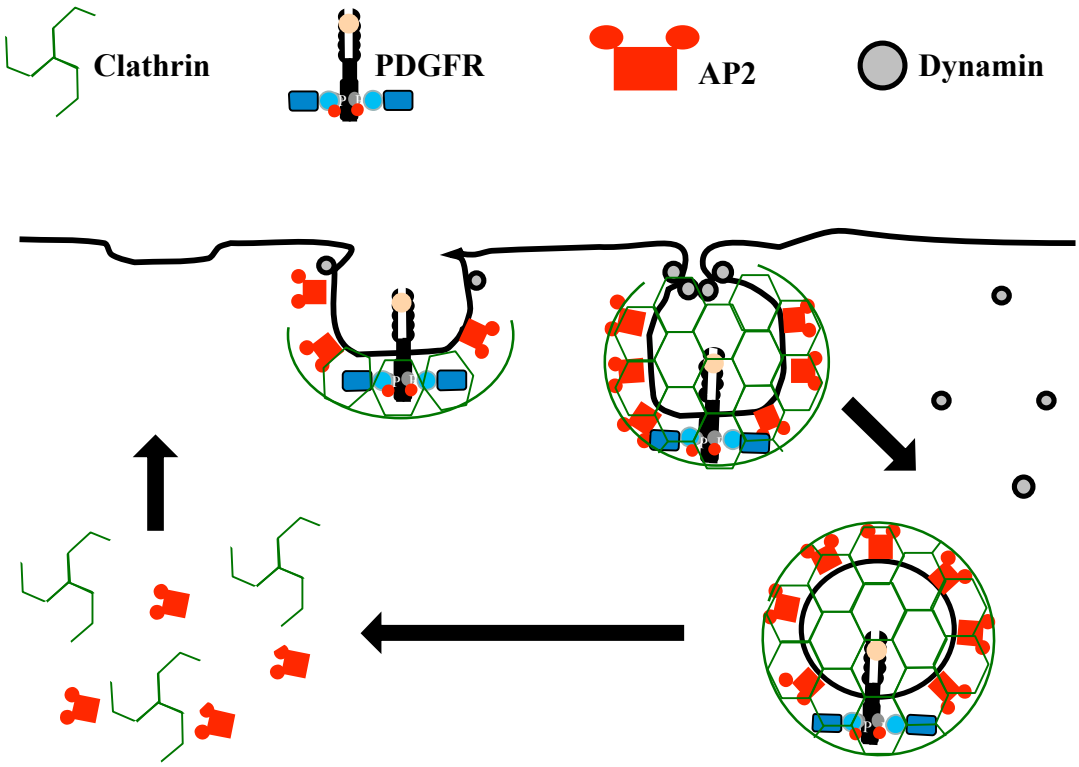

Fig. 1.8. PDGFRs are endocytosed into clathrin-coated vesicles. Clathrin triskelions assemble into a polygonal lattice around endocytosing PDGFR and plasma membrane forming a coated pit. AP2 is recruited to the plasma membrane to mediate clathrin assembly. Dynamin forms a ring around the top of the endocytosing vesicle and mediates membrane scission to release the clathrin-coated vesicle into the cytosol. (Adapted from Conner and Schmid, 2003)

found at the carboxy-terminal of the α and β2-adaptins (Collins *et al*., 2002). The α-adaptin subunit targets AP2 to the plasma membrane and specifies the site of clathrin assembly, whereas the β2-adaptin subunit triggers clathrin assembly (Conner and Schmid, 2003). The μ2 and the smaller σ2 bind tyrosine-based internalization motifs on the activated receptors and help to stabilize the core unit respectively (Conner and Schmid, 2003). AP2 directs clathrin assembly into curved lattices and couples clathrin coated vesicles to cargo recruitment (Brodsky *et al*., 2001).

At the late stages of clathrin-coated vesicle formation, receptors and their bound ligand get concentrated into coated pits which are invaginated plasma membrane that are pinched off to form vesicles (Fig. 1.8). Dynamin self assembles into a collar at the necks of deeply invaginated coated pits (Conner and Schmid, 2003). Dynamin is a large modular GTPase with a PH domain that binds PI3P, a GTPase effector domain (GED), and proline/arginine rich domains which interact with other endocytosis components. Dynamin has its own GAP activity within the GED which is required for self assembly into helical rings and stacks. The exact mechanism as to how dynamin pinches off vesicles is unknown, but it is known that dynamin must undergo GTP hydrolysis driven conformational changes for its activity (Song and Schmid, 2003).

Once the receptors are endocytosed, clathrin is shed from the vesicles and the vesicles are able to fuse with internal early/sorting endosomes (Fig. 1.9) (De Camilli *et al*., 1996). The early/sorting endosome is a key component in the endocytosis pathway as the fate of the endocytosed receptor is decided here. At the early/sorting endosomes receptors are targeted to a variety of pathways. These processes are regulated by a family of small monomeric G proteins, known as Rab proteins (discussed in Section 1.3.2.1). After the release of bound ligand and dephosphorylation, receptors can be quickly recycled back to the plasma membrane for further rounds of activation and signalling. Upon receptor monoubiquitination and through the recognition of bound ubiquitin (Ub) (discussed in Section 1.3.2.2), receptors can be targeted to the multi-vesicular body (MVB) within the late endosome (discussed in Section 1.3.2.3) and degraded in the lysosome.

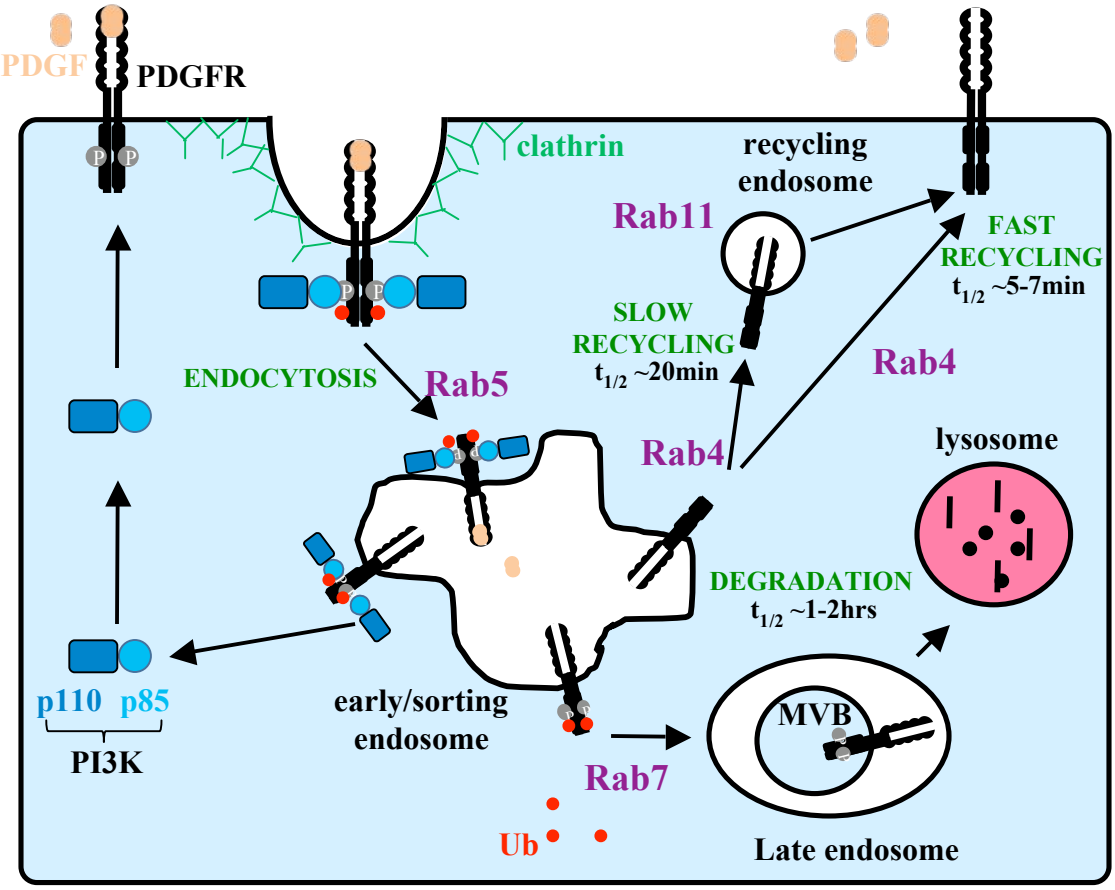

Fig. 1.9. Rab GTPases regulate vesicle fusion events during receptor-mediated endocytosis. Once the receptors are endocytosed, clathrin is shed from the vesicles and the vesicles are able to fuse with internal early endosomes. At the early/sorting endosomes receptors are targeted to a variety of pathways. These processes are regulated by a family of small monomeric G proteins, known as Rab proteins. Rab5 is responsible for regulating the entry of vesicles into the early endosome. Rab4 is responsible for regulating the exit to a recycling pathway, portion of which also involves Rab11, and Rab 7 is responsible for regulating the entry of the vesicles to the MVB and a degradative pathway. After the release of bound ligand and dephosphorylation, receptors can be quickly recycled back to the plasma membrane for further rounds of activation and signalling. Upon receptor monoubiquitination and through the recognition of bound ubiquitin receptors can be targeted to the late endosome within multi-vesicular bodies (MVB) and degraded in the lysosome.

1.3.1.1 Rab proteins

Rab proteins are a part of the Ras superfamily of GTPases (Pereira-Leal and Seabra, 2000). There are five families which make up this superfamily: Rab, Rho/Rac/Cdc42, Ras, Arf, and Ran. The largest family are the Rab proteins which are essential regulators of vesicle transport pathways. There have been more than 60 Rabs identified, each numbered in order of their discovery (Pereira-Leal and Seabra, 2000). Rab proteins can be ubiquitously expressed or tissue specific (Table 1.3) (Stenmark and Olkkonen, 2001). Rab proteins are responsible for regulating vesicle fusion events. Specifically, Rab5 is responsible for regulating the homotypic fusion of early/sorting endosomes and trafficking of receptors. Rab4 is responsible for regulating the exit to a recycling pathway. Rab 11, together with Rab4, is responsible for regulating the slow recycling pathway, and Rab 7 is responsible for regulating the exit of vesicles to the late endosome and lysosomal degradative pathway (Fig. 1.9) (Armstrong, 2000; Bucci *et al*., 1992; Mills *et al*., 1999; Mohrmann and van der Sluijs, 1999; Somsel Rodman and Wandinger-Ness, 2000; Stenmark *et al*., 1994; Ullrich *et al*., 1994).

Rab proteins are approximately 25 kDa proteins (Tuvim *et al*., 2001). They are folded into six β strands (five parallel, one antiparallel) which are surrounded by five α helixes. Rab proteins contain two switch regions crucial for interaction with guanine nucleotide exchange factors (GEF) and GTPase activating proteins (GAP). Switch I is located in the loop 2 region and switch II is located in the loop 4, helix 2 and loop 5 region of the protein (Fig. 1.10) (Tuvim *et al*., 2001)**.** Elements responsible for guanine nucleotide (GDP or GTP) binding, Mg^{2+} binding, and GTP hydrolysis are conserved for all Rab proteins. The area responsible for GTPase activity is located in five loops that connect the α helixes and β sheets. There are several aa which function to bind the phosphate, the nucleotide, the Mg^{2+} molecule or facilitate hydrolysis (Stenmark and Olkkonen, 2001). All Rab proteins can tightly associate with endosomal membranes through a posttranslational modification of two geranylgeranyl (20 carbon polyisoprenoid) groups on two cysteine residues found in aa motifs (CXXX, CC, CXC, CCXX, CCXXX, where X is any aa) near the carboxy-terminal end of the protein (Fig. 1.10; some Rabs only contain one cysteine) (Tuvim *et al*., 2001). Rab proteins are prenylated by the enzyme geranylgeranyl transferase (Seabra *et al*., 1992).

Table 1.3. Rab GTPase subcellular location and function

Name	Localization	Function	Expression
Rab 1	Endoplasmic Reticulum, *cis*-Golgi	ER-Golgi transport	ubiquitous
Rab2	Endoplasmic Reticulum, *cis*-Golgi	Golgi-ER retrograde transport	ubiquitous
Rab3	Synaptic vesicle	Regulation of neurotransmitter release	neurons
Rab4	Early endosome	Endocytic recycling	ubiquitous
Rab5	Early endosome, clathrin-coated vesicles, plasma membrane	Budding, motility, fusion in endocytosis	ubiquitous
Rab6	Golgi	Retrograde golgi traffic	ubiquitous
Rab7	Late endosome	Late endocytic traffic	ubiquitous
Rab8	*Trans*-golgi network, plasma membrane	TGN-PM traffic	ubiquitous
Rab9	Late endosome	LE-TGN traffic	ubiquitous
Rab11	Recycling endosome, *Trans*-golgi network	Endocytic recycling via RE	ubiquitous
Rab27	Melanosomes, granules	Movement of lytic granules and melanosomes towards PM	Melanocytes, platelets, lymphocytes

Adapted from Stenmark and Olkkonen, 2001

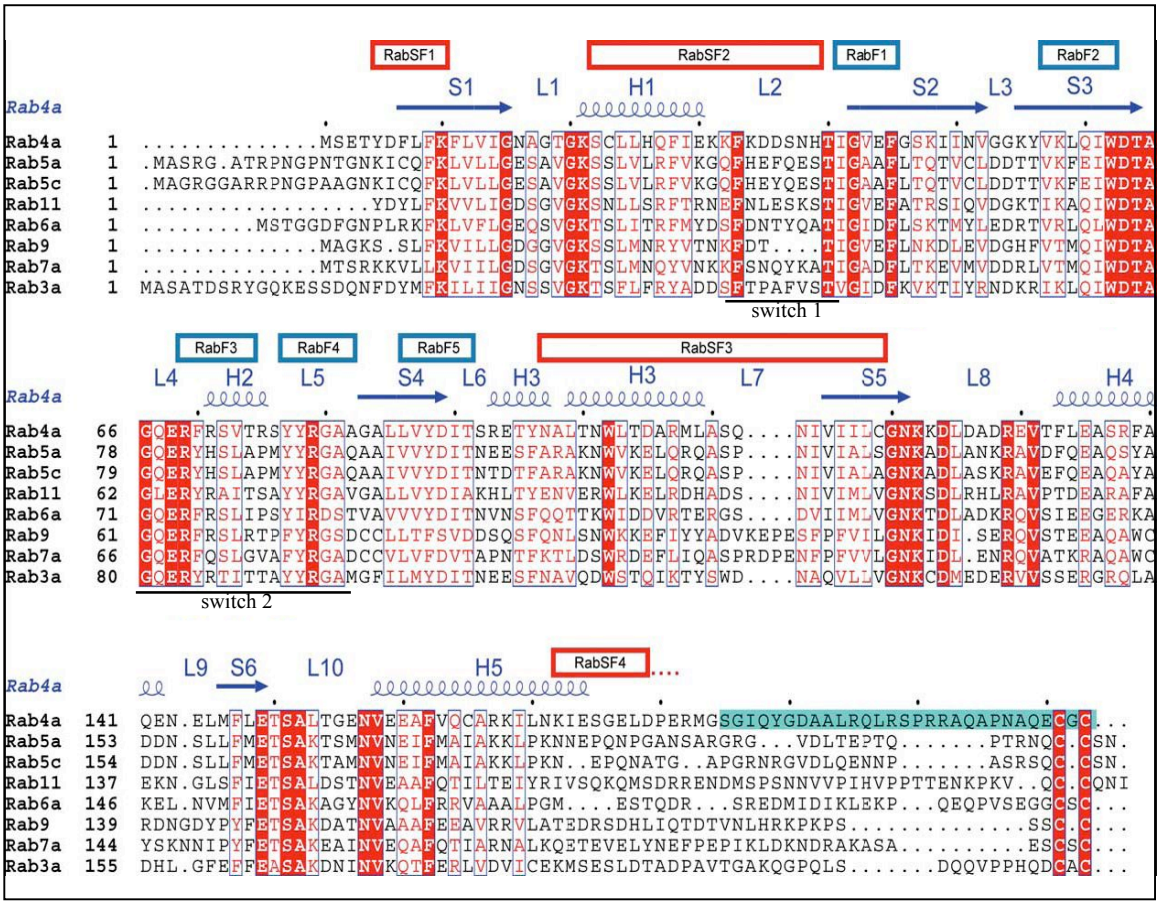

Fig. 1.10. Sequence alignment between human Rab proteins highlighting specific regions within RabGTPases which distinguish them from other GTPases in the Ras superfamily. Rab protein specific sequence regions RabF and RabSF are superimposed on the sequence alignment. RabF regions are conserved between Rab family members but make Rab proteins distinct from other branches of the Ras superfamily. RabSF regions determine specificity of Rab binding partners between other Rab proteins. The red shaded boxes show identical sequence alignment and the red lettering highlights areas of similar sequence. The secondary structure of Rab4a is added to the alignment to give an idea as to where these specific regions are located throughout the Rab proteins (L-loop, S-sheet, H-helix). (The blue highlighted region was added to show a deleted region used in the Huber and Scheidig, 2005 paper and is not important for this thesis) (Reproduced with permission from A.J. Scheidig. (Huber and Scheidig, 2005))

Rab proteins contain specific regions that distinguish them from other GTPases within the Ras superfamily (Fig. 1.10). These specific aa regions are known as Rab F1-5 and Rab SF regions (Stenmark and Olkkonen, 2001). The F1-5 regions are conserved in all Rab families and in conjunction with the SF regions, they determine specificity of binding partners for each individual Rab protein.

Rab proteins are membrane associated molecular switches that regulate the budding, transport and fusion of endosomes. Rab proteins are regulated spatially and by their nucleotide (GDP or GTP) bound state (Stenmark and Olkkonen, 2001). Rab proteins interchange between inactive and active states by exchanging GDP for GTP, respectively. The nucleotide exchange is regulated by GEFs, while GAPs stimulate the hydrolysis of GTP to GDP by the Rab proteins. There is a dramatic conformation change seen within the active site of the Rab protein and their switch domains upon binding to GDP or GTP (Fig. 1.11) (Stenmark and Olkkonen, 2001).

Rab proteins are also regulated spatially (Fig. 1.12). Prior to growth factor stimulation, inactive Rab-GDP is bound to a guanine-dissociation inhibitor (GDI) that masks the geranylgeranyl groups and allows the Rab protein to localize to the cytosol. Upon growth factor stimulation, the GDI is removed through the action of a GDI-displacement factor (GDF) and Rab-GDP is relocalized to an endosomal membrane. GDP is replaced with GTP through the action of a GEF protein. Rab-GTP is activated and is able to bind to specific effector proteins to mediate membrane fusion events. After membrane fusion, the Rab GTPase activity is accelerated by the action of a GAP protein and the bound GTP is hydrolyzed to GDP (Stenmark and Olkkonen, 2001). The Rab protein is inactivated which then allows the GDI protein to bind Rab-GDP and localize it to the cytosol.

Effector proteins of specific Rab proteins are key to Rab function (Stenmark and Olkkonen, 2001). Effector proteins are a heterogeneous group composed of: coil-coil proteins responsible for membrane tethering and docking, enzymes, and cytoskeleton associated proteins. Rab5 is the best characterized Rab protein in regards to function and effector protein associations. Rab5 is responsible for regulating the homotypic fusion of early endosomes and in the trafficking of activated receptor complexes into the early/sorting endosome. Rab5-GTP recruits early endosomal antigen 1 (EEA1) protein to the endosome and is required to facilitate

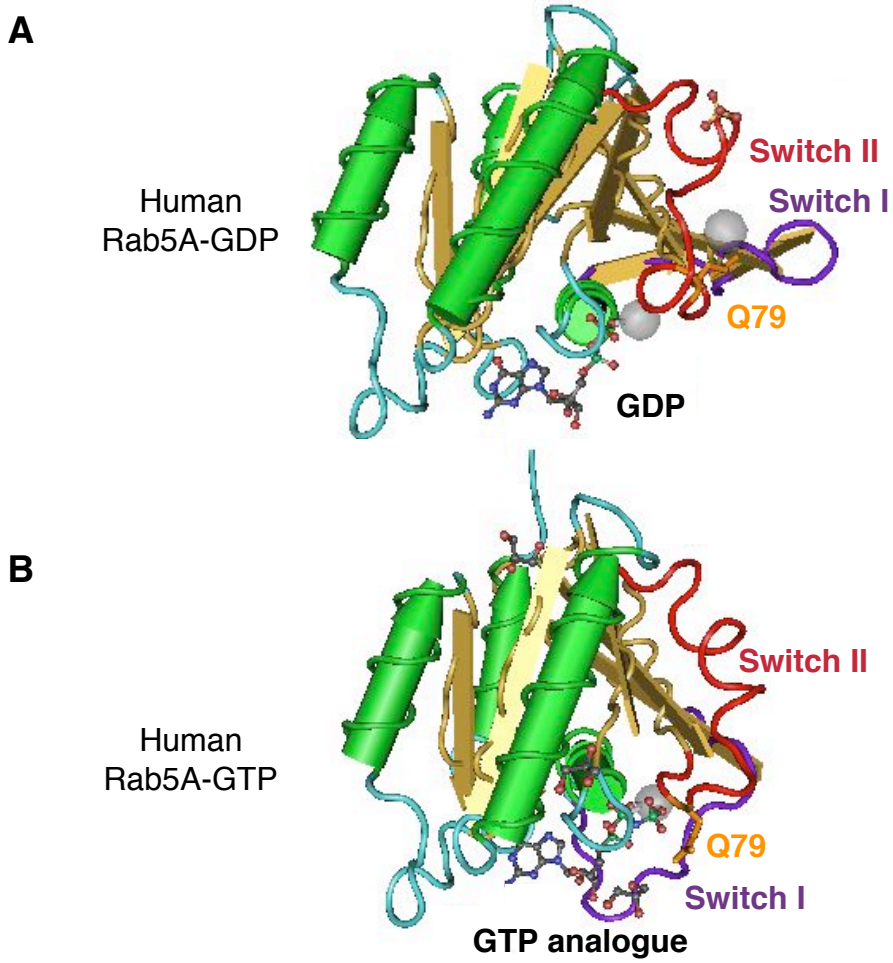

Fig. 1.11. Rab5a active site and switch regions change conformation when bound to GDP or GTP. Crystal structures of Rab5A complexes. Switch I (purple), switch II (red) and the catalytic glutamine (Q79, orange) are highlighted. The nucleotide structures, Mg^{2+} (grey spheres) and small water molecules are also shown. A) Crystal structure of inactive state Rab5A-GDP complex A) Note the catalytic glutamine (Q79) is directed away from the bound GDP as are the switch regions, particularly switch I (purple). B) Crystal structure of active conformation of Rab5A bound to a GTP analogue. Note the repositioning of the catalytic glutamine (Q79) near the gamma phosphate of the bound nucleotide. Compared to the GDP-bound structure in (B), notice the switch regions have moved significantly. From Zhu et al., 2004 and color highlighted using Cn3Dv4.1.

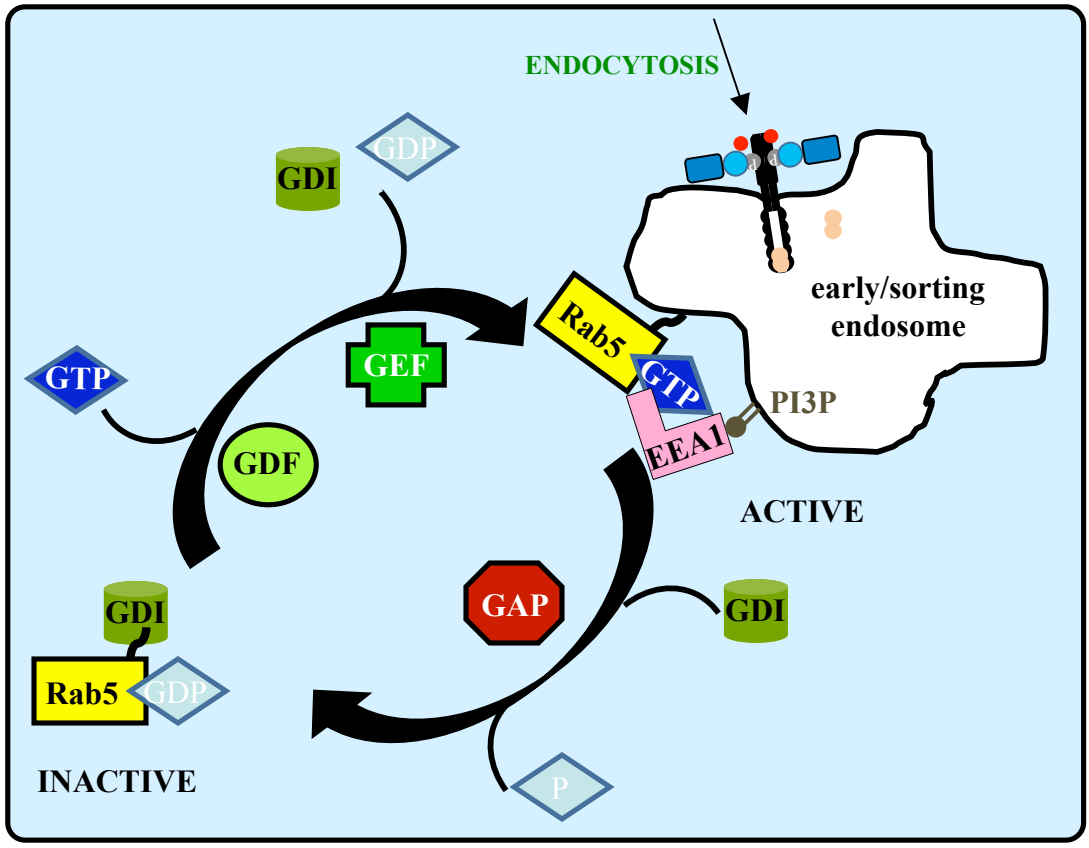

Fig. 1.12. Rab5 GTPase cycles regulate the timing of the assembly/disassembly of multiprotein complexes involved in receptor trafficking. Prior to growth factor stimulation, inactive Rab5-GDP is bound to a guanine-dissociation inhibitor (GDI) which masks the geranylgeranyl groups and allows the Rab5 protein to localize to the cytosol. Upon growth factor stimulation, the GDI is removed through the action of a GDI-displacement factor (GDF) and Rab5-GDP is relocalized to an endosomal membrane where GDP is replaced with GTP through the action of a guanine nucleotide exchange factor (GEF) protein. Rab5-GTP is activated and is able to bind to specific effector proteins such as EEA1 to mediate membrane fusion events. EEA1 helps to tether the two endosomal membranes by binding to Rab5 and PI3P for membrane fusion to take place. After membrane fusion, the Rab5 GTPase activity is accelerated by the action of a GAP protein and the bound GTP is hydrolyzed to GDP. The Rab5 protein is inactivated which allows the GDI protein to bind Rab5-GDP and localize it to the cytosol.

fusion events (Mills *et al*., 1998); (Christoforidis *et al*., 1999a; Rubino *et al*., 2000; Simonsen *et al*., 1998). EEA1 interacts with phosphatidylinositol 3`-phosphate (PI3P) lipids on the endosomal membrane through its FYVE zinc finger domain. EEA1 helps tether incoming early endosomal vesicles containing newly endocytosed PDGFR to the early/sorting endosome by interacting with both Rab5-GTP and PI3P (Fig. 1.13). Rab5 and EEA1 have not been shown to facilitate the actual membrane fusion event but are responsible for tethering the incoming vesicle to the proper endosome. Membrane fusion is likely facilitated by soluble N-ethylmaleimide-sensitive factor attachment protein (SNAP) receptor SNARE proteins.

There are two well-characterized Rab5 mutants used to study Rab5 protein interactions and functions (Liu and Li, 1998). They are Rab5-Q79L and Rab5-S34N. The Rab5-Q79L mutant is locked in the active conformation and only interacts with GTP since mutation of this catalytically important glutamine (Fig. 1.11) renders it GTPase defective, whereas the Rab5-S34N mutant is locked in the inactive conformation and only interacts with GDP. Using these mutants in isolation, it is possible to identify Rab5 binding partners and functions by understanding how the protein behaves in both the inactive and active conformations. These mutants are used in this thesis to determine how the p85 subunit of PI3K interacts with Rab5.

1.3.1.2 RTK mediated monoubiquitination

PDGFRs are targeted for lysosomal degradation by the addition of several single ubiquitin (Ub) molecules which act as a signal for the receptor to be sorted to the degradative pathway (Marmor and Yarden, 2004). Ub is a 76 amino acid polypeptide and Ub conjugation is mediated through a series of enzymatic reactions (Fig. 1.14) (Hershko and Ciechanover, 1998). These reactions include an ATP-dependent conjugation of Ub to the active site cysteine residue of an E1 enzyme and the transfer of Ub to an E2 conjugating enzyme through a thiol-ester linkage. Some E2 enzymes can conjugate Ub directly onto the substrate but in most cases an E3 Ub ligase enzyme is needed. E3 Ub ligases mediate substrate recognition. Several types of E3 ligases exist. There are the “homologous to the E6-AP carboxy terminus” (HECT) domain containing E3 ligases (e.g. Nedd4) which conjugate Ub by proceeding through a thiol-

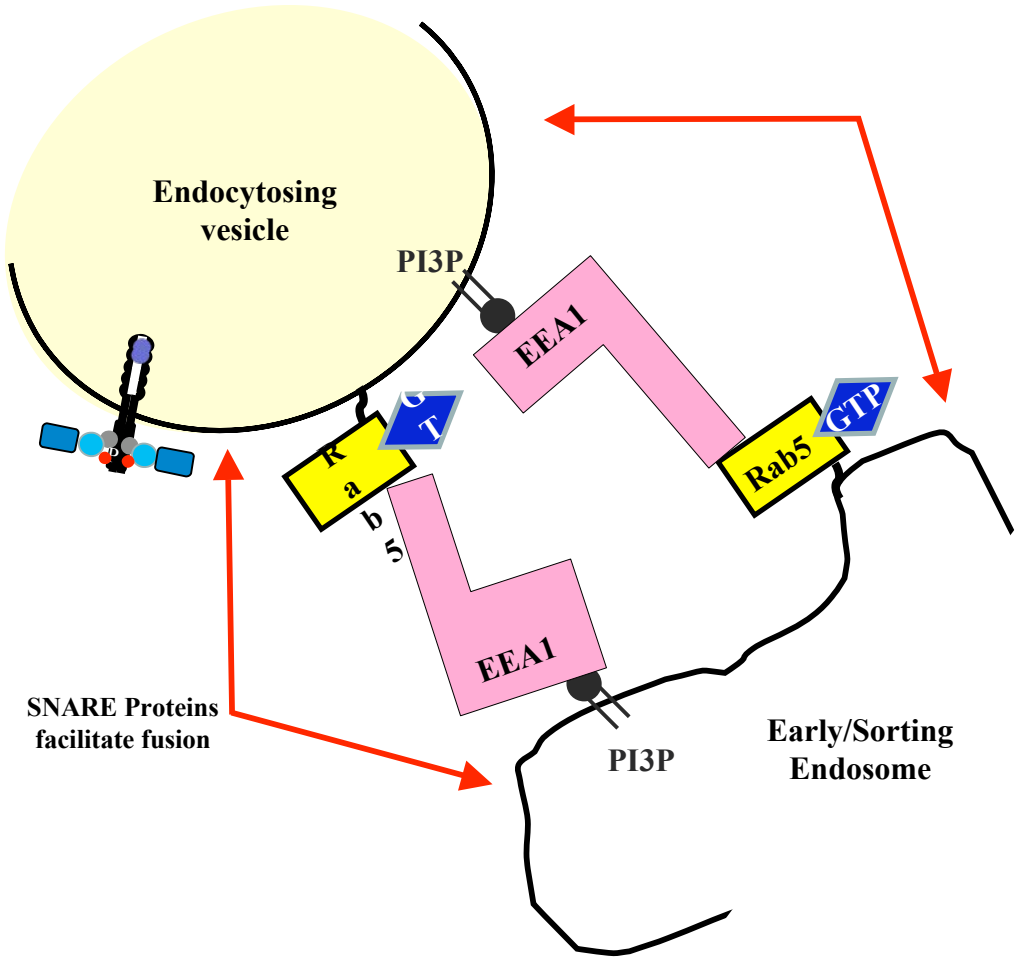

Fig. 1.13. Rab5 and EEA1 are responsible for tethering endocytosing vesicles to early/sorting endsomes to facilitate highly specific membrane fusion events. Rab5-GTP recruits EEA1 to the endosome. EEA1 interacts with PI3P on the endosomal membrane through its FYVE zinc finger domain. EEA1 helps tether incoming vesicles containing newly endocytosed PDGFR to the early endosome by interacting with both Rab5-GTP and PI3P. Rab5 and EEA1 have not been shown to facilitate the actual membrane fusion event but are responsible for tethering the incoming vesicle to the proper endosome. Membrane fusion is likely facilitated by SNARE proteins.

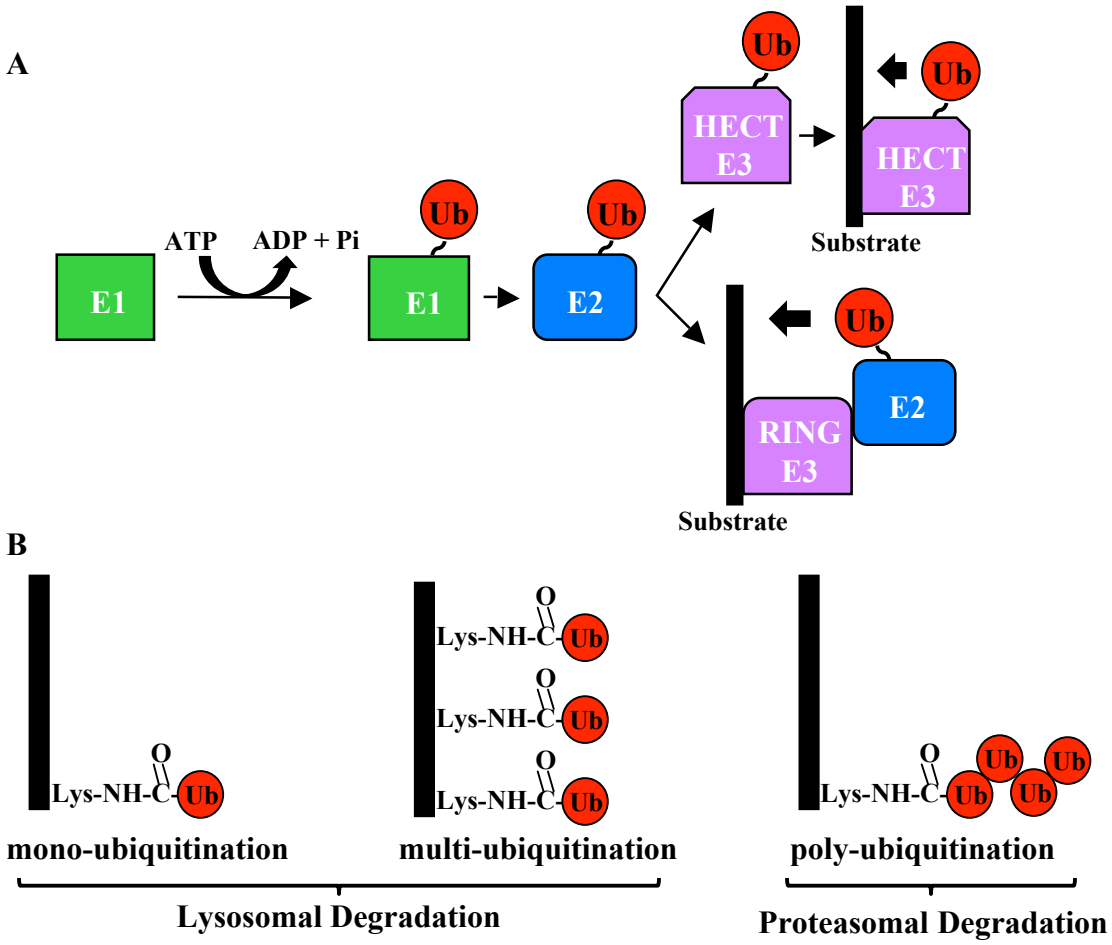

Fig. 1.14. Receptor ubiquitination. A) The ubiquitination reaction consists of three steps: the E1 enzyme mediates the ATP-dependent activation of the C-terminal glycine of ubiquitin, which is conjugated to an active site cysteine through a thiol-ester linkage. Ubiquitin is then transferred to a cysteine in the active site of E2 enzymes. Although some E2s can ubiquitinate substrates directly, in most cases an E3 ubiquitin ligase is required. E3 enzymes mediate ubiquitination in a distinct manner: HECT domain-containing E3s form a thiol-ester linkage with a ubiquitin transferred from the E2, which is subsequently conjugated to the substrate. RING finger E3s function as adaptors that bind both E2 enzymes and substrates to coordinate substrate ubiquitination. Both reactions result in the formation of an isopeptide bond between the C-terminal glycine of ubiquitin and the ε-amino group of a lysine residue within the substrate. B) Several types of substrate modification by ubiquitin can ensue: conjugation with one ubiquitin moiety (mono-ubiquitination), conjugation with multiple ubiquitin monomers (multi-ubiquitination) or the formation of a ubiquitin chain branched at internal lysines within ubiquitin (poly-ubiquitination).

ester:Ub intermediate and the "really interesting new gene" (RING) domain containing E3 ligases (e.g. Cbl) which act as an adaptor E3 ligase which binds to both the substrate and E2 conjugating enzyme.

The Ub molecules are conjugated to the substrate via the ε amino group of lysine residues. There are three possible outcomes of ubiquitination (Fig. 1.14). The substrate can be mono-ubiquitinated (one Ub molecule at one site on the substrate), multi-ubiquitinated (mono-ubiquitinated on several sites) or poly-ubiquitinated (several Ub molecules conjugated into a chain at one site). Mono-ubiquitinated or multi-ubiquitinated proteins are targeted to the lysosome for degradation, whereas poly-ubiquitinated proteins are targeted to the proteasome for degradation. Monoubiquitination is critical in PDGFR signalling for late endosomal sorting and lysosomal degradation of internalized receptors (Marmor and Yarden, 2004).

The Cbl family of E3 ligases have been shown to facilitate the ubiquitination of the PDGFR (Thien and Langdon, 2001); (Tsygankov *et al*., 2001). The structure of Cbl proteins include a tyrosine kinase binding (TKB) domain, a RING domain, a proline rich region, and a Ub-binding Ub associated (UBA) domain. There are three Cbl family members: c-Cbl, Cbl-b, and Cbl-3. The c-Cbl family member has been shown to specifically regulate PDGFR ubiquitination (Miyake *et al*., 1998). The c-Cbl E3 ligase binds the PDGFR at pTyr 1021 and becomes phosphorylated itself by the activated receptor which stimulates c-Cbl Ub ligase activity (Thien and Langdon, 2001; Tsygankov *et al*., 2001).

1.3.1.3 Late endosomal sorting

The early/sorting endosome is different from the late endosome. It is unclear whether the early/sorting endosome matures forming the late endosome or if vesicles are pinched off from the early/sorting endosome and form or fuse with the late endosome. The late endosome is characterized by a decrease in pH and accumulation of hydrolytic enzymes (Marmor and Yarden, 2004). The late endosome contains lysobisphosphatidic acid within the endosome and PI3P at the membrane (Teis and Huber, 2003). Late endosome also contain MVBs and

activated receptors are endocytosed inside the late endosome forming these internal vesicles. Receptors continue to actively signal until they are taken into these MVBs (Clague and Urbe, 2001). Late endosomes fuse with the lysosome where receptor degradation takes place (Marmor and Yarden, 2004). Sorting receptors into the MVB involves many steps and the sequential recruitment of several multi-protein complexes composed of class E vacuolar protein sorting (Vps) proteins (Fig. 1.15) (Urbe, 2005).

Sorting of receptors into the MVB is controlled by several interdependent mechanisms such as conjugating receptors with an Ub molecule, recognition and binding to the ubiquinated receptor and finally the invagination of the late endosomal membrane to form a MVB (Teis and Huber, 2003). The PDGFR is ubiquitinated in response to ligand binding (Marmor and Yarden, 2004). The conjugation of the PDGFR with an Ub molecule is a signal for sorting into the MVB of the late endosome (Urbe, 2005). Effector molecules help with the sorting by binding to Ub through Ub interacting motif (UIM) or UBA domains.

Once at the early/sorting endosome, the hepatocyte growth factor-regulated tyrosine kinase substrate (Hrs) and signal-transducer molecule (STAM) complex interacts with ubiquitinated receptors through the UIM of the Hrs protein (Urbe, 2005). The Hrs/STAM complex recruits the receptor to a specialized area of the early/sorting endosome that is covered with a flat clathrin coat. This clathrin coated area is a concentration device used to trap ubiquitinated receptors for the formation of a MVB (Urbe, 2005).

Hrs plays a central role in MVB formation (Fig. 1.15) (Urbe, 2005). Hrs recruits endosomal sorting complex required for transport (ESCRT) I, II and III which are protein complexes required for MVB formation. ESCRT proteins are sequentially recruited to and activated at the early/sorting endosome. They constitute the core of the MVB formation machinery and act downstream of Hrs/STAM complexes (Katzmann *et al*., 2002; Raiborg *et al*., 2003; Urbe, 2005). Hrs recruits ESCRT I (also known as the tumor susceptibility gene (tsg101)) through a four aa motif PS[T]AP. ESCRT I recruits ESCRT II which is transiently associated with early/sorting endosomal membranes in an ESCRT I-dependent manner. ESCRT II is then able to recruit ESCRT III which facilitates membrane invagination and vesicle formation inside the endosome to form the MVBs. ESCRT III recruits

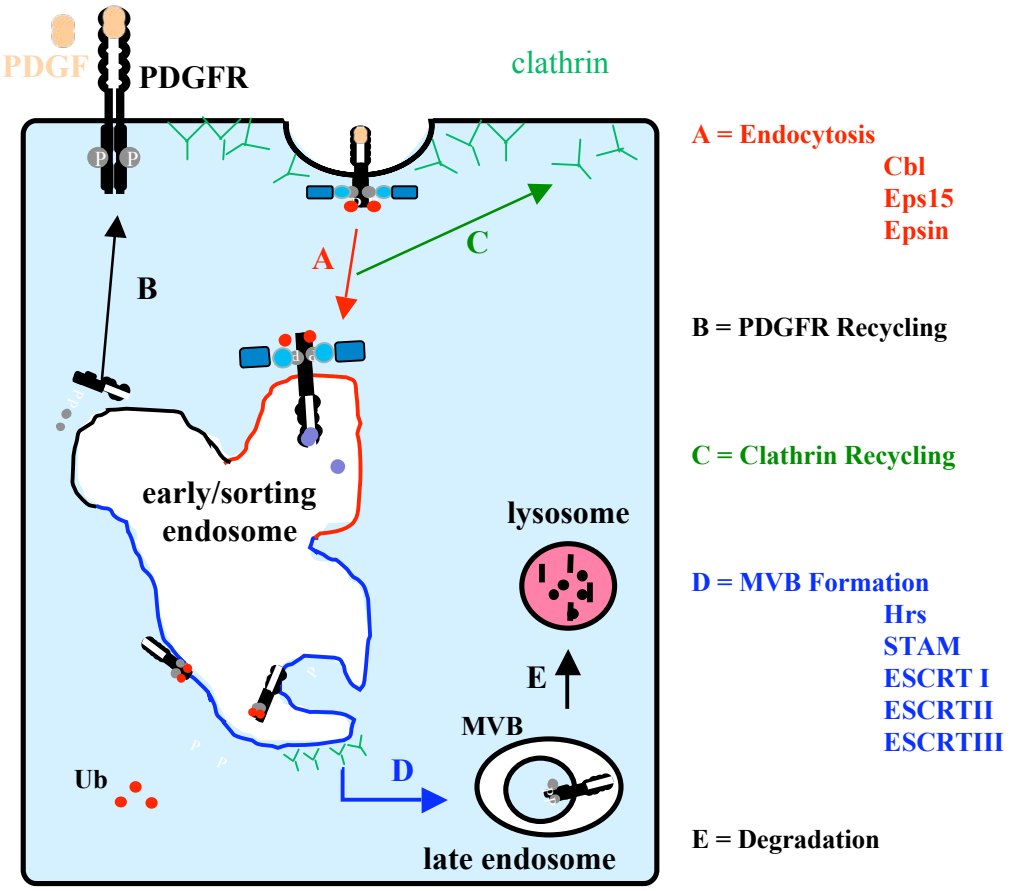

Fig. 1.15. Late Endosomal Sorting. Stimulation with ligand induces activation of PDGFR, autophosphorylation and endocytosis. A) Cbl is recruited to the PDGFR, phosphorylated and ubiquitinates the PDGFR. Ubiquitinated receptors are sorted into clathrin-coated pits by a multiprotein complex that includes coat adaptors such as Epsin and Eps15. B) At the early endosome, PDGFR can be recycled back to the plasma membrane. C) Progression through the endocytic pathway is characterized by the shedding of clathrin, D) a decrease in the internal pH within the vesicles and the accumulation of hydrolytic enzymes. PDGFR trafficking from early/sorting to late endosomes is dependent on its sustained ubiquitination. MVB sorting is regulated through recognition of ubiquitinated cargo by Hrs/STAM complex, ESCRT I (tsg101) and other components of ESCRT complexes. Invagination of the limiting membrane of the MVB forms internal vesicles. This is coupled to receptor de-ubiquitination and dissociation of the ESCRT complex from endosomes, mediated by the ATPase Vps4. Fusion of the late endosome with the lysosome results in degradation of the contents of the internal vesicles.

the deubiquitinating enzyme Doa4 (Amerik *et al*., 2000) before vesicle formation so Ub can be recycled back to the cytosol for further conjugation reactions. The last step in MVB formation is the ATP-dependent dissociation and recycling of the ESCRT proteins by Vps4.

PDGFR endocytosis contains many steps of activation and regulation. There are numberous proteins and functions which, if compromised, could result in defective PDGFR downregulation. The next section will highlight numerous cellular outcomes when several parts of this pathway are interrupted.

1.3.2 Defects in endocytosis and cancer

Receptor overexpression or receptors containing activating mutations have resulted in cancerous phenotypes (Blume-Jensen and Hunter, 2001). Receptor endocytosis is a process which regulates the downregulation of signalling from surface receptors. There are several steps within the endocytic pathway, which, when affected, could result in defective downregulation. It has been shown that mutations involved in MVB sorting signals such as mutations of Ub or ubiquitinating enzymes have all been found in human cancers (Jiang and Beaudet, 2004). The loss of Ub conjugation to activated receptors has resulted in increased recycling of the receptor back to the cell surface for further rounds of activation and signalling (Levkowitz *et al*., 1998). Mutated receptors that can no longer bind Cbl, or Cbl mutations which knock out its E3 ligase activity have also been shown to result in defective receptor downregulation (Bache *et al*., 2004; Peschard and Park, 2003). Further down in the MVB sorting pathway, the ESCRT protein tsg101 has also been linked to the development of tumors (Bache *et al*., 2004; Katzmann *et al*., 2002). As defects in the endocytic pathway can lead to defective receptor downregulation, a better understanding of the pathway and the proteins involved will allow research to evolve to include this pathway in the repertoire of cancer fighting therapies.

1.4 RabGAP function of p85

More recently it is becoming apparent that p85 has regulatory functions beside those involving p110. Our lab specifically has studied the interactions between the p85 subunit and A-Raf (Fang *et al*., 2002; King *et al*., 2000; Mahon *et al*., 2005), ankyrin3 (Ignatiuk *et al*., 2006), and PTEN (unpublished data). We have shown that p85:A-Raf regulates PDGFR function, that p85:ankyrin3 interactions appear to target activated PDGFRs for lysosomal-mediated degradation and that the p85:PTEN interaction significantly increases PTEN lipid phosphatase activity. Of particular interest to this thesis is the discovery that p85 has GAP activity towards Rab5 and Rab4 (Chamberlain *et al*., 2004). It has been shown previously that the p85 subunit of PI3K stays associated with the PDGFR during receptor endocytosis (discussed in Section 1.3.2) (Kapeller *et al*., 1993) and can bind directly to Rab5. As previously discussed, Rab5 is a G-protein which localizes to early and sorting endosomes and regulates the movement of vesicles containing activated PDGFR from the plasma membrane to sorting endosomes (Section 1.3.2.1) (Chamberlain *et al*., 2004). Furthermore, studies have shown that p85 binding sites on PDGFRs are required for proper receptor down-regulation (Joly *et al*., 1994). Thus p85 may play a role in helping to regulate the process of receptor degradation by interacting both with activated receptors and the Rab proteins that control receptor endocytosis and recycling.

GAP domains downregulate G-proteins by stimulating the intrinsic GTPase activity of the G-protein to hydrolyse bound GTP to GDP. GAP proteins function by stabilizing the switch regions of the bound GTPase protein so that the catalytic glutamine residue is positioned properly and by supplying a charged arginine residue to the GTPase active site (Clabecq *et al*., 2000). During the hydrolytic reaction, nucleophilic attack of water upon the γ phosphate of GTP to form GDP + Pi, involves several steps including: deprotonation of the attacking water molecule, transition state complex formation, and rearrangement of the enzyme and solvent. The addition of Mg^{2+} is required for guanine stabilization (Fig. 1.16) (Sprang, 1997).

The p85 subunit of PI3K contains a GAP-like BH domain with sequence homology to RhoGAP proteins involved in regulating Rho GTPases such as Cdc42 and Rac1. In earlier work, p85 was found to bind both proteins but did not posses GAP activity towards either

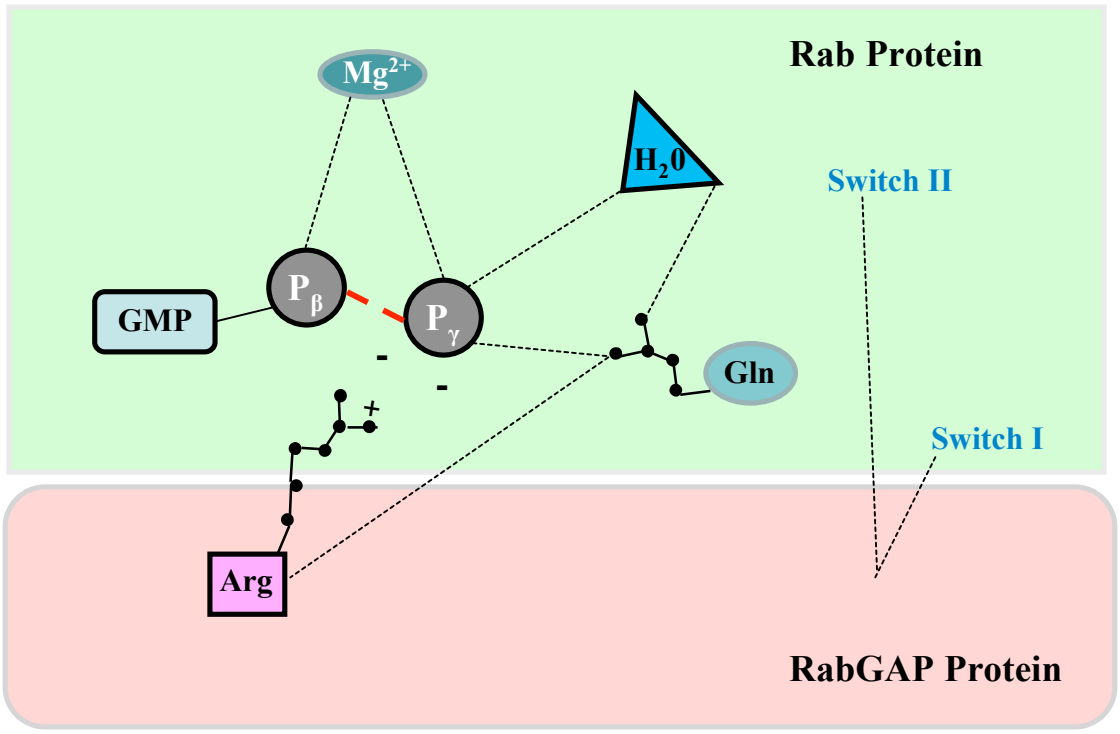

Fig. 1.16. GAP proteins stimulating the intrinsic GTPase activity of Rab proteins to hydrolyse bound GTP to GDP. GAP proteins function by stabilizing the switch regions of the bound Rab protein so that the catalytic glutamine residue is positioned properly and by supplying an arginine residue to the GTPase active site. During the hydrolytic reaction, nucleophilic attack of water upon the γ phosphate of GTP to form GDP + Pi, involves several steps including: deprotonation of the attacking water molecule, transition state complex formation, and rearrangement of the enzyme and solvent. The addition of Mg^{2+} is required for guanine stabilization (Adapted from Scheffzek *et al*., 1998).

protein (Zheng and Guan, 1994); (Bokoch *et al*., 1996). The crystal structure of the p85 BH domain revealed a distinct folding pattern capable of binding a G-protein suggesting that p85 may possess GAP activity towards an unidentified G-protein (Musacchio *et al*., 1996). Later work, from our laboratory, revealed the p85 protein had GAP activity encoded in its BH domain selective for Rab5, Rab4, but not Rab11 (Chamberlain *et al*., 2004). It was also found to possess GAP activity towards Cdc42 and Rac1 but at higher concentrations of p85 than had been previously tested. The ability of p85 to possess GAP activity towards Rab5 and Rab4 suggested that p85 may play a central role in coordinating receptor endocytosis and cell signalling. To investigate this hypothesis our lab generated several p85 domain mutants and studied their effects on normal receptor endocytosis and cell signaling (discussed in Section 1.4.1). The results of these studies, in particular the results from the p85-ΔBH, p85-R274A and the p85-Δ110 mutants, lead to us to hypothesize a new model of p85 interaction with Rab5 and activated receptors known as the 'hand-off" model (discussed in Section 1.4.2).

1.4.1 p85-R274A, p85-ΔBH and p85-Δ110 mutants of p85

Stable NIH 3T3 cell lines were produced, expressing mutants of p85 that contained different p85 domain combinations, to study the effects each mutant had on receptor endocytosis and cell signalling. The proteins were expressed as FLAG-tagged fusion proteins for detection. Cell lines expressing two of these mutants, p85-ΔBH (deletion of the BH domain and flanking proline rich regions) and p85-R274A (point mutation within the BH domain) have been characterized (Chamberlain *et al*., 2004). Both mutants were tested for RabGAP activity. As the GAP activity was found to be encoded in the BH domain, it was expected, and confirmed, that each mutant would show reduced GAP activity towards Rab5 (Fig. 1.17) (Chamberlain *et al*., 2004). The GAP activity of the p85-R274A mutant was reduced more so than that of the p85-ΔBH mutant. Both mutants were then tested for their ability to bind Rab5. The p85-wt bound to both Rab5-GTP and Rab5-GDP. However, the p85-ΔBH protein bound only Rab5-GTP and the p85-R274A protein only bound to Rab5-GDP (Fig. 1.18) (Chamberlain *et al*., 2004). Although defective for RabGAP activity, each mutant retained the domain responsible for

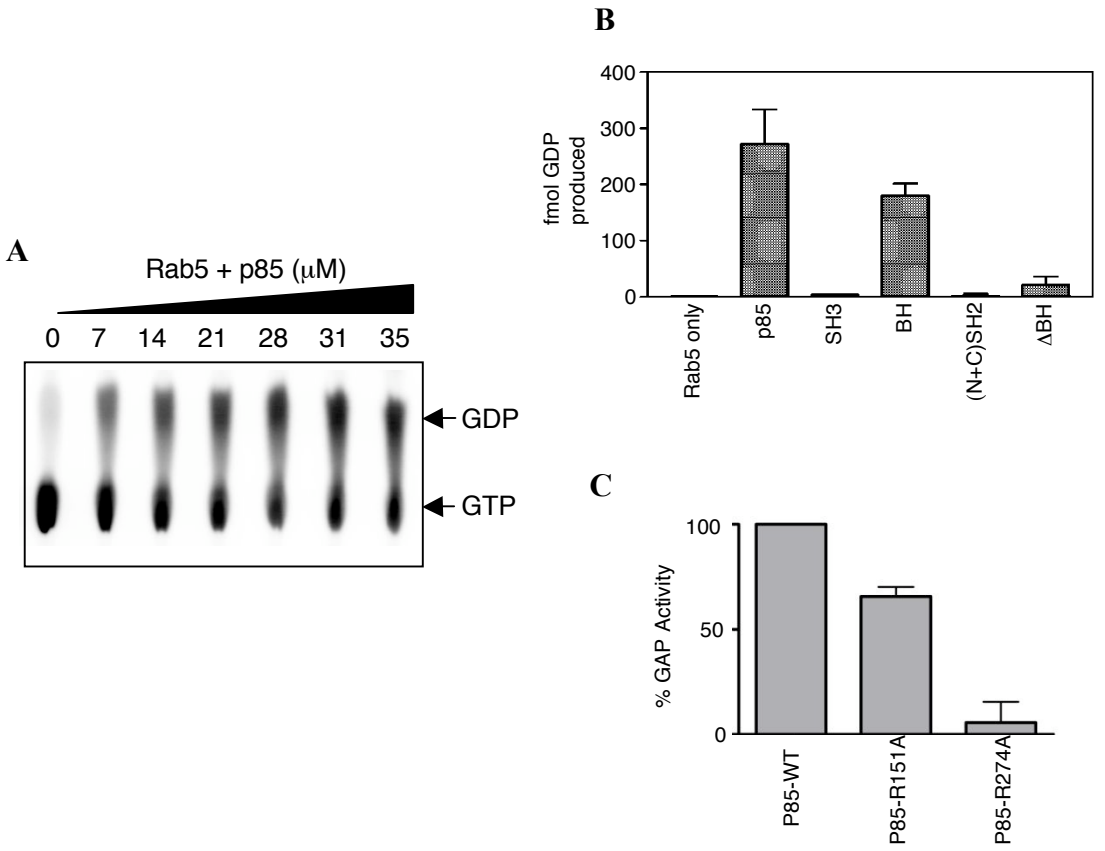

Fig. 1.17 The BH domain of the p85α encodes Rab5 GAP activity. Rab5 was loaded with [α^{32}P]GTP, and hydrolysis to [α^{32}P]GDP was assayed for 10 min in the absence and presence of increasing concentrations of p85 as indicated. A) Nucleotides were resolved by thin layer chromatography and visualized using a phosphorimager. B) GAP assay testing the ability of different domains of p85 (10 μM each) to stimulate the GTPase activity of Rab5. C) GAP assay comparing the ability of wild type (p85-WT) and mutant (p85-R151A and p85-R274A) p85 proteins to accelerate the GTPase activity of Rab5. Reproduced with permission from Chamberlain *et al.* (2004).

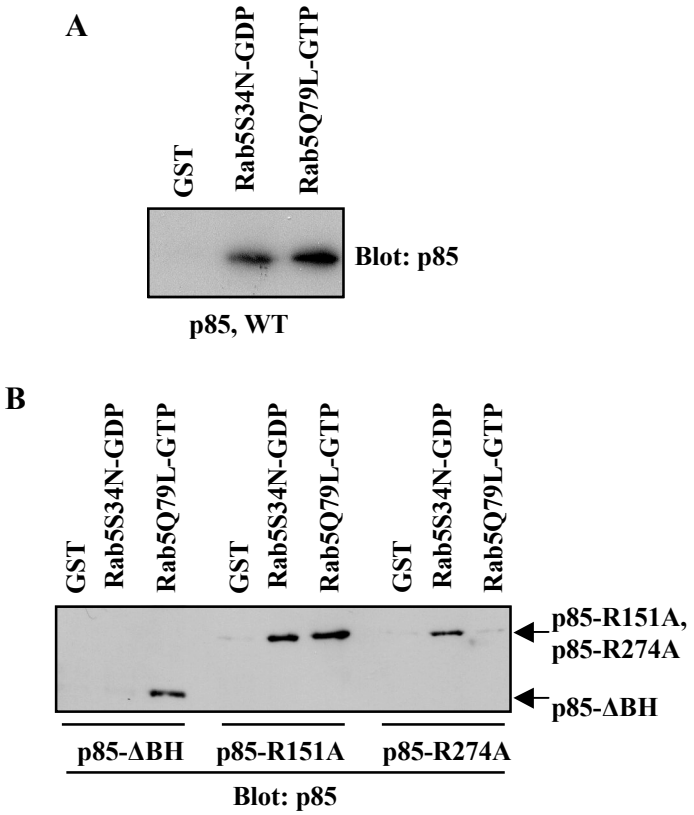

Fig. 1.18. The p85 protein binds directly to Rab5-GTP and Rab5-GDP. GST and GST-Rab5 were immobilized on glutathione Sepharose beads and loaded with the indicated nucleotide. Purified PreScission-cleaved p85 was added and bound p85 was detected after washing, using an immunoblot analysis with anti-p85 antibodies. A) GST and GST-Rab5 mutants known to selectively bind GDP (S34N) or GTP (Q79L) were used in a pull-down assay with wild type p85 protein B) the indicated p85 mutants were tested for their abilities to bind to GST (control), GST-Rab5S34N-GDP, and GST-Rab5Q79L-GTP as described above. Reproduced with permission from Chamberlain et al. (2004).

binding the p110 catalytic subunit for PI3K and was therefore tested to determine if/how PI3K subunit associations was affected by the mutants. Both mutants were tested for their ability to bind to p110α and as expected both mutants were able to interact with p110α and stimulate PI3K activity to a degree comparable to that of the full length p85 (Fig. 1.19) (Chamberlain *et al*., 2004). Because each mutant did possess defective RabGAP activity, the two proteins were tested for their ability to affect PDGFR downregulation and activation as compared to control NIH 3T3 cells and cells expressing p85-wt. The normal degradation of the PDGFR was slowed down by both mutants, with p85-R274A exerting a greater effect (Fig. 1.20) (Chamberlain *et al*., 2004). PDGFR activation was assessed by tyrosine phosphorylation of the PDGFR and the ability of the PDGFR to activate downstream signalling pathways such as the PI3K/Akt and Ras/MAPK pathway. Cells expressing the p85-R274A and p85-ΔBH proteins showed enhanced PDGFR tyrosine phosphorylation (Fig. 1.20). The cells did, however, show near normal activation/phosphorylation of Akt as compared to control cells, but showed an increase in MAPK activation/phosphorylation; this was particularly true for p85-R274A expressing cells (Fig. 1.21) (Chamberlain *et al*., 2004). Lastly, the cells were tested for PDGFR associations during growth factor stimulations. The p85-R274A mutant remained associated with the receptor for longer periods of time as compared to p85-wt (Fig. 1.22) (Chamberlain *et al*., 2004).

Upon further investigation of cells expressing the p85-R274A mutant, our lab has now shown that defective Rab GAP activity leads to tumour formation in nude mice (Fig. 1.23) (Chamberlain *et al*., 2008). These cells possess the hallmarks of transformed cells. We show p85-R274A expressing cells have several characteristics indicative of deregulated growth. These cells show a loss of contact inhibition for cell growth and are able to grow independent of attachment (Fig. 1.24) (Chamberlain *et al*., 2008). Furthermore, the co-expression of a dominant negative Rab5-S34N mutant with p85-R274A could block p85-R274A-induced transformed properties (Fig. 1.25) (Chamberlain *et al*., 2008).

Similar experiments that were used to characterize the p85-ΔBH and p85-R274A cell lines were used to begin characterizing other p85 mutant cell lines (unpublished data). In particular, the p85-Δ110 mutant, which no longer bound the p110 catalytic subunit of PI3K due

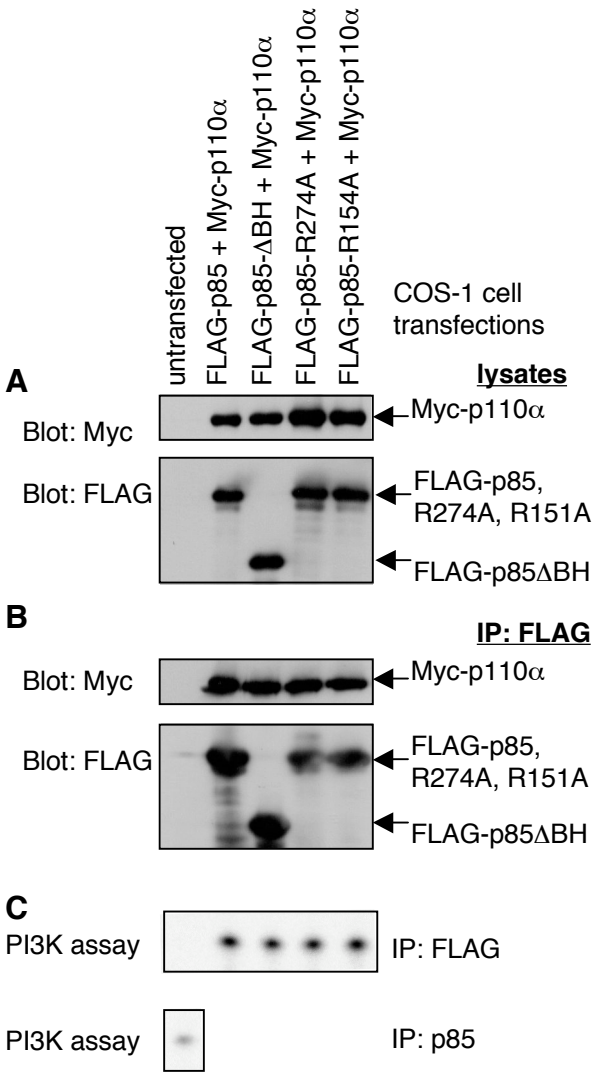

Fig. 1.19. The p85 BH domain mutants retain their ability to bind to p110 and associate with PI3K activity. COS-1 cells were cotransfected with the indicated FLAG-p85 encoding plasmid together with one encoding Myc-p110, or left untransfected as a control. A) lysates (20 µg of total protein) from each were immunoblotted with anti-Myc antibodies, stripped, and reprobed with anti-FLAG antibodies. B) lysates (200 µg of total protein) were immunoprecipitated (IP) with anti-FLAG antibodies and immunoblotted with anti-Myc antibodies, stripped and reprobed with anti-FLAG antibodies. C) anti-FLAG immunoprecipitates were assayed for associated PI3K activity. Radiolabeled PI3K lipid products were resolved by thin layer chromatography and visualized using a phosphorimager. As a positive control, an anti-p85 immunoprecipitate of lysates from untransfected NIH 3T3 cells was also assayed for associated PI3K activity. Reproduced with permission from Chamberlain et al. (2004).

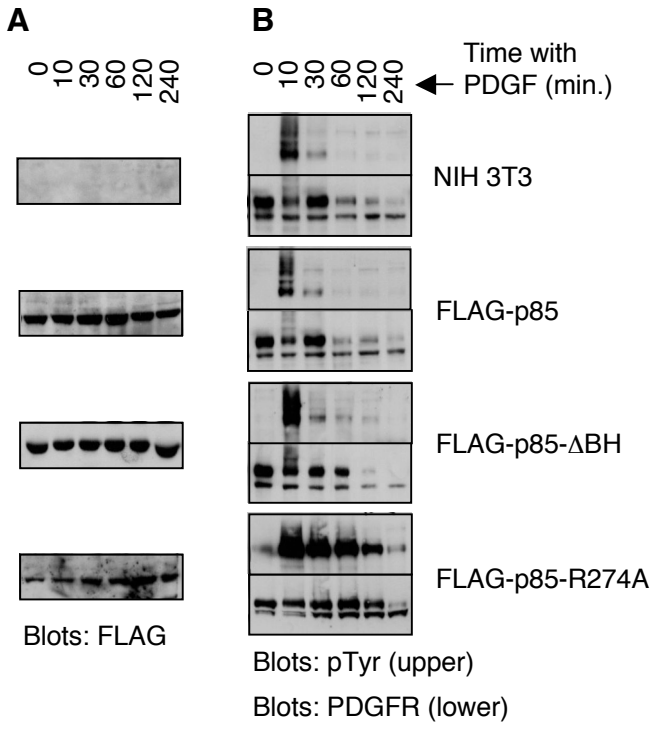

Fig. 1.20. Overexpression of FLAG-p85-R274A slows the down-regulation of the activated PDGFR. Untransfected NIH 3T3 cells, or cells stably expressing wild type FLAG-p85, FLAG-p85-ΔBH, or FLAG-p85-R274A, were stimulated with PDGF BB for the indicated times. Cell lysates (20 μg of protein per lane) were probed in an immunoblot analysis with the indicated antibodies. Results are typical for at least three independent experiments. Reproduced with permission from Chamberlain et al. (2004).

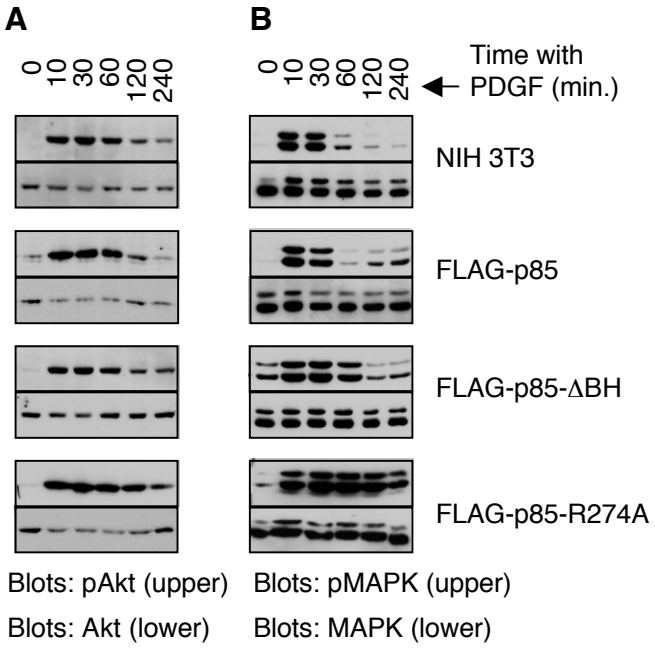

Fig. 1.21. Overexpression of FLAG-p85-R274A activates the MAPK pathway. Untransfected NIH 3T3 cells, or cells stably expressing wild type FLAG-p85, FLAG-p85-ΔBH, or FLAG-p85-R274A, were stimulated with PDGF BB for the indicated times. Cell lysates (20 μg of protein per lane) were probed in an immunoblot analysis with the indicated antibodies. Results are typical for at least three independent experiments. Reproduced with permission from Chamberlain et al. (2004).

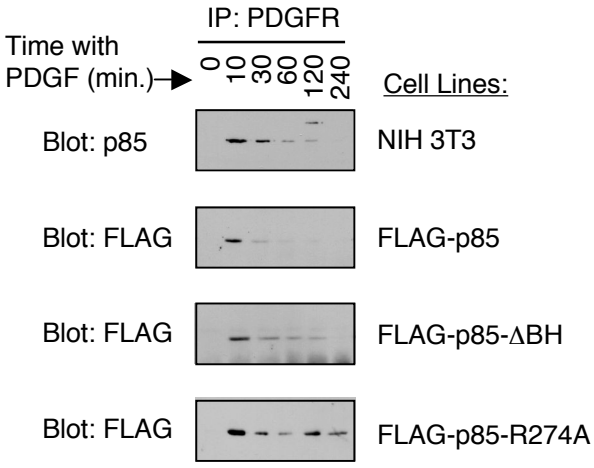

Fig. 1.22. The p85 BH domain mutants retain their ability to bind to activated PDGFRs. NIH 3T3 cells stably expressing the indicated FLAG-p85 proteins were stimulated for various times with PDGF BB. Lysates (200 μg) from each cell line were immunoprecipitated (IP) with anti-PDGFR antibodies and immunoblotted with anti-FLAG antibodies (for cells expressing FLAG-p85, FLAG-p85 BH, and FLAG-p85-R274A), or with anti-p85 antibodies (for untransfected NIH 3T3 cells). Reproduced with permission from Chamberlain et al. (2004).

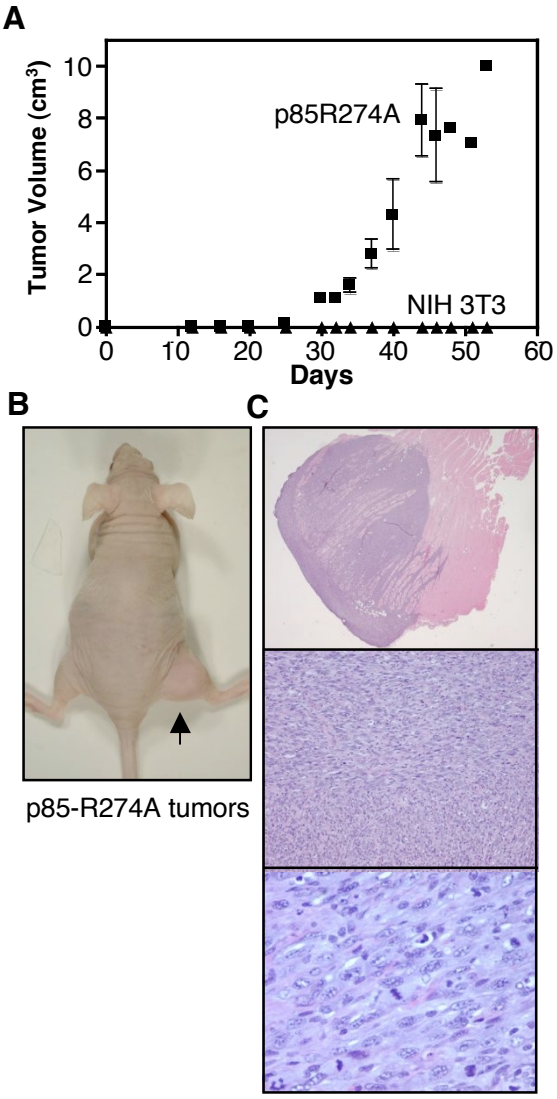

Fig. 1.23. The p85-R274A-expressing cells form tumors in nude mice. NIH 3T3 or p85-R274A cells (2.5 x 10^6) were injected subcutaneously into the right flank of each of four nude mice. A) the average tumor volume was plotted over time for mice injected with p85-R274A-expressing cells (*squares*) or control NIH 3T3 cells (*triangles*). B) a mouse injected with p85-R274A-expressing cells with the tumor indicated by the *arrow* is shown. C) hematoxylin-eosin staining shows the architecture of a typical tumor. The *top panel* shows the tumor infiltrating the muscle (x10 magnification). The *middle panel* shows the fascicles and spindle architecture of the tumor (x100). The *bottom panel* shows a typical high-powered (x400) field of view. Reproduced with permission from Chamberlain et al. (2008).

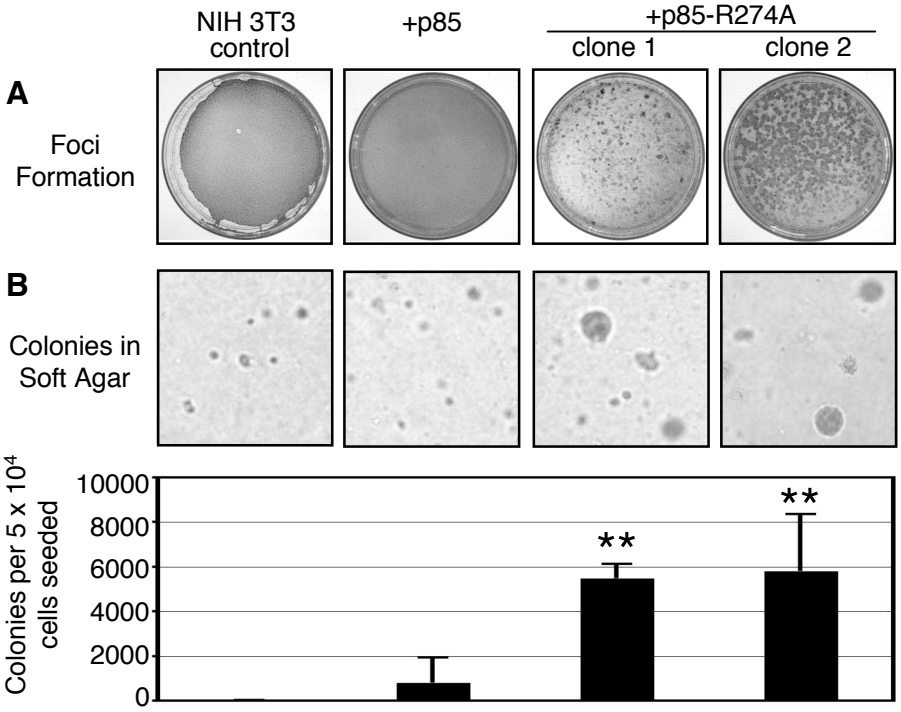

Fig. 1.24. p85-R274A-expressing cells lack contact inhibition and anchorage dependence for growth, indicative of transformed cells. A) the indicated cell lines were plated (2.5 x 10^5 cells/10-cm plate), and after 14 days of growth, the cells were stained with Giemsa and viewed for focus formation. A typical result from one of three independent experiments is shown. B) cells (5 x 10^4) were plated in soft agar and grown for 20 days. A typical field of view is shown. The mean ± S.D. of the number of colonies formed per 5 x 10^4 cells plated from three independent experiments is shown. **, $p < 0.001$ compared with the NIH 3T3 control. Reproduced with permission from Chamberlain et al. (2008).

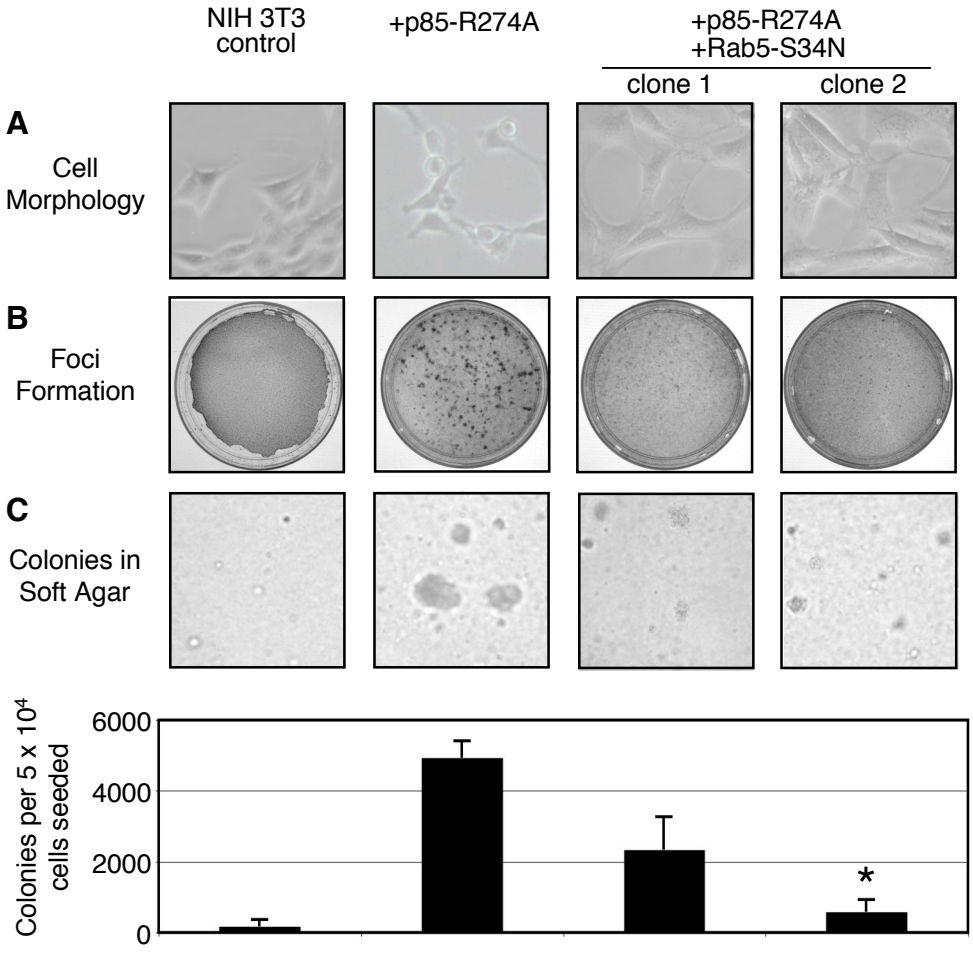

Fig. 1.25. Coexpression of Rab5-S34N reverts the transformed properties of p85-R274A-expressing cells. A) flattened morphology of cells expressing both Rab5-S34N and p85-R274A. B) reduced focus formation upon coexpression of Rab5-S34N with p85-R274A. Experiments were carried out as for Fig. 1.24, and a typical result from one of three independent experiments is shown. C) reduced anchorage-independent growth in soft agar of cells coexpressing Rab5-S34N and p85-R274A. Experiments were as described for Fig. 1.24, where the mean ± S.D. from three independent experiments was determined. *, $p < 0.01$ compared with p85-R274A cells. Reproduced with permission from Chamberlain et al. (2008).

to a well characterized small deletion (aa 478-513) in the p110 binding domain (Klippel *et al*., 1993), was studied. As expected, this mutant did not bind to p110α (Fig. 1.26). Unexpectedly, p85-Δ110 overexpression had little or no effect on PDGFR-associated PI3K activity (Fig. 1.27). The p85-Δ110 protein was also found to spend longer periods of time associated with the activated receptor during time course experiments as compared to control p85 protein, suggesting that it was not released from the receptor (Fig. 1.27). As noted earlier, this was also observed for the p85-R274A protein.

These observations led us to investigate how p85 interacted with Rab5 during endocytosis. The results shown by the mutant p85-R274A, p85-ΔBH and p85-Δ110 proteins influenced a proposed model of interaction between p85 and Rab5 during receptor endocytosis known as the "hand-off" model (Section 1.4.2).

1.4.2 "Hand-off" model to describe the interaction between p85 and Rab5 during PDGFR endocytosis

How p85 may interact with activated receptors, p110β, and Rab5 can be explained using the sequential "hand-off" model (Fig. 1.28). Previous studies have shown Rab5-GTP associates with p110β but not p110α and that the p110β protein is known to specifically bind to Rab5-GTP and not to Rab5-GDP (Christoforidis *et al*., 1999b). These same studies showed that p85 was able to interact and bind to Rab5 only when associated with p110β (Christoforidis *et al*., 1999b). As stated previously, it is now known p85 can interact with Rab5 directly (Chamberlain *et al*., 2004). This model suggests p85 assists in Rab5 relocalization to the endosomal membrane, early in receptor endocytosis, perhaps acting as a GDF. Prior to growth factor stimulation, inactive Rab5-GDP bound to a GDI protein is localized to the cytosol. Upon growth factor stimulation, Rab5-GDP is relocalized to the endosomal membrane. Since p85 can bind directly to Rab5-GDP and is known to remain bound to the tyrosine phosphorylated PDGFR during endocytosis, this interaction may assist in Rab5 relocalization and ensure that Rab5 is targeted to the correct endosomal compartment (Kapeller *et al*., 1993).

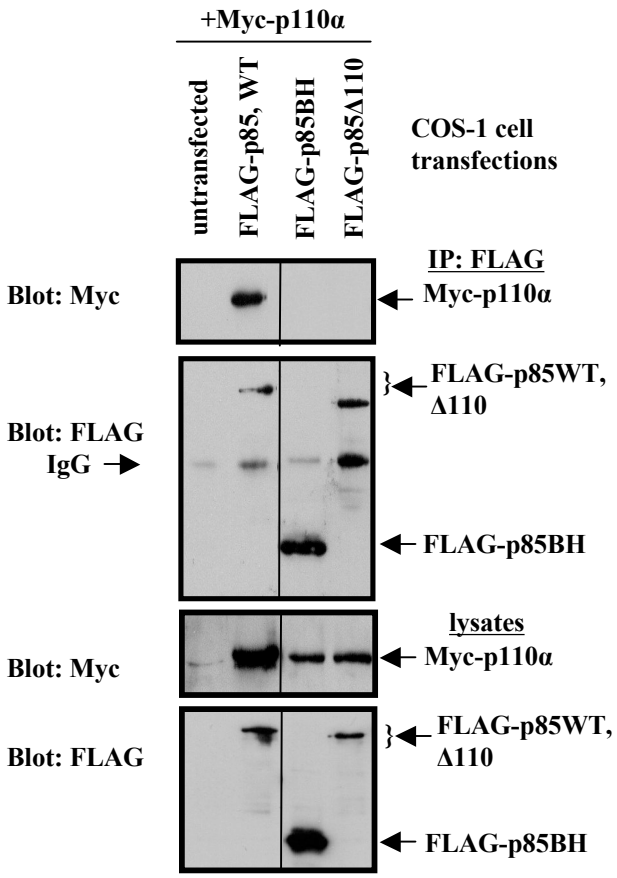

Fig. 1.26. Mutant FLAG-p85 proteins behave as expected with regard to their ability to bind to the catalytic subunit of PI3 kinase, p110. COS-1 cells were cotransfected with each of the FLAG-p85 plasmids together with a plasmid encoding N-terminal triple Myc (EQKLISEEDL)-tagged p110. Three days after transfection, cells were lysed and immunoprecipitated with anti-FLAG antibodies and tested for associated Myc-p110 protein with a Myc immunoblot (upper) and a control FLAG immunoblot (lower). The p85-BH results are not important for this thesis. (Experiments performed by John Hanson and Dean Chamberlain)

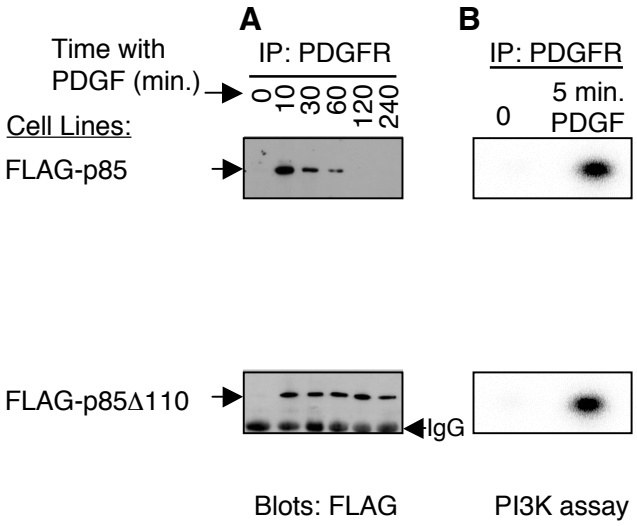

Fig. 1.27. The p85-Δ110 protein binds to the activated PDGFR for longer periods of time as compared to p85-wt but does not interfere with PDGFR-associated PI3 kinase activity. NIH 3T3 cells were stimulated with PDGF. A) Anti-PDGFR immunoprecipitations followed by anti-FLAG immunoblots were tested for PDGFR associations. B) Anti-PDGFR immunoprecipitations were tested for PI3 kinase activity. (Experiments performed by John Hanson and Dean Chamberlain)

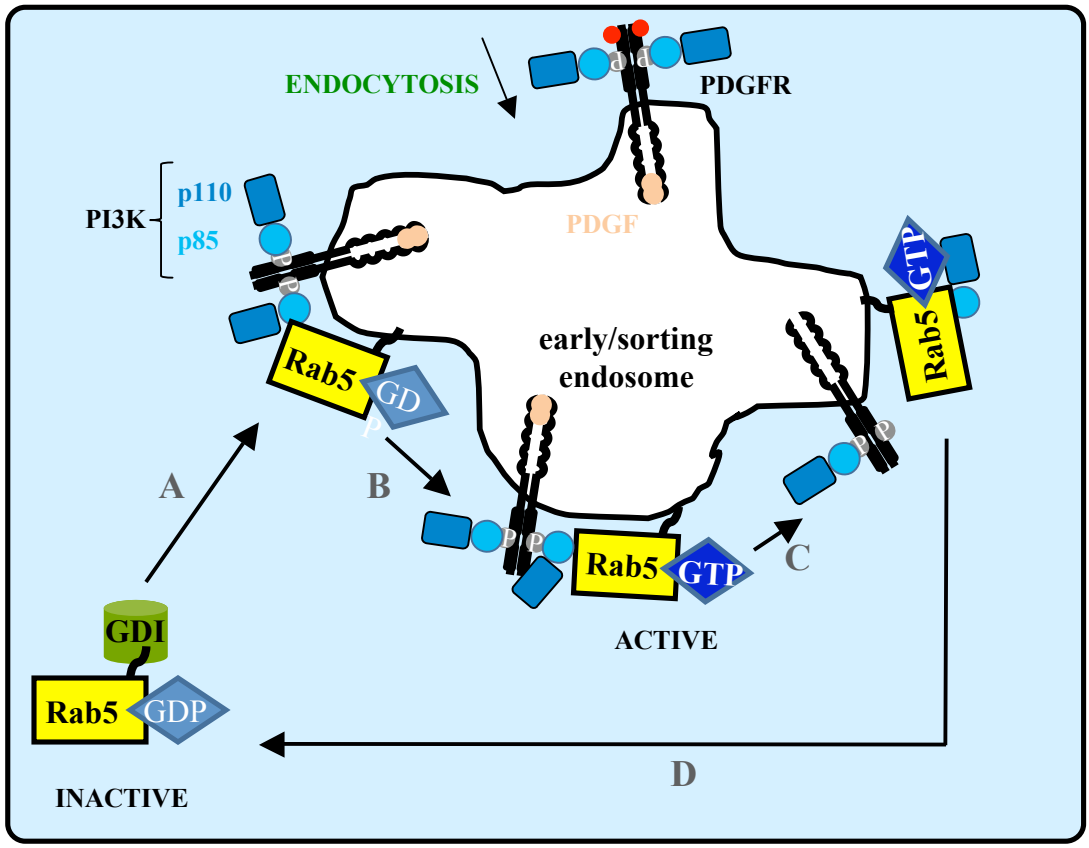

Fig. 1.28. Sequential "hand-off" model to describe p85 interactions with activated receptors, p110β, and Rab5. A) Prior to growth factor stimulation, inactive Rab5-GDP bound to a GDI protein is localized to the cytosol. Upon growth factor stimulation, Rab5-GDP is relocalized to the endosomal membrane. Since p85 can bind directly to Rab5-GDP and is known to remain bound to the tyrosine phosphorylated PDGFR during endocytosis, this interaction may assist in Rab5 relocalization and ensure that Rab5 is targeted to the correct endosomal compartment by acting as a GDF. B) Rab5 exchanges its GDP for GTP through the action of a GEF. Rab-GTP is the active conformation important for vesicle fusion events in receptor trafficking. C) The p85 protein directly binds Rab5-GTP and p110β. The p110β protein is known to specifically bind to Rab5-GTP and not to Rab5-GDP (Christoforidis *et al.*, 1999). We hypothesize that both p85 and p110β bind Rab5-GTP and the formation of this trimeric complex allows the release of p85 from the receptor with a corresponding increase in p85 RabGAP activity. D) The GAP activity of p85 could then stimulate the hydrolysis of GTP to GDP by Rab5 whereby Rab5-GDP would leave the membrane and bind GDI to return to the cytosol.

Thus, PDGFR-associated p85 may act as a GDF. Rab5 exchanges its GDP for GTP through the action of a GEF. Rab-GTP is the active conformation important for vesicle tethering events resulting in receptor trafficking. The p85 protein directly binds Rab5-GTP and p110β. We hypothesize that both p85 and p110β bind Rab5-GTP and the formation of this trimeric complex allows the release of p85 from the receptor with a corresponding increase in p85 Rab GAP activity. The GAP activity of p85 could then stimulate the hydrolysis of GTP to GDP by Rab5 whereby Rab5-GDP would leave the membrane and bind GDI to return to the cytosol.

The results shown by the mutant p85-ΔBH, p85-R274A, and p85-Δ110 proteins influenced the proposed model. The p85-wt protein can bind to Rab5 in both GDP and GTP conformations. We hypothesize that the ability of the p85 protein to bind to Rab5-GDP may help to localize the Rab5 protein to membranes containing activated receptors undergoing endocytosis. The p85-ΔBH only binds Rab5-GTP; therefore cells expressing this mutant will lose p85-dependent Rab5 membrane localization possibly resulting in this targeting process being less efficient. After nucleotide exchange the p85-ΔBH can bind to Rab5-GTP and p110 resulting in release from the receptor. The p85-ΔBH cannot, however, effectively accelerate Rab5 GTPase activity since its BH domain is missing, thus Rab5 remains on the membrane in its active GTP-bound form promoting vesicle fusion events. On the other hand, p85-R274A binds only Rab5-GDP and would still be able to help localize Rab5 to those specific membranes. The p85-R274A mutant would not be able to bind to Rab5-GTP after Rab5 nucleotide exchange or stimulate GTP hydrolysis. The p85-R274A mutant would not be able to form the trimeric complex between p110β and Rab5 and would not be released from the receptor. The p85-R274A mutant would remain bound to the PDGFR. Rab5-GTP would stay associated with the membrane for longer periods of time, as compared to the p85-ΔBH expressing cells, promoting vesicle fusion events. The p85-Δ110:Rab5 binding specificities and GAP activity are unknown. However, this mutant cannot bind p110 and remains associated with the activated PDGFR during time-course experiments. As defined by our model, cells expressing this mutant would have the same phenotype as those expressing p85-R274A. The p85-Δ110 still contains its BH domain suggesting it would possess GAP activity, as this activity is independent of PI3K activity. However, without the ability of p85-Δ110 to bind p110, the p85, p110β, and Rab5 would not be released from the PDGFR and the GTPase

activity would not be fully increased. The p85-Δ110 would remain bound to the PDGFR. This would again suggest Rab5 would remain associated with the membrane in its active state promoting vesicle fusion. As p85 was found to have GAP activity towards both Rab5 and Rab4, the model would suggest an increase in membrane fusion events for both the endocytic and recycling pathways. The net effect would be decreased receptor degradation due to fewer opportunities for the receptor to be targeted to the degradative pathway.

2.0 RATIONALE AND OBJECTIVES

2.1 Rationale

The main focus of our laboratory is to better understand the function of the Class IA PI3K, p85:p110. Our studies focus on understanding how the subunits of PI3K, mainly the p85 subunit, interact with effector molecules and how these interactions influence cell signalling. Previously our lab has studied the interactions between the p85 subunit with A-Raf (Fang *et al*., 2002; King *et al*., 2000; Mahon *et al*., 2005) and Ankyrin 3 (Ignatiuk *et al*., 2006). Currently our lab has begun to characterize the interactions between p85 and Rab5 (Chamberlain *et al*., 2004; Chamberlain *et al*., 2008). The realization that p85 could be involved in other activities beside p110 regulation led the way to investigate the functions of different domains of p85 by creating several p85 mutants and stably expressing them in NIH 3T3 cells. Cells were then studied to determine the effects the p85 mutants had on PDGFR signalling and the cellular consequences brought about due to these effects (Section 1.4.1) The characterizations of the mutant p85-R274A, p85-ΔBH and p85-Δ110 proteins influenced a proposed model of the interaction between p85 and Rab5 during PDGFR endocytosis known as the "hand-off" model (Section 1.4.2).

2.2 Objectives

The main goal of this project was to characterize the interactions between the p85 protein with activated PDGFR and Rab5. The experimental objectives were as follows:

1. To determine the p85 domains involved in binding Rab5-GDP and Rab5-GTP.
2. To determine the mechanism(s) of defective PDGFR degradation in cells expressing the p85-R274A mutant.

3.0 MATERIALS AND METHODS

3.1 Materials

3.1.1 Reagents and Supplies

All of the chemicals and enzymes used were of analytical grade or higher and were purchased from VWR, BDH or Sigma unless otherwise stated. Glutathione Sepharose beads (Amersham Pharmacia Biotech), Protein G Agarose (Sigma), and Protein A Sepharose beads (Sigma) were prepared according to the manufacturer's instructions and were stored at 4°C, stable for several months. Glutathione Sepharose beads were used for the purification of GST fusion proteins and pull-down experiments, while Protein G Agarose and Protein A Sepharose beads were used for immunoprecipitation (IP) experiments. Premade TrueBlot anti-Rabbit Ig IP beads (eBioscience) were used according to the manufacturer's instructions for IP experiments and stored at 4°C.

Several primary antibodies were used for the immunoprecipitation, immunofluorscence and immunoblotting experiments. The antibodies were obtained from a variety of different sources and are described in Table 3.1. Anti-PDGFR 958 (Santa Cruz Biotechnology, sc-432) and anti-rabbit IgG agarose conjugate (Santa Cruz Biotechnology, sc-2345) were used in the immunoprecipitation experiments. Anti-Rab5 (Abcam, #ab50523), anti-Rab4 (BD Transduction Laboratories, #610888), anti-phosphoPDGFR (pY857) (Santa Cruz Biotechnology, sc-12907-R) and secondary antibodies Alexa 488 (green) and Alexa 594 (red) (Molecular Probes) were used in the immunofluorescence experiments. The following primary antibodies were used for immunoblotting: anti-ubiquitin P4D1 (Santa Cruz Biotechnology, sc-8017), anti-pTyr (pY20) (Santa Cruz Biotechnology, sc-508), anti-PDGFRβ 2B3 (New England Biolaboratory, 3175), anti-phosphoPDGFR (pY1021) (Santa Cruz Biotechnology, sc-12909-R), anti-Cbl 7G10 (Millipore, 05-440), anti-FLAG M2 (Sigma, F3165), anti-p85-N-SH3 (Upstate Biotechnology Institute, 05-217), affinity purified anti-p85-BH (specific for amino acids: 78-332, (Chamberlain *et al*., 2004)) and affinity purified anti-p85-(N+C)SH2 (specific for amino acids: 312-722, Fang *et al*., 2002; (King *et al*., 2000). The secondary antibodies used were horseradish peroxidase-coupled anti-mouse IgG (Santa Cruz Biotechnology, sc-

Table 3.1. Primary antibodies used for immunoprecipitation (IP), Western Blot (WB), and immunofluorescence (IF)

Antibody Specificity	Company, Catalog #	Species	Concentration used	Application	Figure
Anti-PDGFR (958)	Santa Cruz Biotechnology, sc-432	rabbit	5 µg/mL 1 µg/mL 0.5 µg/mL	IP WB IF	4.8, 4.9 4.10 4.11, 4.12
Anti-PDGFR (2B3)	New England Biolabs, 3175	mouse	1 µg/mL	WB	4.8
Anti-Rab5	Abcam, #ab50523	mouse	1 µg/mL	IF	4.11, 4.13
Anti-Rab4	BD Transduction Laboratories, #610888	mouse	3 µg/mL	IF	4.12, 4.14
Anti-phospho PDGFR (pY857)	Santa Cruz Biotechnology, sc-12907-R	rabbit	0.5 µg/mL	IF	4.13, 4.14
Anti-phospho PDGFR (pY1021)	Santa Cruz Biotechnology, sc-12909-R	rabbit	1 µg/mL	WB	4.8
Anti-pTyr (pY20)	Santa Cruz Biotechnology, sc-508	mouse	1 µg/mL	WB	4.8
Anti-ubiquitin (P4D1)	Santa Cruz Biotechnology, sc-8017	mouse	1 µg/mL	WB	4.8
Anti-Cbl (7G10)	Millipore, 05-440	mouse	1 µg/mL	WB	4.8, 4.9
Anti-FLAG (M2)	Sigma, F3165	mouse	5 µg/mL	WB	4.8
Anti-p85 (N-SH3)	Upstate Biotechnology Institute, 05-217	mouse	2 µg/mL	WB	4.2, 4.4, 4.8
Anti-p85 (BH)	Anderson, affinity purified (to amino acids: 78-332)	rabbit	1 µg/mL	WB	4.2, 4.4, 4.5,4.7
Anti-p85 ((N+C)SH2)	Anderson, affinity purified (to amino acids: 312-722)	rabbit	1 µg/mL	WB	4.2, 4.4

2005) and horseradish peroxidase-coupled anti-rabbit IgG (Santa Cruz Biotechnology, sc-2004).

3.1.2 Plasmids and Vectors

The pGEX6P1 vector (Amersham Pharmacia Biotech) is designed for isopropyl β-D-thiogalactopyranoside (IPTG)-induced protein production in bacteria. High levels of glutathione S-transferase (GST) fusion proteins are produced after transformation with this vector. This vector contains an ampicillin resistance gene and encodes a PreScission protease cleavage site (LEVLFQ*GP, the asterisk indicates the cleavage site). The protease cleavage site, situated between GST and the fusion protein, is important to allow removal of the GST portion during protein purification. The pGEX6P1 vector was used to express the bovine p85-wild type (wt, aa 1-724) and p85 mutant proteins: p85-R274A (aa 1-724), p85-SH3 (aa 1-83), p85-SH3-Pro-BH-Pro (aa 1-332), p85-Pro-BH-Pro (aa 77-322), p85-Pro-BH (aa 79-301), p85-BH-Pro (aa 110-332), p85-BH (aa 110-301), p85-(N+C)SH2 (aa 314-724), p85-N-SH2 (aa 314-446), p85-C-SH2 (aa 614-724), p85-p110B (p110 binding domain, aa 431-623), p85-ΔBH (aa 1-83, 314-724), p85-ΔSH3 (aa 78-724), p85-Δ110 (aa 1-477, 514-724). Plasmids containing the dog Rab5 mutant sequences (Rab5-Q79L and Rab5-S34N, aa 2-215) were generously provided by Dr. M. Zerial from the Max Planck Institute of Molecular Cell Biology and Genetics, Dresden, Germany.

The pFLAG3 vector was a modification of the HA3 vector and was described previously (Chamberlain *et al*., 2004). This vector is designed to make fusion proteins containing three copies of the FLAG epitope (DYKDDDDK) fused to the N-terminus of the protein. This vector is a mammalian expression plasmid and contains both ampicillin and Geneticin resistance genes. The pFLAG3 vector was used to express the bovine p85 wild type and p85 mutant proteins in eukaryotic stable cell lines.

3.1.3 Bacterial Strains

The pGEX6P1 plasmids were expressed in both *Escherichia coli* (*E. coli*) BL21 cells

[F^- *ompT hsdS*$_B$ ($r_B^- m_B^-$) *gal dcm*] (Novagen) and *E. coli* TOP10 cells [*F*$^-$ *mcrA (mrr*$^-$*hsdRMS*$^-$ *mcrBC) 80lacZM15 lacX74 recA1 ara139 (ara-leu)7697 galU galK rpsL (StrR) endA1 nupG*] (Invitrogen). The pGEX6P1 plasmids were expressed in the *E. coli* BL21 cells for protein purification experiments as these cells are protease deficient, thereby decreasing protein degradation. The pGEX6P1 plasmids were expressed in the *E. coli* TOP10 cells for the production of plasmid DNA. Both *E. coli* strains were grown in Luria-Bertani Broth (LB, Sigma) containing 1%(w/v) bacto-tryptone, 0.5%(w/v) bacto-yeast extract and 1%(w/v) sodium chloride (NaCl) pH 7.0, per litre and 100 μg/mL ampicillin (LBA, Sigma).

3.1.4 Mammalian Cell lines

NIH 3T3 mouse fibroblast cells were obtained from American Type Culture Collection. NIH 3T3 cells were maintained in Dulbecco's Modified Eagle Medium (DMEM, Gibco) supplemented with 10% fetal bovine serum (FBS, Hyclone) 100 units/ml penicillin G and 100 μg/ml streptomycin (P/S, Gibco) and grown at 37°C with 5% CO_2. NIH 3T3 cells stably transfected with pFLAG3 plasmids containing p85-wt and p85-R274A cDNA (Chamberlain *et al*., 2004; King *et al.,* 2000) were grown in selection media (DMEM + 10% FBS + P/S) containing 400 μg/mL Geneticin (G418, Gibco).

3.2 Methods

3.2.1 Protein Analysis

3.2.1.1 Sodium dodecyl sulphate (SDS)-polyacrylamide gel electrophoresis (PAGE)

For protein visualization by either Coomassie blue staining or Western blot analysis, proteins were resolved by SDS-PAGE using the Mini-Protean II apparatus (Bio-Rad) (Laemmli, 1970). SDS-PAGE consists of two parts for each gel; resolving and stacking. The resolving gel contained between 7.5%-15% acrylamide solution (29.2:0.8 acrylamide: bisacrylamide, 37 mM Tris-HCl pH 8.8 and 0.1% (w/v) SDS) was poured and polymerized first by the addition of 0.06% (w/v) ammonium persulfate (APS, Sigma) and 0.1% (v/v) N,N,N',N'-

Tetra-methylethylenediamine (TEMED, Bio-Rad). Water-saturated butan-1-ol (100 µl, Bio-Rad)) was added to the top of the resolving gel to keep air away from the gel during polymerization. After polymerization (45 min), the butan-1-ol was removed and replaced with a two mL stacking gel containing 4.5% acrylamide solution, 125 mM Tris-HCl pH 6.8 and 0.1% (w/v) SDS. The stacking gel was also polymerized by the addition of APS and TEMED, but was let to sit for only eight min instead of 45 min. A 15-well teflon comb was inserted into the stacking gel to form wells. After the completed gel was cast, the gel was assembled into the electrophoresis apparatus. The protein samples were prepared in SDS sample buffer (62.5 mM Tris-HCl pH 6.8, 5% (v/v) β-mercaptoethanol, 2.3% (w/v) SDS, 0.1% (w/v) bromophenol blue, 10% (v/v) glycerol) and were heated for five min at 100°C. Prestained molecular weight markers (Fermentas, #SM0671, 170, 130, 100,70, 55, 40, 35, 25, 15, 10 kDa) or unstained molecular weight markers (Fermentas, #SM0661, 200, 150, 120, 100, 85, 70, 60, 50, 40, 30, 25, 20, 15, 10, kDa) and the protein samples were loaded onto the gel and resolved by electrophoresis at a constant voltage of 180 V in running buffer (25 mM Tris, 250 mM glycine and 0.1% (w/v) SDS) until the bromophenol blue dye was off the bottom of the gel (Laemmli, 1970). To visualize the proteins within the gel, the gel was stained with Coomassie blue stain (0.14% (w/v) Coomassie blue R-250, 41.4% (v/v) methanol and 5.4% (v/v) acetic acid) for 30 min at room temperature (RT) with shaking and destained (41.4% (v/v) methanol and 5.4% (v/v) acetic acid) until the protein bands were visible. A picture of the gel was taken using a Gel Doc 2000 (Bio Rad).

3.2.1.2 Western blot analysis

Following electrophoresis (section 3.2.1.1) the SDS-PAGE gel was incubated for 15 min in transfer buffer (48 mM Tris pH 9.2, 39 mM glycine, 0.0375% (w/v) SDS, 20% (v/v) methanol). During the incubation, six pieces of 3MM filter paper (Whatman) were soaked in transfer buffer and one piece of nitrocellulose membrane (Scheicher and Schuell) was soaked in distilled water. A Panter semi-dry Electroblotter Owl Separation System (VWR) was used at a constant current of 400 mA (15 min/gel being transferred) to transfer the proteins from the gel to the nitrocellulose membrane. Following the transfer, the nitrocellulose membrane was

blocked for one hour at RT or overnight at 4°C in blocking solution (5% Carnation skim milk powder in TBST (100 mM Tris-HCl pH 8, 150 mM NaCl, 0.05% polyoxyethylenesorbitan monolaurate (Tween-20))). After blocking, the membrane was probed with primary antibody in blocking solution overnight at 4°C at the concentrations listed in Table 3.1. The membrane was then washed three times in TBST for eight min each and incubated with a secondary antibody conjugated to horseradish peroxidise (1:2000) for either one hour at RT (or overnight at 4°C) and washed three times in TBST for five min each. The nitrocellulose membrane was incubated for one min in Western Lighting enhanced chemiluminescence reagent (Perkin Elmer) and in a dark room exposed to X-Omat Blue XB-1 film (Kodak). Exposures ranged from one sec to 30 min. The film was developed using a Kodak M35A X-Omat processor.

To reprobe the membrane with different primary antibodies, the membrane was incubated in stripping buffer (62.5 mM Tris-HCl pH 6.8, 2% (w/v) SDS, 100 mM β-mercaptoethanol) for 30 min at 60°C. The membrane was washed three times in TBST for five min and incubated in blocking solution. The nitrocellulose membrane was reprobed as described above.

3.2.1.3 Induction and purification of GST fusion proteins

E. coli BL21 cells transformed with the pGEX6P1 vector encoding the protein of interest was inoculated into LBA (100 mL) and allowed to grow overnight at 37°C with shaking (300 rpm). The entire overnight culture was added to one litre of LBA and allowed to grow at 37°C with shaking (300 rpm) until an OD_{600} value of 0.5-0.7 was reached. To induce the expression of the GST fusion protein, IPTG (Sigma) was added to a final concentration of 0.1 mM and the one litre culture was allowed to grow for four hours at 37°C with shaking (300 rpm). The cells were pelleted by centrifugation at 6000 x g for 15 min at 4°C. The one litre culture pellets were either lysed immediately or frozen at -20°C until use.

3.2.1.3.1 GST-p85 fusion protein purification

For cell lysis, culture pellets were weighed and resuspended in PreScission buffer (150

mM NaCl, 1 mM ethylenediaminetetraacetic acid (EDTA), 1 mM dithiothreitol (DTT), 50 mM Tris-HCl, pH 7.0) (8 mL/1.6 g cells). Lysozyme (IGN Biochemicals) was added to a final concentration of 1 mg/mL and cells were lysed on ice for 45 min. Cells were sonicated three times 30 sec on a setting of 3.0 using a microtip and a Model 250/450 Sonifier (Branson Ultrasonics) with two min of chilling on ice between each treatment. Triton X-100 (Sigma) was added to a final concentration of 1% (v/v) to decrease bacterial protein interactions. Cell lysates were centrifuged at 22 000 x g for 30 min at 4°C to remove insoluble material and unbroken cells. The supernatant was filtered using a 0.45 µM cellulose acetate membrane (Nalgene) to remove particulates and was incubated with one mL of glutathione Sepharose beads (50% slurry) (Amersham Pharmacia Biotech) for one hour at RT with agitation. GST fusion proteins bound to beads were pelleted by centrifugation at 675 x g for 5 min at 4°C. Beads were washed six times, each time in 30 mL PreScission buffer and transferred to a 1.5 mL microcentrifuge tube in a total volume of one mL (50% slurry).

For protein purification, the GST tag was cleaved from the GST-p85 wild type and GST-p85 mutant fusion proteins using PreScission protease (Amersham Pharmacia Biotech; 40-160 µL/1 litre culture, determined empirically) 16-64 hr at 4°C with nutating. The cleaved protein fraction was recovered from the supernatant the next day by centrifugation of the beads at 2000 x g for five min at 4°C. The beads were washed six times with one mL PreScission buffer to recover any of the cleaved protein trapped in the beads, until an absorbance of <0.1 at OD_{280} was reached in the washes. Individual aliquots of the cleaved fraction (5 µL each), of each wash containing cleaved protein (5 µL each) and beads before and after cleavage (5 µL each), were resolved by SDS-PAGE (7.5%-15%) and visualized by Coomassie Blue staining to determine protein yield and cleavage efficiency. The cleaved protein fractions and washes containing the desired protein were pooled into an Amicon Ultra Centrifugal Filter (molecular weight cut off 5-30 kDa, Millipore), the buffer was replaced with a protein storage buffer (20 mM Tris-HCl pH 8.0, 100 mM NaCl, 1 mM DTT and 1 mM EDTA) and the sample volume was reduced to 800 µL. Glycerol (to 20% v/v) was added to the protein to decrease protein shearing during freezing.

To decrease non-specific binding to GST and glutathione Sepharose beads during pull-

down experiments, concentrated p85 proteins were precleared by incubation with 500 µg GST bound to glutathione Sepharose beads + 100 µL glutathione Sepharose beads (50% slurry) overnight at 4°C. GST immobilized on beads and any non-specific binding proteins were removed from the p85 preparations by centrifugation at 12 000 x g for 10 min at 4°C. The supernatant containing the purified p85 wild type and p85 mutants were precleared three times each. The protein concentrations were determined by Lowry assay (Sigma) according to the manufacturer's instructions. Protein aliquots were flash frozen in liquid nitrogen prior to storage at -80°C for future use in pull-down experiments.

3.2.1.3.2 Preparation of GST-Rab5 fusion proteins bound to glutathione Sepharose beads for pull-down experiments

For the preparation of GST alone (control) and GST-Rab5 mutants bound to beads, 50 mL culture pellets were obtained by resuspending the one litre culture pellet prior to any freezing (Section 3.2.1.3) in 10 mL of phosphate buffered saline (PBS, 137 mM NaCl, 2.7 mM KCl, 4.3 mM Na_2HPO_4, 1.4 mM KH_2PO_4, pH 7.3) + protease inhibitors (1 mM 4-(2-Aminoethyl) Benzenesulfonyl Fluoride Hydrochloride, 10 µg/mL aprotinin and 10 µg/mL leupeptin) and then dividing the suspension into 500 µL aliquots in 1.5 mL microcentrifuge tubes. The cells were pelleted by centrifugation at 12 000 x g for two min at 4°C and the supernants were discarded. Samples were either lysed immediately or frozen at -20°C until use. For cell lysis, culture pellets (i.e. 50 mL culture worth) were resuspended in one mL PBS + protease inhibitors and sonicated (section 3.2.1.1.1) three times 10 sec on a setting of 1.5. Cell lysates were centrifuged at 12 000 x g for 10 min at 4°C to remove insoluble material and unbroken cells. The supernatant was incubated with 200 µL of glutathione Sepharose beads (50% slurry) (Amersham Pharmacia Biotech) and agitated for one hour at RT. GST fusion proteins bound to beads were pelleted by centrifugation at 2000 x g for two min at 4°C. Beads were washed three times each in one mL PBS and made up to a final volume of 500 µL suspensions. The beads were diluted 1/10 in a new microcentrifuge tube and 2-10 µL of protein suspensions were resolved by SDS-PAGE (12 %) and visualized using Coomassie Blue staining to determine protein purity and concentration. The protein concentration was

estimated by comparison with bovine serum albumin (BSA) standards (0.5-8.0 μg) resolved along side the protein of interest. All protein-bead suspensions were stored at 4°C and were stable for up to three weeks. Protein stability was checked weekly by resolving the proteins on an SDS-PAGE gel and staining the proteins using Coomassie Blue staining to check for degradation.

3.2.1.4 Pull-down experiments

The p85 wild type and p85 mutant proteins were further precleared with GST bound to glutathione Sepharose beads (200 μg GST immobilized on glutathione Sepharose beads) and 50 μL glutathione Sepharose beads (50% slurry) for two hours at 4°C. During p85 wild type and p85 mutant protein preclearing**,** GST (10 μg), GST-Rab5-Q79L (10 μg), and GST-Rab5-S34N (10 μg) bound to glutathione Sepharose beads were added to separate microcentrifuge tubes. An extra 30 μL of glutathione Sepharose beads (50% slurry) were added to each tube to increase the bead pellet for easy visualization. The beads were washed with 500 μL of dilution buffer (20 mM Tris-HCl pH 7.5, 1 mM DTT, 5 mM $MgCl_2$, 20% (v/v) glycerol). The beads were collected by centrifugation at 2000 x g for two min at 4°C and the supernatant was removed. The beads were incubated with 500 μL Buffer A (20 mM Tris-HCl pH 7.5, 1 mM DTT, 10 mM EDTA, 5% (v/v) glycerol, 0.1% (v/v) Triton X-100, 10 μg/ml leupeptin, 10 μg/ml aprotinin) for 20 min at RT to strip off any nucleotide bound to the GST-Rab5 proteins. The beads were collected as described above and the supernatants removed. The beads were incubated in 400 μL of Buffer B/C (20 mM Tris-HCl pH 7.5, 1 mM DTT, 10 mM $MgCl_2$, 5% (v/v) glycerol, 0.1% (v/v) Triton X-100, 0.1% (v/v) Tween-20, 10 μg/mL leupeptin, 10 μg/mL aprotinin) + the nucleotide indicated below for 30 min at RT:

1. GST (negative control) had no nucleotide added.
2. GST-Rab5-Q79L was incubated with 200 μM guanosine 5` triphosphate (GTP, Sigma).
3. GST-Rab5-S34N was incubated with 200 μM guanosine 5` diphosphate (GDP, Sigma).

The beads were collected as described above and the supernatant removed. The beads were

blocked in 500 µL blocking solution (5% Carnation skim milk powder in Buffer B/C + nucleotide as described above) for 30 min at 4°C. After 20 min of this blocking step, the precleared p85 wild type and p85 mutant proteins were centrifuged at 12 000 x g for 10 min at 4°C to separate the protein in the supernatant from the preclearing beads (discarded). For the protein binding reaction, either p85 wild type (1 µg) or p85 mutants (1-10 µg) were added directly to the blocking beads and allowed to bind for one hour at 4°C. The beads were collected as described above and washed three times each with one mL IP-Wash buffer (50 mM Tris-HCl pH 7.5, 150 mM NaCl, and 1% (v/v) onidet P40 (NP-40, USB). Washes ranged from 10 sec to five min with or without nutating. The beads were collected as described above, supernatant removed and SDS sample buffer (15 µL) was added. The samples were frozen at -20°C until use or immediately resolved by SDS-PAGE (Section 3.2.1.1) followed by Western blot analysis (Section 3.2.1.2).

3.2.2 Molecular Biology

3.2.2.1 Polymerase chain reaction (PCR)

Primers (Invitrogen) were designed to amplify the cDNA corresponding to the BH domain of the p85 subunit of PI3K. A unique restriction enzyme site was incorporated at both the 3` and 5` ends for easy subcloning. There were four primers designed to amplify the regions encoding the BH domain plus the N-terminal proline rich region (p85-Pro-BH), the C-terminal proline rich region (p85-BH-Pro) or to exclude both regions (p85-BH). These are described in Table 3.2. For the PCR reaction, 0.5 mL microcentrifuge tubes were used. The reaction was carried out in a total volume of 100 µL. The following were added to the PCR reaction (final concentrations): 1x Pfu buffer (Fermentas), 5% (v/v) dimethyl sulfoxide, 0.02 mM dNTPs (each), 10 ng template pGEX6P1-p85 wild type DNA, 0.1 µM 5` primer, 0.1 µM 3` primer and 2.5 units Pfu enzyme (Fermentas). The PCR reaction was initially set at 95°C for 4 min. This was followed by 40 cycles of 95°C for 30 sec (to denature double stranded template DNA and primers), 56°C for 30 sec (to anneal the primers to the template DNA), and 72°C for one min (to extend the DNA). A final 72°C step (for seven min for further DNA extensions) was included. Aliquots of the PCR product (10 µL), 1 kb DNA ladder (Fermentas,

Table 3.2. Primers used to amplify the p85-BH domain with and without the Pro-rich regions

p85 domain	Amino Acids Encoded	5 ` primer	3 ` primer
p85-Pro-BH	79-301	5´-ACC ACA AAG GAT CCG GAA GGA AAA AGA TCT CGC CTC CCA-3´	5´-CCA GAA TTC GCG TTC ATT CCA TTC GG-3´
p85-BH-Pro	110-332	5´-GCA GGA TCC CAA CAA GCT TCC ACT CTC-3´	5´-CAT CAC GGG AAT TCA TTC AGC ATC TTG TAA AGA CAT ATT-3´
p85-BH	126-298	5´-GCA GGA TCC CAA CAA GCT TCC ACT CTC-3´	5´-CCA GAA TTC GCG TTC ATT CCA TTC GG-3´

— BamHI Site

— EcoRI Site

#SM0313, 10000, 8000, 6000, 5000, 4000, 3000, 2500, 2000, 1500, 1000, 750, 500, 250) and 100 bp DNA ladder (Fermentas, #SM0243, 1031, 900, 800, 700, 600, 500, 400, 300, 200, 100, 80) were resolved on a 1% agarose gel (0.4 g agarose in 1x Tris Acetic Acid EDTA (TAE, 40 mM Tris acetate and 2 mM Na_2EDTA) and 1 µg/mL ethidium bromide) at a constant current of 100 V for 25 min to check for the presence and size of the PCR product. The remaining PCR product was visualized using a Gel Doc 2000 (Bio Rad). The PCR product was purified using a QIAquick PCR Purification kit (Qiagen) following the manufacturer's instructions.

3.2.2.2 Digestions and ligations

The inserts encoding the p85-Pro-BH, p85-BH-Pro, and p85-BH amplified by PCR had a unique restriction enzyme site incorporated at each end during amplification: BamHI at the 5` end and EcoRI at the 3` end. The p85-Pro-BH, p85-BH-Pro, and p85-BH encoding DNA were inserted into the multiple cloning site of the pGEX6P1 vector using the BamHI and EcoRI restriction sites. The pGEX6P1 was chosen as it would produce GST fusion proteins for easy purification later on. The p85-Pro-BH, p85-BH-Pro, p85-BH encoding PCR inserts, and pGEX6P1 vector DNA were digested separately in a total volume of 40 µL. The following was added to the digestion reaction (final concentrations): 1x Phorall buffer (Amersham Pharmacia Biotech), 2 µg of the individual PCR product or pGEX6P1 vector DNA, 20 units BamHI (New England Biolabs), and 20 units EcoRI (New England Biolabs). The reactions were incubated at 37ºC for one hour. The digested products were purified using a QIAquick PCR Purification kit (Qiagen) following the manufacturer's instructions but eluted in a smaller volume of 25 µL. An aliquot of the newly digested cDNA (2 µL) was resolved on a 1% agarose gel and visualized as described (Section 3.2.2.1).

The p85-Pro-BH, p85-BH-Pro, p85-BH encoding cDNA concentrations were compared to the restricted pGEX6P1 vector DNA to perform the ligation reaction. For the ligation reaction 6x molar excesses insert DNA was added to the vector DNA (~200 ng) with 10 µL of 2x Quick ligation buffer (New England BioLabs) in a total volume of 20 µL. To start the reaction, one µL of Quick T4 DNA Ligase (New England BioLabs) was added and allowed to

sit for 20 min at RT.

To express the clonal product, 10 µL of the ligation mix was added to competent *E. coli* TOP10 (200 µL) cells (Hanahan, 1983) and incubated on ice for 10 min. The plasmid DNA was transformed into the *E. coli* TOP10 cells by heat shocking the cells at 42ºC for two min followed by five minute incubation on ice. LB (800 µL) was then added to the cells and they were incubated at 37ºC for 30 min to allow expression of the plasmid. The cells successfully expressing the plasmid DNA were selected for by plating the cells onto an LBA agar plate (LBA + 0.02% agar (w/v), Sigma). The cells grew overnight at 37ºC.

To confirm the pGEX6P1 vector contained the proper insert, *E. coli* TOP10 colonies were inoculated into five mL LBA and grown overnight at 37ºC. Plasmid DNA was isolated from overnight cultures using a QIAprep Spin Miniprep Kit (Qiagen) as per the manufacturer's instructions. The plasmid DNA (2 µL of 50 µL preparation) was digested with BamHI (10 units) and EcoRI (10 units) as described above, and the digests were resolved on a 1% agarose gel and visualized as described (Section 3.2.2.1). Plasmids containing inserts were sequenced to ensure there were no mutations in the insert introduced during the PCR reaction. The DNA was sent to the National Research Council of Canada Plant Biotechnology Unit for sequencing.

The plasmid DNA that contained both the vector and insert of the proper size was transformed into *E. coli* BL21 for future induction (Section 3.2.1.3) and purification of GST fusion proteins (Section 3.2.1.3.1).

3.2.3 Cell Culture Techniques

3.2.3.1 Growth factor stimulations

NIH 3T3 cells and NIH 3T3 cells stably expressing FLAG-p85 wild type and FLAG-p85-R274A were grown to 70% confluency on 10 cm plates. The cells were starved in starving media (DMEM + 0.5% FBS + P/S) for 24 hours at 37°C. After 24 hours, two mL of starving media were removed from each plate of cells and PDGF was added to a final concentration of 50 ng/mL. The remainder of the starving media was removed from each plate of cells and

replaced with the two ml of starving media + PDGF. Cells were stimulated for 0, 5, 10, 20, 30, or 60 min at 37°C. After stimulation, the cells were placed on ice, washed with five mL ice cold PBS and each plate was lysed in one mL of PLC lysis buffer (50 mM Hepes pH 7.5, 150 mM NaCl, 10% (v/v) glycerol, 1% (v/v) Triton X-100, 1.5 mM $MgCl_2$, 1 mM ethyleneglycol-bis (B-aminoethylether) N,N,N,N, tetraacetic acid (EGTA), 10 mM sodium pyrophosphate (NaPPi), and 100 mM NaF) + protease inhibitors + 1 mM sodium orthovanadate (Na_3VO_4, Sigma). The lysed cells were scraped and transferred to a 1.5 mL microcentrifuge tube. The cell debris and unbroken cells were removed by centrifugation at 12 000 x g for 10 min at 4°C. The supernatant containing soluble protein was transferred to a new microcentrifuge tube and frozen at -80°C.

3.2.3.2 PDGFR immunoprecipitations

After cell stimulations (Section 3.2.3.1), the PDGFR was immunoprecipitated from the cell lysates. The protein concentration from the cell lysates was determined by Lowry assay (Sigma) according to the manufacturer's instructions. The cell lysates (500 µg) were transferred to new microcentrifuge tubes. The lysates were precleared, to decrease any non-specific binding, with anti-rabbit IgG agarose conjugate (5 µg, Santa Cruz Biotechnology, sc-2345) and either 30 µL of Protein A Sepharose beads (Sigma), 30 µL of Protein G Agarose beads (Sigma) or 50 µL of TrueBlot beads (eBioscience) for 30 min at 4°C. The beads and non-specifically associating proteins were removed by centrifugation at 12 000 x g for 10 min at 4°C. The supernatant was incubated with anti-PDGFR 958 (5 µg, Santa Cruz Biotechnology, sc-432) and either 30 µL of Protein A Sepharose beads (Sigma), 30 µL of Protein G Agarose beads (Sigma) or 50 µL of TrueBlot beads (eBioscience) for 1.5 hours at 4°C. The beads were centrifuged at 2000 x g for two min at 4°C and washed three times each in one mL HNTG (20 mM HEPES, pH 7.5, 150 mM NaCl, 0.1% (v/v) triton X-100, 10% (v/v) glycerol, + 1 mM Na_3VO_4 (Sigma) and centrifuged as described above. The supernatant was discarded and SDS sample buffer (15 µL) was added to the beads. The samples were frozen at -20°C until use or immediately resolved by SDS-PAGE (7.5%) (Section 3.2.1.1) for Western blot analysis (Section 3.2.1.2).

3.2.3.3 Biotin assay

NIH 3T3 cells and NIH 3T3 cells stably expressing FLAG-p85 wild type and FLAG-p85-R274A were grown to 70% confluency on 10 cm plates. The cells were starved in starving media (DMEM + 0.5% FBS + P/S) for 24 hours at 37°C. After 24 hours, two ml of starving media were removed from each plate of cells and PDGF was added to 50 ng/mL. This media was left at 37°C until use. Controls included:

1. MOCK - not treated with biotin, unstimulated and kept at 4°C during the entire experiment to assess how much receptor is non-specifically recovered by the streptavidin IP in the absence of any biotin labelling.
2. 4°C – treated with biotin and stimulated as long as the longest time point of the experiment, however kept at 4°C (on ice) during the experiment to prevent endocytosis and to assess how much endocytosis is occurring at 4°C (on ice).
3. 0 min stimulation – treated with biotin and not stimulated, therefore kept on ice for the entire experiment to assess how efficiently the biotin label is removed from the cell surface.

The cells were washed once with five mL 4°C PBS^{++} (PBS + 1 mM $MgCl_2$ and 2.5 mM $CaCl_2$). Cells were incubated with 1.5 mg/mL EZ-LinkTM Sulfo-NHS-SS-Biotin (biotin, PIERCE, #21335) in PBS^{++} for 20 min at 4°C (1.5 mL/10 cm plate). Cells were washed three times with five mL cold 50 mM glycine in PBS^{++} to quench unlinked biotin. Cells were stimulated with the PDGF in starving media (removed earlier) for 0, 10, 20, 30, 40, or 60 min as described (Section 3.2.3.1) at 37°C. The cells were placed on ice and washed three times with five mL cold PBS^{++} followed by three washes with five mL ice cold glutathione cleavage buffer (50 mM L-glutathione reduced (Sigma), 75 mM NaCl, 10 mM EDTA, 1% fatty acid free BSA (w/v), and 0.075 N NaOH) to cleave surface biotin. Cells were washed three times with five mL ice cold 5 mg/mL Iodoacetamide in PBS^{++} to quench the reaction. Cells were washed once with five mL PBS^{++} and lysed as described (Section 3.2.3.1). Biotinylated proteins (150 µg as determined by lowry) were immunoprecipiated as described (Section 3.2.3.2) with 50 µL UltraLink Immobilized Strepavidin (PIERCE) beads overnight at 4°C. The beads were washed three times each in five mL HNTG discarding the supernatant. SDS sample buffer (20 µL) was added to the beads. The samples were frozen at -20°C until use or immediately resolved by

SDS-PAGE (7.5%, note 1.5 mm thick) (Section 3.2.1.1) followed by Western blot analysis (Section 3.2.1.2).

3.2.3.4 Immunofluorescence and confocal microscopy

NIH 3T3 cells and NIH 3T3 cells expressing FLAG-p85 wild type and FLAG-p85-R274A were seeded onto a four-well chamber slide (VWR, CA62405-176) (1.0 x 10^4 cells/well). The next day the cells were incubated in one mL starving media overnight and were about ~60% confluent. The cells were stimulated with PDGF as described previously (50 ng/mL, 300 µL/well) for 0, 10, 30 or 120 min at 37°C. The media was removed from each well and the cells were washed twice with one mL PBS + 1 mM sodium azide (NaN_3, BDH). The cells were fixed with 500 µL 14% paraformaldehyde in PBS for 30 min at RT. The paraformaldehyde was removed and the cells were washed three times with one mL PBS + NaN_3. The cells were incubated undisturbed with 500 µL 0.05% saponin (Sigma) in PBS+NaN_3+ 1% BSA for 30 min at RT to permeabilize the cells. The cells were washed three times in one mL PBS+NaN_3+BSA. The cells were incubated with primary antibody (anti-PDGFR 958 (0.5 µg/mL, Santa Cruz Biotechnology, sc-432), anti-Rab5 (1 µg/mL, Abcam, #ab50523), anti-Rab4 (3 µg/mL, BD Transduction Laboratories, #610888), anti-phosphoPDGFR (pY857) (0.5 µg/mL, Santa Cruz Biotechnology, sc-12907-R)) as indicated in each figure overnight at 4°C. When probing with more than one primary antibody at a time, it was important that each was raised in a different species (mouse or rabbit) for accurate binding of the fluorescently tagged secondary antibody. The next day, the cells were washed three times with one mL PBS+NaN_3+BSA. On the last wash, the cells were incubated in one mL PBS+NaN_3+BSA for 10-20 min nutating slowly at RT. The Alexa 488 (green) or Alexa 594 (red) (5 µg/mL, Molecular Probes) secondary antibodies were added to each well and allowed to incubate at RT in the dark. When probing with more than one secondary antibody at a time, it was important that each secondary antibody recognized different species (mouse or rabbit) and that each secondary antibody was represented by a different fluorophore (red or green) for accurate identification later on. The cells were washed in the dark as described after the primary antibody. Once the washing was complete, the chamber portion of the chamber slide

was removed to isolate the slide. The slide was dried completely in the dark and a single large cover slip (VWR, #48393241) was mounted onto the slide using ProLong Gold antifade reagent/mounting medium (Invitrogen). The slides were stored in the dark at either 4°C for short term storage or -20°C for longer storage.

Immunofluorescence images were generated using an Olympus F300 confocal microscope (Dr. Mousseau, Dept. Of Psychiatry, University of Saskatchewan) using an UPLanSApo 100x oil immersion objective with a numerical aperture of 1.40. Images were selected based on representative cells showing high fluorescence intensity to insure there was no bleed through from the red channel to the green channel when two antibodies were used. The fluorescence intensity (PMT setting) was adjusted to decrease or increase the red or green fluorescence to make them similar to each other. To decrease background, the Gain and Offset settings were also adjusted. After the primary settings were identified, cells were analyzed by fast Z-sectioning (XYZ) taking image slices through the cell at different depths. Once the middle of the cell was identified, cells were analyzed by slow Z-sectioning (XY) and Kalman analysis. Several scans at the same depth were taken and the intensities for each were averaged to generate one image. The picture was saved and the process was repeated for all other cells in the experiment using the exact same settings.

4.0 RESULTS

4.1 Interaction of p85 with Rab5

The p85 wild type protein can bind to Rab5 directly (Chamberlain *et al*., 2004). It has been shown that p85 wild type can bind to both the inactive Rab5-GDP conformation and the active Rab5-GTP conformation, while some p85 mutants show a strong preference for only Rab5-GDP or Rab5-GTP (Chamberlain *et al*., 2004). To characterize the function of the p85:Rab5 interaction in cells, the aim of this work was to generate a p85 mutant unable to bind Rab5 by focusing on which domains of p85 were needed for Rab5 binding.

4.1.1 Purification of wild type and p85 mutant proteins

The p85 regulatory subunit is made up of five domains. To determine which domains of p85 were required for Rab5 binding, mutant p85 proteins were made which contained one or more domains of p85 in different combinations (p85-wt, p85-R274A, p85-SH3, p85-SH3+Pro-BH-Pro, p85-Pro-BH-Pro, p85-ΔBH, p85-Δ110, p85-N-SH2, p85-C-SH2, p85-(N+C)SH2, p85-p110B, p85-ΔSH3) (Fig. 4.1). Purified proteins were needed to assay the direct interaction between p85 and Rab5. GST-p85 proteins were bacterially expressed, bound to glutathione Sepharose beads, and the p85 portion was cleaved from the GST using a PreScission protease. Isolated p85 proteins were concentrated using Amicon Ultra filters. The p85 preparations were precleared by incubation with GST (500 μg) bound to glutathione Sepharose beads overnight at 4ºC. Proteins were precleared three times to decrease non-specific interactions between the p85 preparations and the GST and/or glutathione Sepharose beads. Protein concentrations were determined and the p85 proteins were resolved using SDS-PAGE. The p85 proteins were visualized by Coomassie Blue staining as well as Western Blot analysis (Fig. 4.2). The proteins obtained were approximately 90-100% pure. The smaller bands present in lanes 1, 2, 9, 13, 14, and 15 are likely degradation products of the p85 proteins possibly due to freezing and thawing the proteins for storage, since they react with the anti-p85 antibodies (Fig. 4.2B).

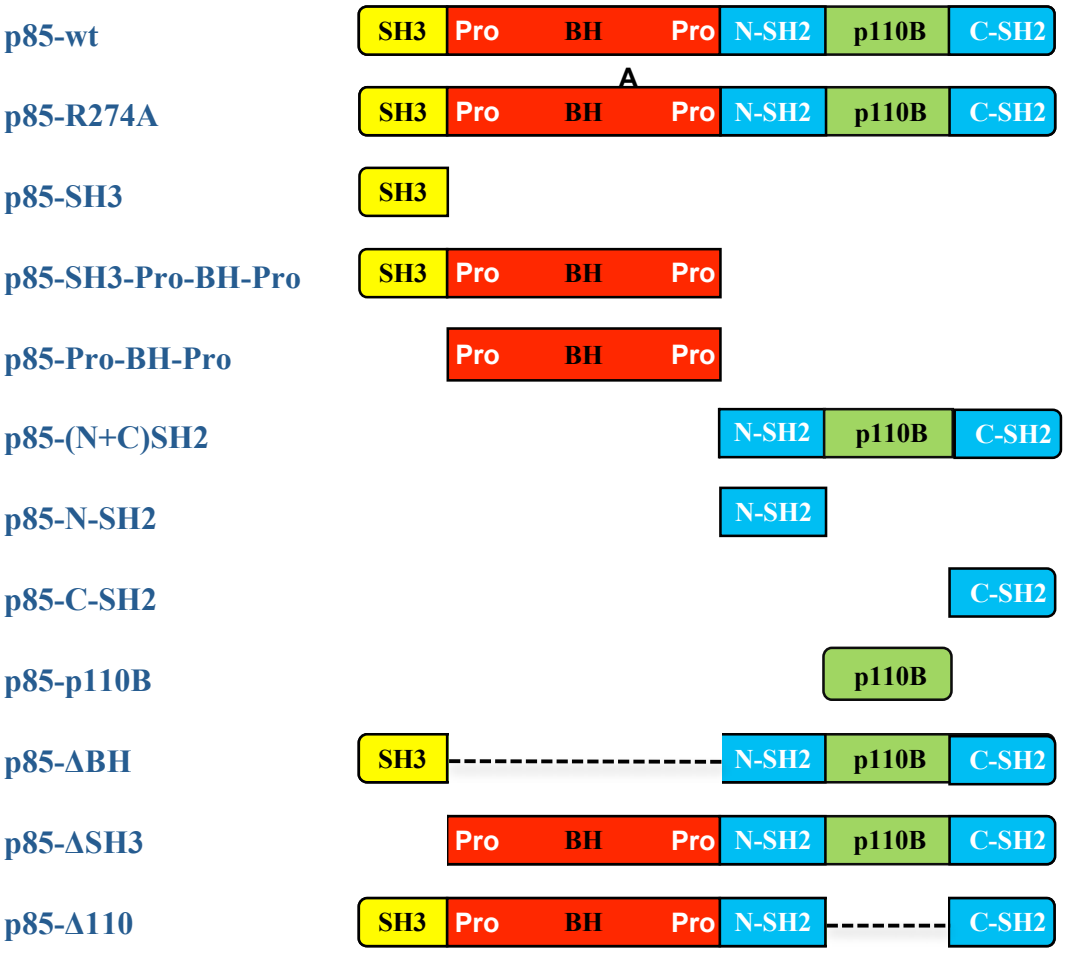

Fig. 4.1. Domain stucture of p85-wt and p85 mutants. The p85 mutants were overexpressed in bacterial systems as glutathione S-transferase (GST) fusion proteins. GST-p85 fusion proteins were isolated by binding to glutathione Sepharose beads. The p85 proteins were cleaved from the GST rendering purified proteins.

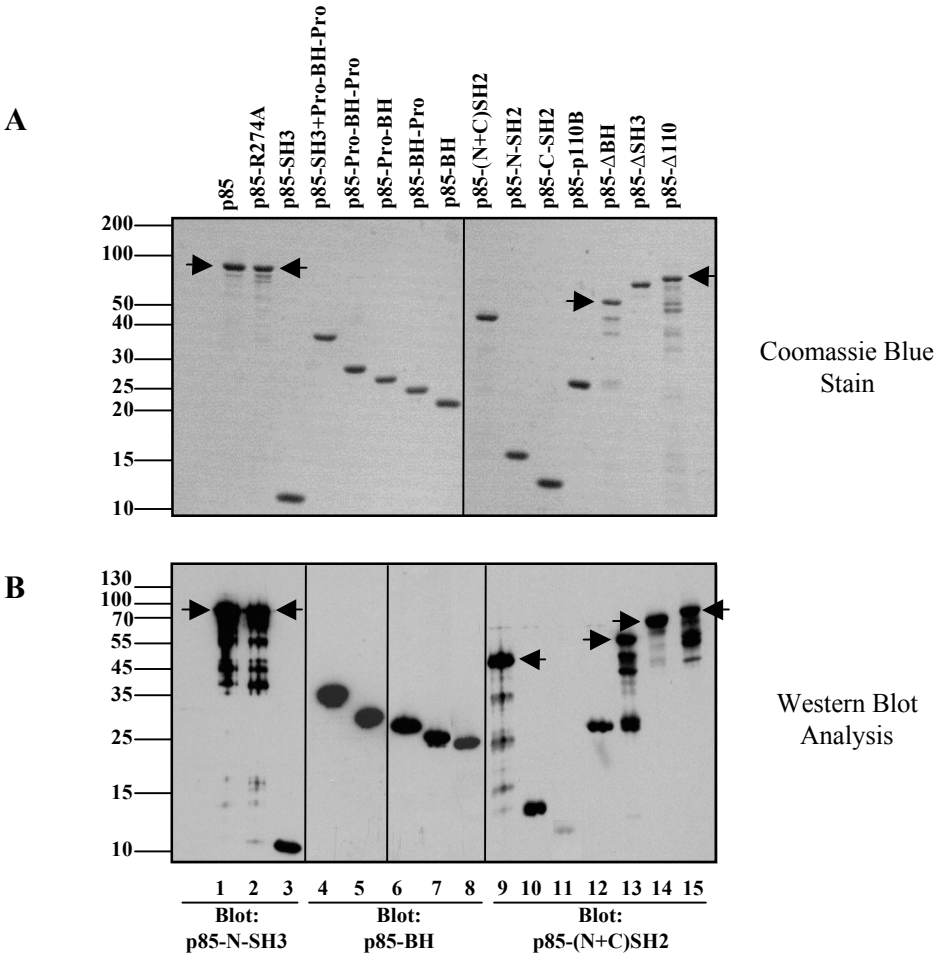

Fig. 4.2. Purified p85 protein domains. Bacterially expressed GST-p85 fusion proteins were induced for 4 hrs at 37ºC with 0.1 mM of IPTG. Proteins were bound to glutathione Sepharose beads and removed from GST using PreScission cleavage. Isolated p85 proteins were concentrated using 5000-30000 MWCO Amicon Ultra filters. Protein concentrations were determined and 1 µg of each protein was resolved using SDS-PAGE. The proteins were visualized by A) Coomassie Blue stain with unstained kDa molecular weight markers (Fermentas, #SM0661) and B) Western Blot analysis with prestained kDa molecular weight markers (Fermentas, #SM0671). The p85 proteins were transferred to nitrocellulose, blocked and probed with anti-p85-N-SH3, anti-p85-BH, and anti-p85-(N+C)SH2 antibodies. Bound antibodies were detected using IgG-linked to horseradish peroxidase and visualized using chemilluminescence. Where multiple bands were observed, an arrow indicates the size of the full-length protein.

4.1.2 GST-Rab5 pull-down experiments using different p85 domains

The ability of different domains of p85 to bind to Rab5, as well as their preference for the inactive Rab5-GDP or active Rab5-GTP conformations was tested. Two Rab5 mutants were used which preferentially bound either GTP or GDP (Liu and Li, 1998). GST-Rab5-S34N bound GDP and GST-Rab5-Q79L bound GTP. Mutant GST-Rab5-S34N and GST-Rab5-Q79L were bacterially expressed as GST fusion proteins and were immobilized on glutathione Sepharose beads along with a GST negative control for the GST pull-down experiments (Fig. 4.3). Each immobilized GST-Rab5 mutant was loaded with its respective nucleotide. GST, GST-Rab5-S34N and GST-Rab5-Q79L were incubated with purified p85 proteins in a solution containing 5% milk blocking reagent. The beads were then washed and samples were resolved using SDS-PAGE. Control samples consisting of GST and Rab5 bound to glutathione Sepharose beads without incubation with p85 proteins were also resolved by SDS-PAGE. Control samples were loaded to ensure there was no cross reactivity between the anti-p85 antibodies with the GST-Rab5 proteins and/or non-specific binding of p85 to GST and/or the glutathione Sepharose beads. A Western Blot analysis was performed using p85 protein specific antibodies (Fig. 4.4).

Initially there were twelve p85 proteins (Fig. 4.1) tested for Rab5 binding. Of these twelve p85 mutants: four did not bind either Rab5 mutant (N-SH2, C-SH2, p110B and SH3), two bound significantly better to Rab5-GDP (R274A and Δ110), two bound better to Rab5-GTP (ΔBH and Pro-BH-Pro) and two bound to both Rab5 mutants (p85-wt and (N+C)SH2) though the p85-(N+C)SH2 was not as convincing (Fig. 4.4). The remaining two p85 mutants (SH3-Pro-BH-Pro and ΔSH3) proved difficult to test due to non-specific binding interactions with the GST control sample (Fig. 4.5). Samples p85-wt, p85-R274A, and p85-ΔBH were tested previously and are shown in Fig. 1.18 (Chamberlain *et al*., 2004). As each protein behaved differently, optimizing the experiments to decrease non-specific interactions was a large problem. Numerous combinations and concentrations of salt and detergents (20 mM Tris-HCl pH 7.5, 1 mM DTT, 5 or 10 mM $MgCl_2$, 10 mM EDTA, 50-150 mM NaCl, 0.1%-1% Triton-X 100, and 0.1%-1% Tween 20) within the buffers were altered. Numerous washing conditions (10 sec-5 x 5 min washes in IP wash buffer (50 mM Tris-HCl pH 7.5, 150-500 mM

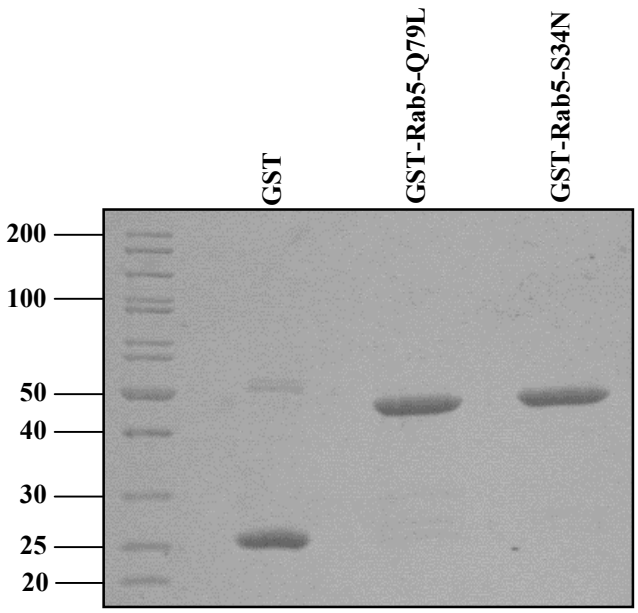

Fig. 4.3. GST and GST-Rab5 fusion proteins bound to glutathione Sepharose beads. Bacterially expressed GST-Rab5 fusion proteins were induced for 4 hrs at 37ºC with 0.1 mM of IPTG. Proteins were bound to glutathione Sepharose beads and 5 µg of each was resolved using SDS-PAGE. The proteins were visualized by Coomassie Blue stain.

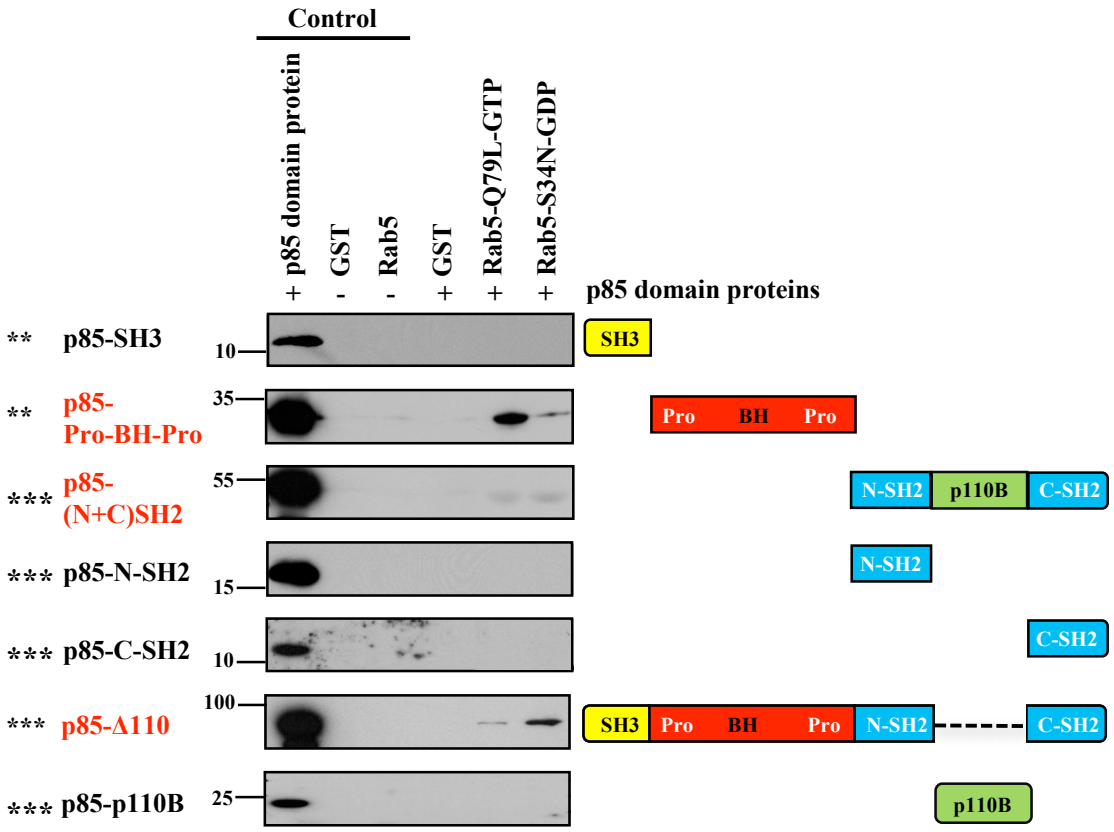

Fig. 4.4. GST-Rab5 pull-down experiments using different p85 domains. GST, GST-Rab5-S34N and GST-Rab5-Q79L (10 µg) were loaded with their respective nucleotide, and were incubated with 5 µg of purified p85 proteins in a 500 µl solution containing 5% milk blocking reagent. Samples recovered with the beads were resolved using SDS-PAGE. Western Blot analysis was performed using p85 protein specific antibodies (*** anti-p85-(N+C)SH2, * anti-p85-N-SH3, and ** anti-p85-BH). Samples p85, p85-ΔBH and p85-R274A were supplied by Chamberlain *et. al.*, 2004 and are shown in Fig. 1.18. Red lettering represents p85 domains which have bound Rab5 mutants. Results are representative of three independent experiments.

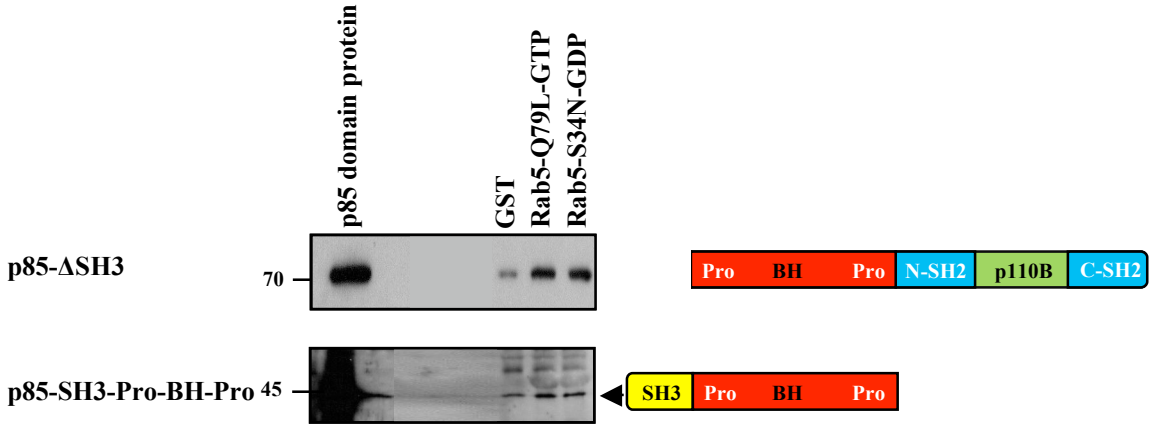

Fig. 4.5. p85 mutants bind non-specifically with the GST negative control in pull-down experiments. GST, GST-Rab5-S34N and GST-Rab5-Q79L (10 µg) were loaded with their respective nucleotide, and were incubated with 5 µg of purified p85 proteins in a 500 µl solution containing 5% milk blocking reagent. Samples were resolved using SDS-PAGE and Western Blot analysis was performed using the p85 protein specific antibody anti-p85-BH. Where multiple bands were observed, an arrow indicates the size of the correct protein. Results are representative of three independent experiments.

NaCl and 1% NP-40)) and countless protein preclearing steps with 100-500 µg GST immobilized on glutathione Sepharose beads overnight at 4°C were performed to try to decrease non-specific binding. The difficulties were not resolved using these strategies.

The results of the successful binding experiments indicated that there were at least two domains of p85 involved in binding to Rab5: one within the p85-Pro-BH-Pro region and one outside of this region, that has not been localized further (Fig. 4.4). The p85-Pro-BH-Pro protein fragment that bound to Rab5 contained the BH domain and two flanking proline-rich regions. To further characterize this interaction, three new protein fragments missing either the N-terminal, C-terminal flanking proline-rich regions, or both (BH-Pro, Pro-BH, and BH respectively) (Fig. 4.6) were generated. Each of these proteins was tested to determine whether or not the proline rich regions were important for Rab5 binding. The regions encoding each of these p85 proteins were amplified by PCR and the DNA was inserted into a pGEX6P1 vector at BamHI and EcoRI sites. After sequencing the DNA to confirm the integrity of these new clones, proteins were bacterially expressed as GST-p85 fusion proteins and cleaved from GST as before. Pull-down experiments were carried out as before. The p85-BH domain containing no proline rich regions bound to Rab5 in its GTP bound state though less well, suggesting that these proline rich regions were not absolutely required for Rab5 binding (Fig. 4.7A). Both p85-Pro-BH and p85-BH-Pro bound non-specifically to the GST control sample and binding specificities could not be resolved (Fig. 4.7B). The p85-ΔBH protein, missing the entire Pro-BH-Pro domain, still bound to Rab5-GTP suggesting additional domain(s) of p85 also contribute to Rab5 binding (Fig. 1.18).

The other important domain contributing to Rab5 binding may be the p85-SH3 domain although when used as an isolated domain it did not bind to Rab5 in either active or inactive conformation (Fig. 4.4). Domains comprising the C-terminal portion of the protein (p85-N-SH2, p85-C-SH2 and p85-p110B) showed no significant binding to Rab5 either (Fig. 4.4). Although there may be minimal binding to Rab5 by the p85-(N+C)SH2 domain, the bands were shifted on the SDS-PAGE gel suggesting they were of the wrong molecular weight to correspond to the p85 protein. It is possible that the bands seen were background GST-Rab5 protein cross-reactivity but the control lane where only the GST-Rab5 bound to beads in the

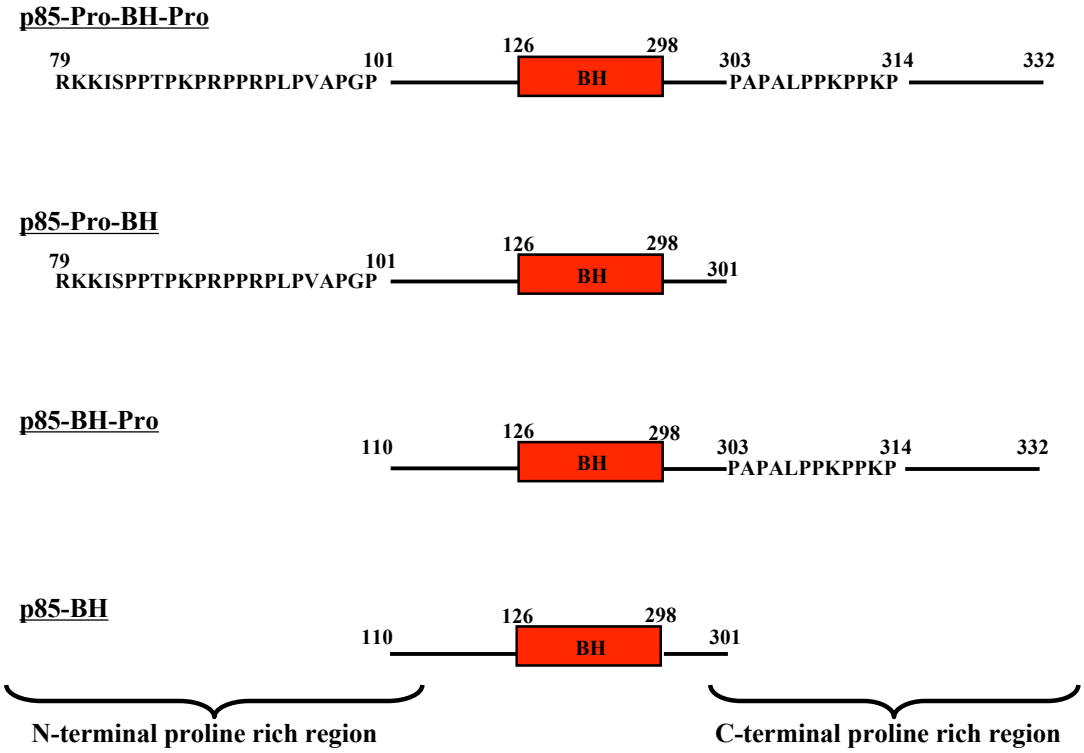

Fig. 4.6. Domain structure of different p85-BH proteins generated. The p85-Pro-BH, p85-BH-Pro, and p85-BH encoding DNA were amplified by PCR and were inserted into the multiple cloning site of the pGEX6P1 vector using the restriction sites BamHI and EcoRI. Proteins were bacterially expressed, isolated by binding to glutathione sepharose beads and cleaved from GST as described previously.

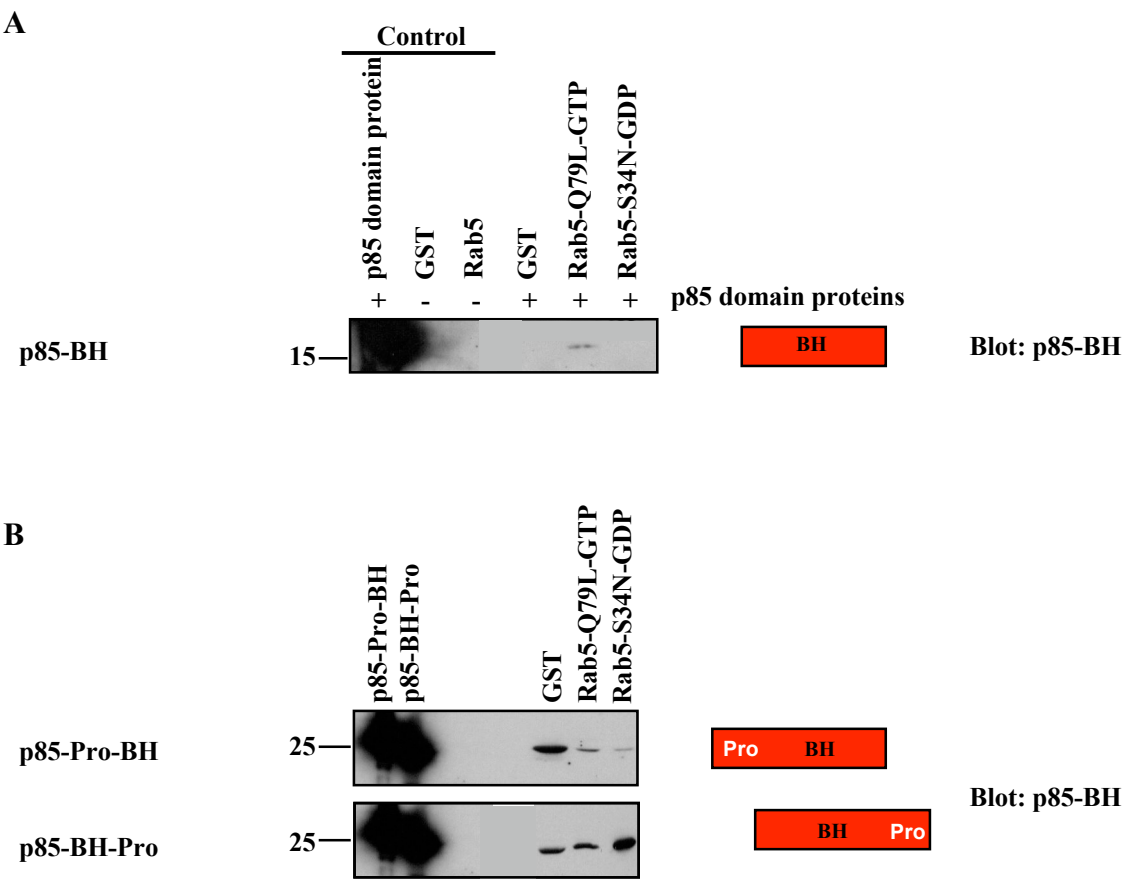

Fig. 4.7. Contribution of the Pro-rich regions flanking the p85-BH domain to Rab5 binding. GST, GST-Rab5-S34N and GST-Rab5-Q79L (10 µg) were loaded with their respective nucleotide, and were incubated with 5 µg of purified p85 proteins in a 500 µl solution containing 5% milk blocking reagent. Samples were resolved using SDS-PAGE and Western Blot analysis was performed using an anti-p85-BH antibody. A) GST pull-down experiment showing the p85-BH domain containing no Pro-rich regions binds to Rab5. B) p85-Pro-BH and p85-BH-Pro have non-specific interactions with the negative control in GST pull-down experiments. Results are representative of three independent experiments.

absence of added p85, did not show a similar band. Further characterization of the domains responsible for p85:Rab5 binding still needs to be investigated to identify the other important domain(s) contributing to Rab5 binding and to fully understand the importance of the selective binding of the p85 mutants to inactive and active Rab5 conformations.

4.2 Mechanism as to how expression of the p85-R274A mutant leads to decreased PDGFR degradation

Previously, the activation and PDGFR degradation patterns in NIH 3T3 cells, p85 wild type expressing and p85-R274A expressing cells was determined (Chamberlain *et al*., 2004). NIH 3T3 cells expressing the p85-R274A mutant displayed increased and prolonged PDGFR activation as compared to both control cells. The increase in PDGFR activation, as determined by tyrosine phosphorylation, resulted in a minor increase in Akt activation and a substantial increase in MAPK signalling. In addition to the increased levels of PDGFR activation and downstream signalling, a reduction in PDGFR degradation was observed in cells expressing p85-R274A, compared to p85-wt and NIH 3T3 control cells. The goal of these next studies was to determine how PDGFR downregulation was being altered in these cells by examining PDGFR monoubiquitination, a modification required for lysosomal sorting, and PDGFR degradation.

4.2.1 PDGFR Monoubiquitination

To determine whether the delayed PDGFR degradation was due to a lack of PDGFR ubiquitination, the PDGFR ubiquitination status in each of the cell lines (NIH 3T3, p85-wt, and p85-R274A) was studied. Stable cell lines expressing FLAG-p85-wt, FLAG-p85-R274A and control NIH 3T3 cells were tested to determine the effect of p85 mutant expression on PDGFR ubiquitination, activation state and degradation. Cells were starved 24 hrs in advance of stimulation and stimulated for 0, 5, 10, 20, 30, and 60 min with PDGF. PDGFR was immunoprecipitated and samples were resolved using SDS-PAGE. Western blot analysis was performed using antibodies specific for ubiquitin, phosphotyrosine, phosphotyrosine1021 (Cbl

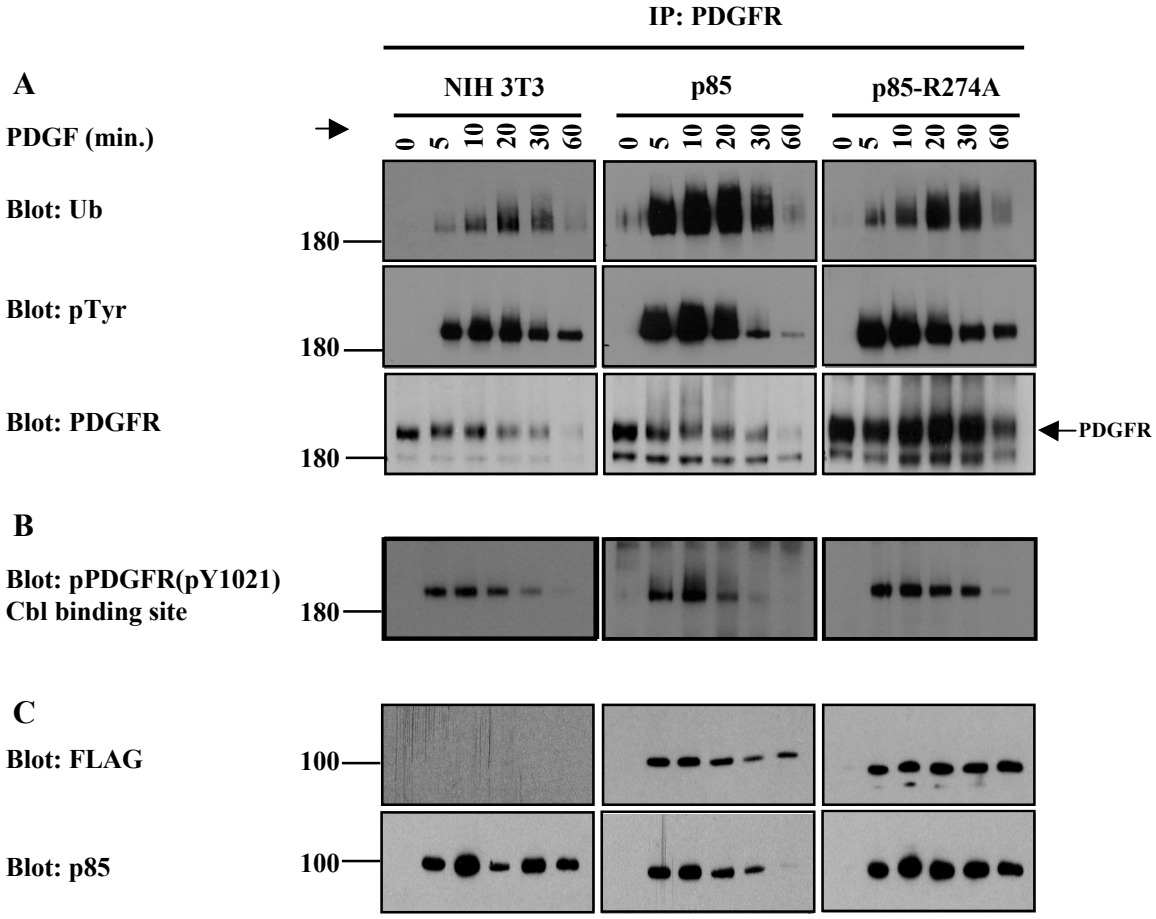

Fig. 4.8. PDGFR is ubiquitinated but has decreased receptor degradation in cells expressing the p85-R274A mutant. Stable cell lines expressing p85-wt, and p85-R274A and control NIH 3T3 cells were stimulated with PDGF for the indicated time. PDGFR was immunoprecipitated and samples were resolved using SDS-PAGE. A) Western blot analysis was performed using antibodies specific for ubiquitin, pTyr, and PDGFR. B) Western blot analysis was performed using antibodies specific for pY1021 of the PDGFR. C) Western blot analysis was performed using antibodies specific for FLAG and p85. Results are representative of three independent experiments.

binding site on PDGFR), FLAG, p85 and PDGFR (Fig. 4.8).

To confirm previous observations of increased and prolonged activation but delayed PDGFR degradation displayed by the p85-R274A expressing cells (Chamberlain *et al*., 2004), PDGFR activation state, ubiquitination, and degradation (Fig. 4.8A) levels were examined first. Both the p85-R274A and p85-wt expressing cells showed an increase in activation (Fig. 4.8A; pTyr blot) as compared to NIH 3T3 cells. Differences in prolonged activation were evident between the p85-R274A expressing cells and the NIH 3T3 cells. These results did not fully agree with those observations seen by Chamberlain *et al*. (2004) where the p85-R274A cells showed a significant difference in prolonged activation as compared to both other cell types (Chamberlain *et al*., 2004). The discrepancies between the prolonged activation levels seen in each cell line could be a result of the type of experiment used in each case. Chamberlain *et al*. (2004) were looking at PDGFR activation levels using total cell lysates over a four hr time course whereas the experiments examined here were of PDGFR IPs over a one hr time course. Most of the differences observed by Chamberlain *et al*. (2004) were observed between the 30 min to four hr time frame. Further, the IP experiments provide a sampling of the PDGFR present and typically do not recover all of the PDGFR present in the cell lysate. As such, as the total PDGFR levels decrease, the PDGFR IP may recover a greater portion of the total receptors remaining in the cell lysate. Thus, PDGFR IPs are a good way to look for post-translational modifications on the PDGFR, but are not quantitative if the PDGFR levels are changing over time. In agreement with the observations seen by Chamberlain *et al*. (2004) the p85-R274A expressing cells showed decreased PDGFR degradation as compared to both NIH 3T3 cells and p85-wt expressing cells. The PDGFRs in p85-R274A expressing cells showed intermediate ubiquitination levels that were greater than those observed in NIH 3T3 cells, yet less than in p85-wt expressing cells. However, cells expressing the p85-R274A mutant showed decreased PDGFR degradation compared to that observed in control cells. This suggests that defective ubiquitination, required for lysosomal sorting, was not the cause of the decreased PDGFR degradation.

Knowing the PDGFR was indeed ubiquitinated in all of these cell lines, the ability of the PDGFR to associate with several known proteins important for sorting the receptor to the

late endosome or lysosome was investigated. Cbl, Hrs and Eps15 are found at the early endosome, whereas STAM and tsg101 are found at the late endosome and lysosome (Urbe, 2005). Several of these proteins bind monoubiquitinated protein, including receptors, and are themselves monoubuquitinated. The PDGFR binds, via its phosphorylated Y1021 residue, the E3 ubiquitin ligase Cbl (Thien and Langdon, 2001); (Tsygankov *et al*., 2001). This site was phosphorylated in all cell lines after stimulation with PDGF but remained phosphorylated longer in p85-R274A expressing cells (Fig. 4.8B). The PDGFR was ubiquitinated and the Cbl binding site was phosphorylated, therefore anti-PDGFR immunoprecipitates were probed for Cbl to determine if the protein responsible for conjugating ubiquitin to the PDGFR was associated with the PDGFR. Cbl binding was detected at all time points but it seemed the binding detected was a non-specific interaction to either the IP beads used in the experiment or the rabbit IgG as the binding was seen even when the cells were unstimulated (i.e. in the absence of pY1021 phosphorylation of the PDGFR), as well as in the control anti-rabbit IgG immunoprecipitation lanes (Fig. 4.9A).

Several different IP beads, Protein G Agarose (Sigma) and TrueBlot anti-rabbit Ig IP beads (eBiosciences), were tested to decrease the non-specific Cbl binding. All of the beads used were able to strongly bind rabbit derived antibodies. The Protein G Agarose and TrueBlot beads differed from the Protein A beads in that they recognized and bound a different section of the rabbit IgG. The TrueBlot beads system were also different because this system used a unique secondary antibody designed to recognize native primary antibody (i.e. the one used to probe the blot) and therefore showed less background when immunoblotting since its ability to recognize the denatured IP antibody was diminished. All beads tested still showed non-specific Cbl binding (Fig. 4.9B). PDGFR association of several other proteins important for PDGFR degradation was tested similarily by western blotting: Hrs, Eps15, STAM and tsg101. After several attempts, there was either not enough protein associating with the PDGFR to detect or the antibodies were not sensitive enough to detect any of these proteins.

Lastly, p85 associations with the PDGFR were studied to look for endogenous p85 associated with the PDGFR and to look for FLAG-p85-wt or FLAG-p85-R274A associated

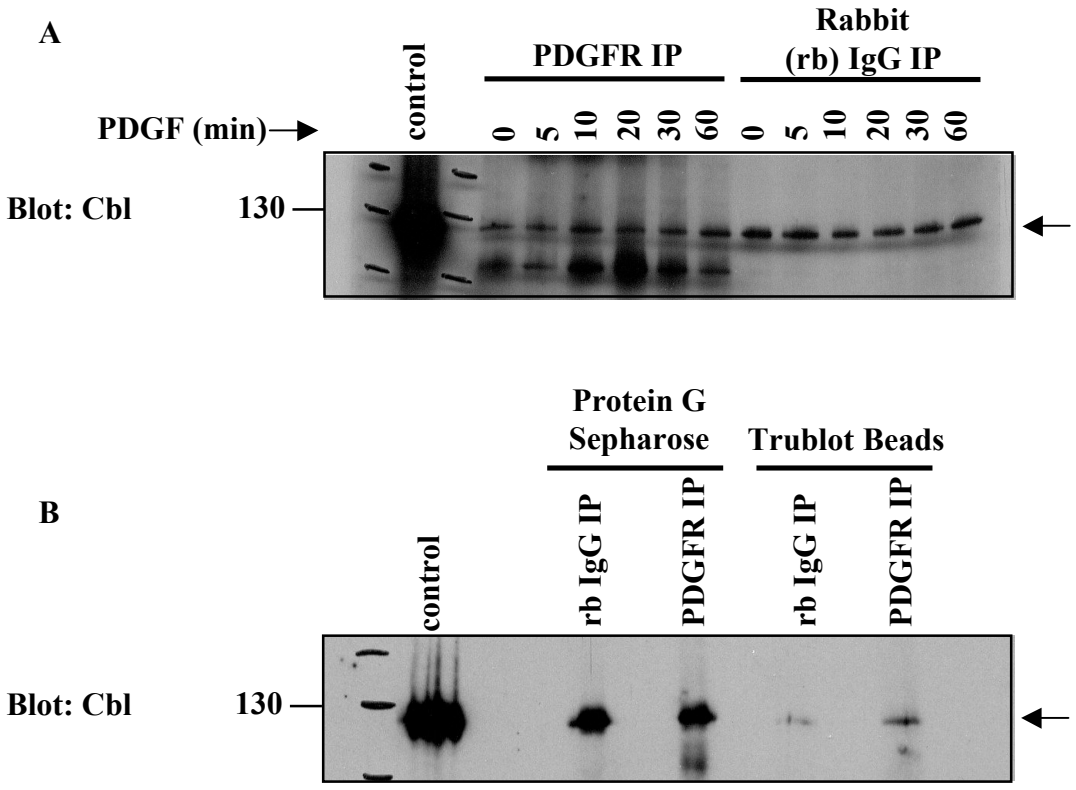

Fig. 4.9. Cbl bound non-specifically to the immunoprecipitation beads and/or the constant regions of the antibodies. Stable cell lines expressing p85 wild type were stimulated with PDGF for the indicated time. PDGFR was immunoprecipitated and samples were resolved using SDS-PAGE. Western blot analysis was performed using antibodies specific for Cbl. A) Immunoblot showing non-specific binding in the rabbit (rb) IgG control. B) Cbl binding was tested using two different types of immunoprecipitation beads on NIH 3T3 lysates (500 µg) that were stimulated with PDGF for 10 min. The control lanes were unstimulated NIH 3T3 cells (25 µg). Results are representative of two independent experiments.

with the PDGFR. Anti-p85 and anti-FLAG antibodies were used to probe anti-PDGFR immunoprecipitates (Fig. 4.8C). All p85 proteins were found to be associated with the PDGFR after stimulation with PDGF, however p85 proteins remained associated for longer periods of time in p85-R274A expressing cells.

Results from the IP experiment show the PDGFR was still being ubiquitinated in all cell lines (Fig. 4.8). Although Cbl associations could not be determined due to non-specific binding to the beads, these data suggested it was not the ubiquitination process that was causing a lack of PDGFR degradation seen in cell lines expressing the p85-R274A mutant. The observed results may be due to defects in the sorting process, as the amount of PDGFR was prolonged in the p85-R274A expressing cells as compared to control cells.

These results led to two hypotheses: i) the decreased PDGFR degradation could be due to a lack of receptor endocytosis where the PDGFR would not be taken into the cell via endocytosis but would be left on the cell surface to continue signaling and/or ii) the decreased PDGFR degradation in p85-R274A expressing cells could be a result of more rapid endosomal receptor trafficking. The p85-R274A mutant has defective RabGAP activity (Chamberlain *et al*., 2004) towards both Rab5 and Rab4, allowing them to remain in their active state longer. Thus, Rab5 (PDGFR endocytosis from the plasma membrane) and Rab4 (PDGFR recycling to the plasma membrane) may be expected to promote rapid PDGFR endocytosis and recycling with reduced opportunities for sorting to a degradative late endosomal/lysosomal pathway.

4.2.2 PDGFR endocytosis as determined by cell-surface biotinylation and uptake

To test whether or not the PDGFR was being endocytosed, the receptors on the surface of the cell were labelled with biotin, induced to endocytose, surface biotin was removed, and the internalized receptors were analyzed using strepdavidin IPs and anti-PDGFR immunoblotting (Fig. 4.10A). Sharon Poland, a fellow graduate student in the laboratory, performed Biotin Assays on stable cell lines expressing FLAG-p85 wild type, FLAG-p85-R274A and control NIH 3T3 cells. Cells were starved for 24 hours and incubated with biotin at 4°C (on ice) to label surface proteins, but at temperatures that did not allow for receptor

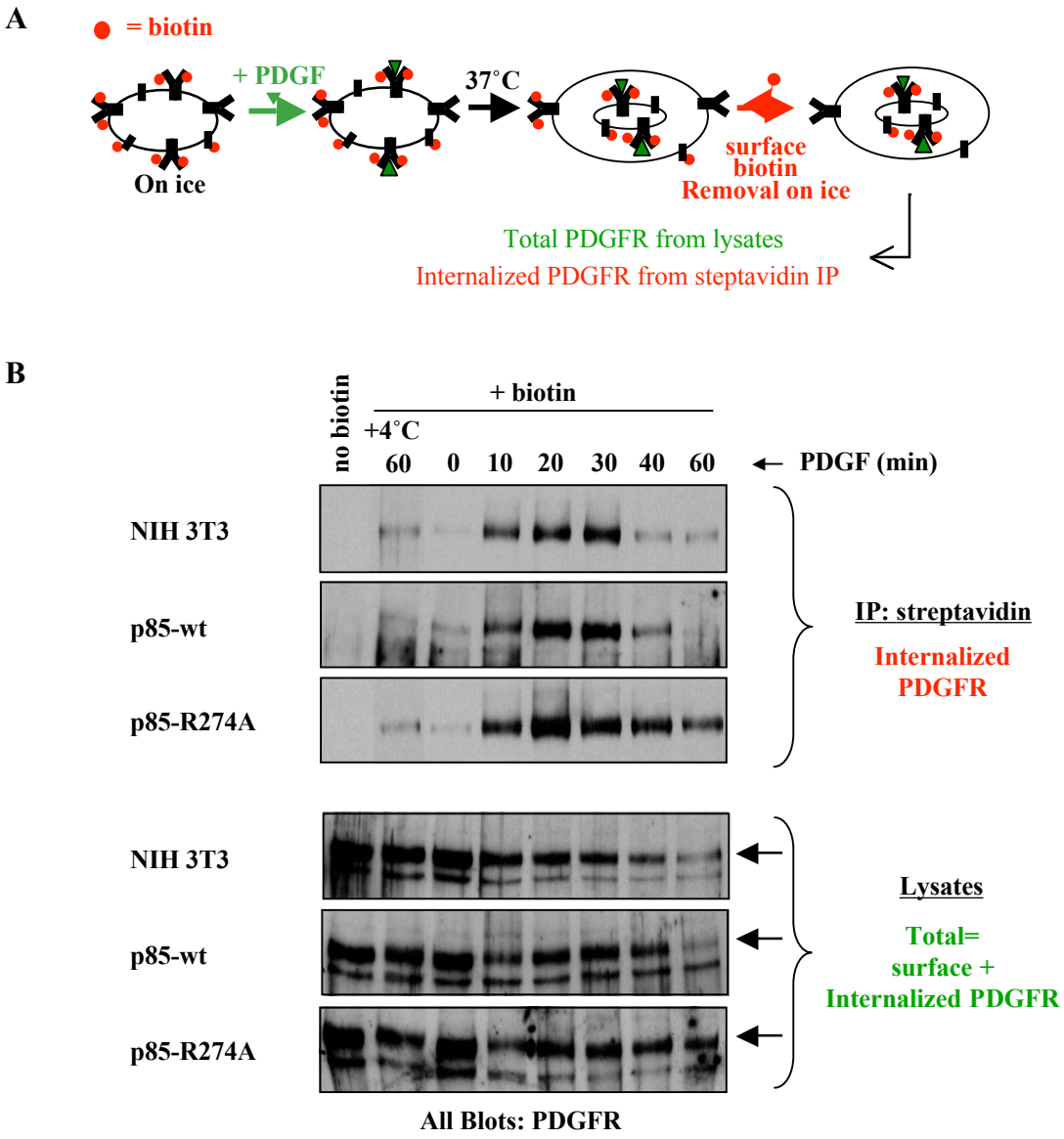

Fig. 4.10. Increased internalization of PDGFR in cells expressing the RabGAP-defective p85-R274A mutant. A) Surface proteins were labeled with biotin and stimulated with PDGF for the indicated times after which the surface biotin was stripped off. Lysates (150 µg) were immunoprecipitated with streptavidin beads to recover the internalized biotinylated proteins. B) Samples were resolved by SDS-PAGE and immunoblotted with PDGFR antibodies. C) Total cell lysates were immunoblotted with the PDGFR antibodies to detect total (surface + internalized) PDGFR levels. Results are representative of three independent experiments performed by Sharon Poland.

endocytosis. The cells were then stimulated at 37°C for 0, 10, 20, 30, 40, and 60 min with PDGF to allow endocytosis of proteins, including the PDGFR. Cells were placed on ice to halt PDGFR trafficking and surface biotin was stripped off using glutathione so only the proteins endocytosed would be biotin-labeled. Biotinylated proteins were immunoprecipitated using streptavidin beads and samples were resolved using SDS-PAGE. Western blot analysis was performed using antibodies specific for the PDGFR (Fig. 4.10B).

There were three controls used in this experiment. The first was the MOCK (no biotin) control. These cells were not treated with biotin, were unstimulated and kept at 4°C (on ice) during the entire experiment. This control was used to test for any antibody cross-reactivity with the IP samples. There was little or no antibody cross-reactivity seen in any cell line. The second control was the 4°C control. These cells were treated with biotin and stimulated as long as the longest time point of the experiment (60 min), however the cells were kept at 4°C (on ice) during the entire experiment. This control was used to determine the amount of PDGFR endocytosis that can occur at 4ºC (on ice) upon PDGF stimulation, when the cells were treated at temperatures that should not allow for receptor endocytosis. There was minimal yet similar PDGFR endocytosis seen in all cell lines. The third control was the 0 min stimulation control. These cells were treated with biotin but not stimulated and therefore kept on ice for the entire experiment. This control was used to determine the efficiency of biotin removal from the cell surface.

The levels of the PDGFR were similar in all cell lines (Fig. 4.10B; lysates) and PDGFR endocytosis was observed in all cell lines tested (Fig. 4.10B; IP: strepdavidin). The p85-R274A expressing cells showed increased levels of internalized PDGFR peaking at 20 min that were maintained over the entire time course as compared to control cells (Fig. 4.10B). As another control, total cell lysates were probed for the PDGFR to determine if the PDGFR was being degraded throughout the time course (Fig. 4.10B). There was less degradation seen in the p85-R274A cells compared to the control NIH 3T3 cells and p85-wt expressing cells at the 60 min time point. The degradation seen was not significant enough to suggest total PDGFR levels would influence the amount of PDGFR internalized at the earlier time points. Results suggest PDGFRs are concentrated in an intracellular compartment and the reduced degradation of the PDGFR observed in the p85-R274A expressing cells was not the result of PDGFRs

trapped at the plasma membrane.

4.2.3 PDGFR trafficking visualized using immunofluorescence and confocal microscopy

To test whether or not the defective PDGFR degradation in the p85-R274A expressing cell line was due to defective endosomal trafficking of the PDGFR, Andrea Hawrysh, a research technician in the laboratory, performed a series of coimmunofluorescence experiments with control NIH 3T3, p85 wild type, and p85-R274A expressing cells to determine the cellular effects of the p85-R274A mutant on PDGFR trafficking through Rab5- and Rab4-containing vesicles or compartments. Rab5 localizes to the early and sorting endosomes where it regulates the movement of vesicles containing activated PDGFR from the plasma membrane to sorting endosomes. Rab4 localizes to sorting and recycling endosomes and regulates the movement of vesicles containing inactivated PDGFR from the sorting endosomes back to the plasma membrane. Experiments were used to compare the trafficking of PDGFRs in Rab5-positive and Rab4-positive vesicles. Cells were plated in multi-well chamber slides and grown to 60% confluency. Cells were starved overnight and stimulated with PDGF for 0, 10, 30 or 120 min. Samples were fixed using paraformaldehyde and permeabilized using saponin. Cells were incubated with antibodies specific for PDGFR, Rab5, Rab4, and phosphotyrosine 857 (phosphospecific antibody indicative of PDGFR activation; pY857) to assess activation state of the PDGFR within these compartments.

Prior to PDGF stimulation all three cell lines appeared the same (Fig. 4.11-4.14). There was no colocalization between either the PDGFR or the activated PDGFR (pY857) with either Rab5-positive or Rab4-positive vesicles. The three cell lines behaved differently after PDGF stimulation. In comparison to NIH 3T3 cells and the p85-wt expressing cells, PDGFR colocalization with Rab5-positive and Rab4-positive vesicles in p85-R274A expressing cells were found to colocalize more in intracellular compartments.

The most notable difference seen between all three cell lines were observed after 30 min of PDGF stimulation. The PDGFR was found to accumulate in intracellular compartments in cells expressing the p85-R274A mutant. The PDGFR partially colocalized to the perinuclear

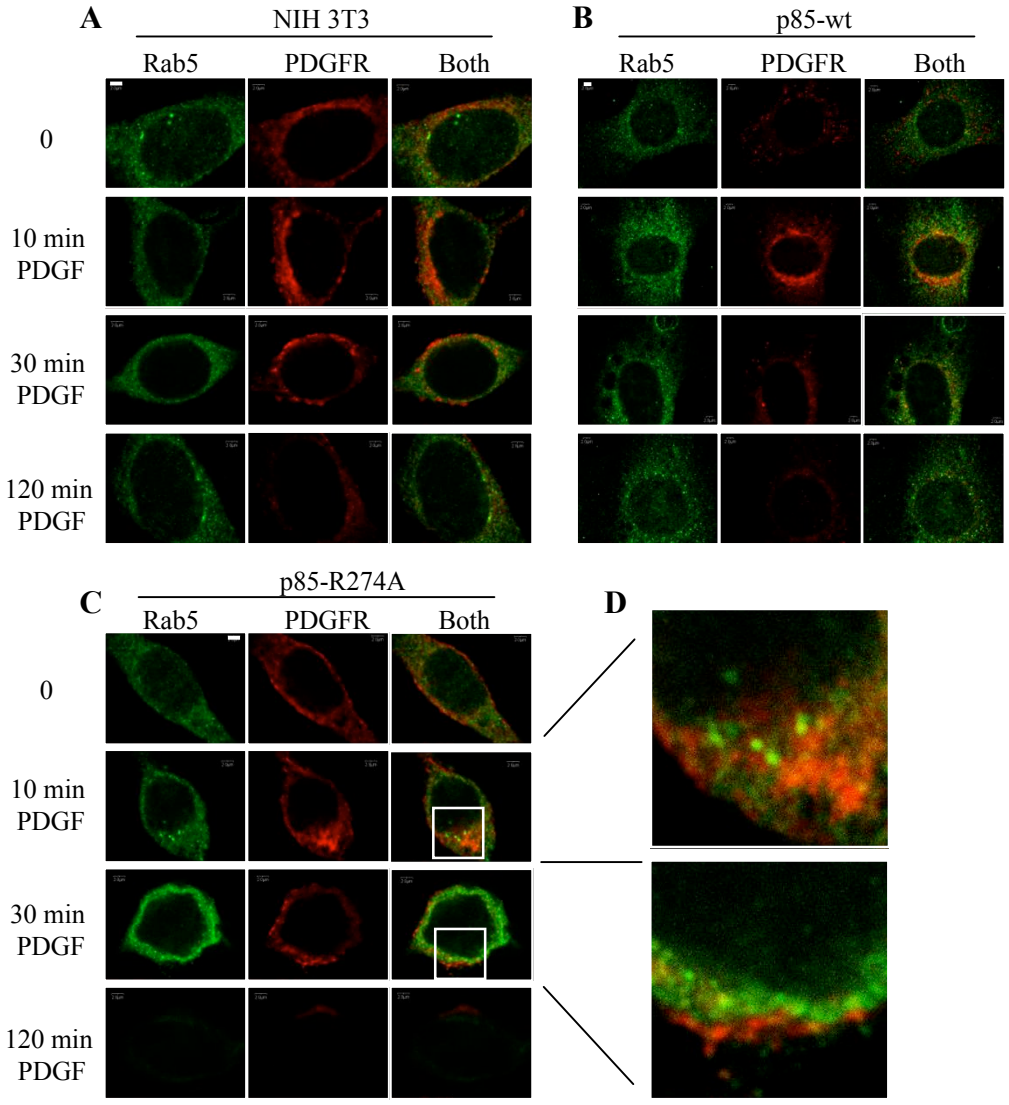

Fig. 4.11. Accumulation of perinuclear Rab5-positive vesicles and peripheral PDGFR-positive vesicles in p85-R274A-expressing cells stimulated with PDGF for 30 min. Control NIH 3T3 (A) cells and cells stably expressing (FLAG-)p85 (B) or (FLAG-) p85-R274A (C) were stimulated with PDGF for the indicated times, fixed, permeabilized, and probed with primary antibodies specific for Rab5 and PDGFR. Secondary antibodies conjugated to Alexa 488 (green) or Alexa 594 (red) were used to visualize the localization of Rab5 (green) and the PDGFR (red). Colocalization is observed as yellow (Both). The cells were visualized using confocal microscopy. Note the cells expressing FLAG-p85 are somewhat larger than the other two cell types are shown 40% smaller to fit into the frame. D) Selected boxed areas were enlarged for a more detailed view. Scale bar, 2 μm for all. Results are representative of three independent experiments performed by Andrea Hawrysh. These experiments were made possible by access to the confocal microscope by Dr. Mousseau, Dept. of Psychiatry.

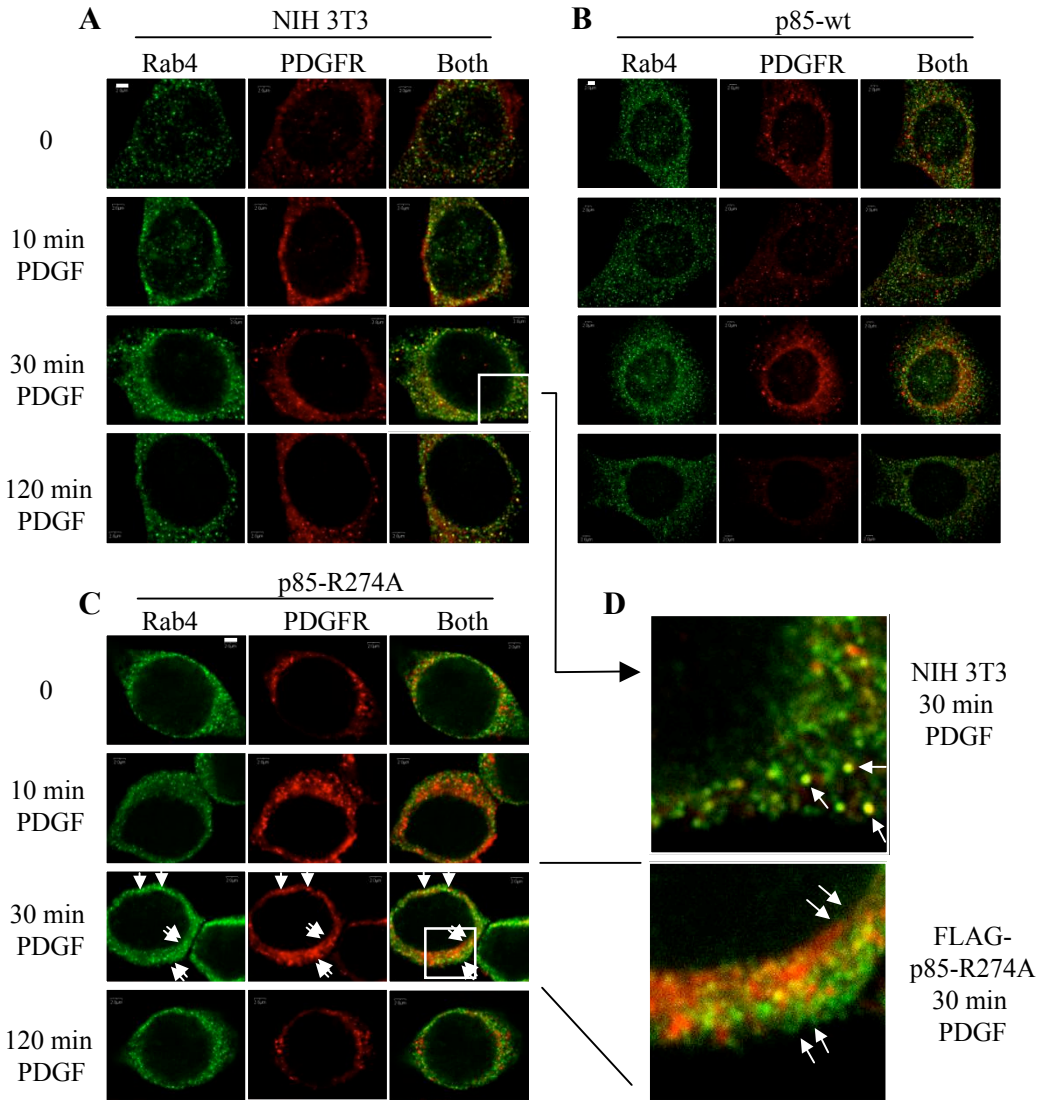

Fig. 4.12. Increased perinuclear PDGFR-positive vesicles and partial colocalization with peripheral Rab4-positive vesicles in cells expressing p85-R274A. Cells were treated as in Fig. 4.11 and probed to visualize the localization of Rab4 (green) and the PDGFR (red). Colocalization is observed as yellow (Both). Arrows indicate punctate colocalization. D) Selected boxed areas were enlarged for a more detailed view. Scale bar, 2 µm. Results are representative of three independent experiments performed by Andrea Hawrysh. These experiments were made possible by access to the confocal microscope by Dr. Mousseau, Dept. of Psychiatry.

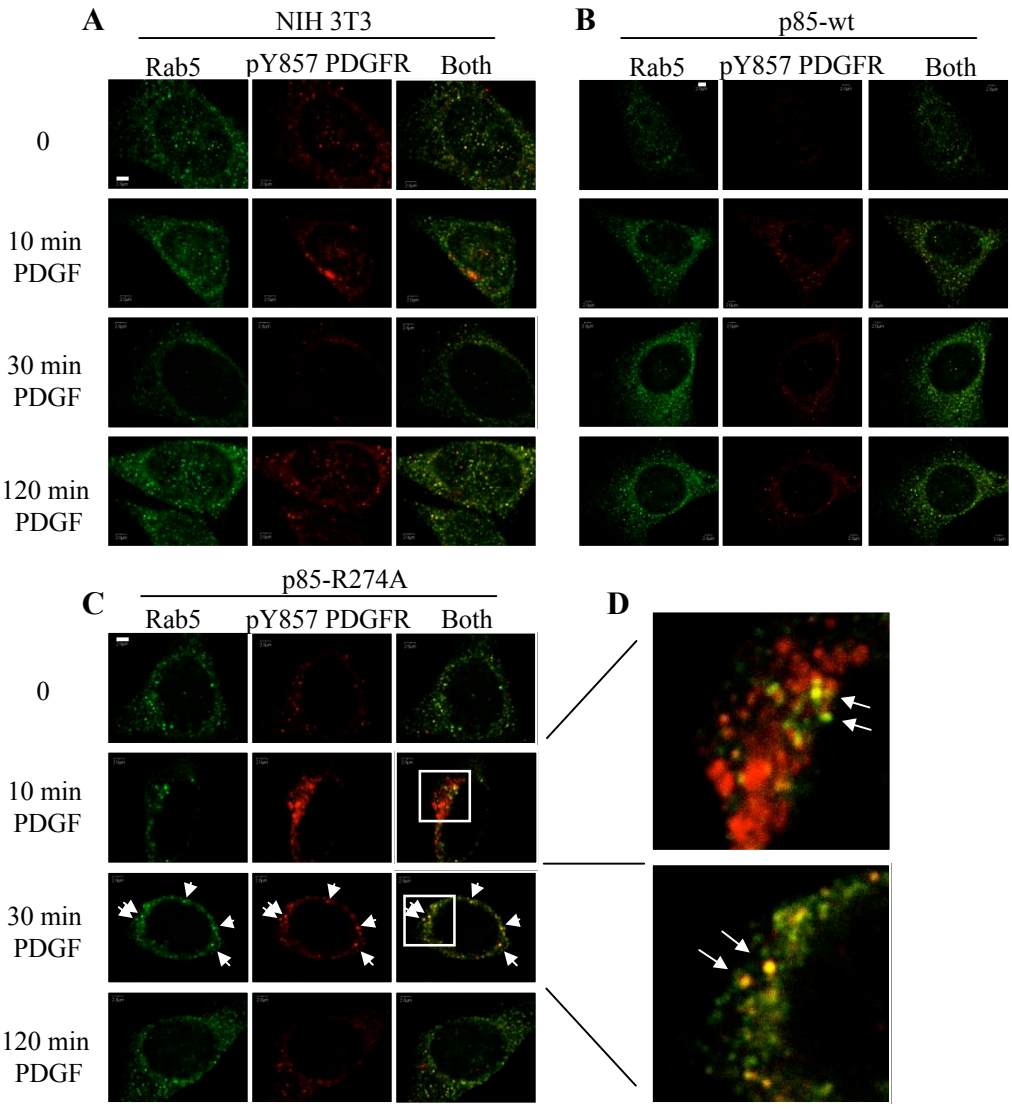

Fig. 4.13. Colocalization of activated PDGFR (pY857) in Rab5-positive vesicles within p85-R274A-expressing cells after 30 min of PDGF stimulation. Cells were treated as in Fig. 4.11 to visualize the localization of Rab5 (green) and phosphorylated PDGFR (pY857; indicative of activated PDGFR) (red). Colocalization is observed as yellow (Both). Arrows indicate punctate colocalization. (D) Selected boxed areas were enlarged for a more detailed view. Scale bar, 2 µm. Results are representative of three independent experiments performed by Andrea Hawrysh. These experiments were made possible by access to the confocal microscope by Dr. Mousseau, Dept. of Psychiatry.

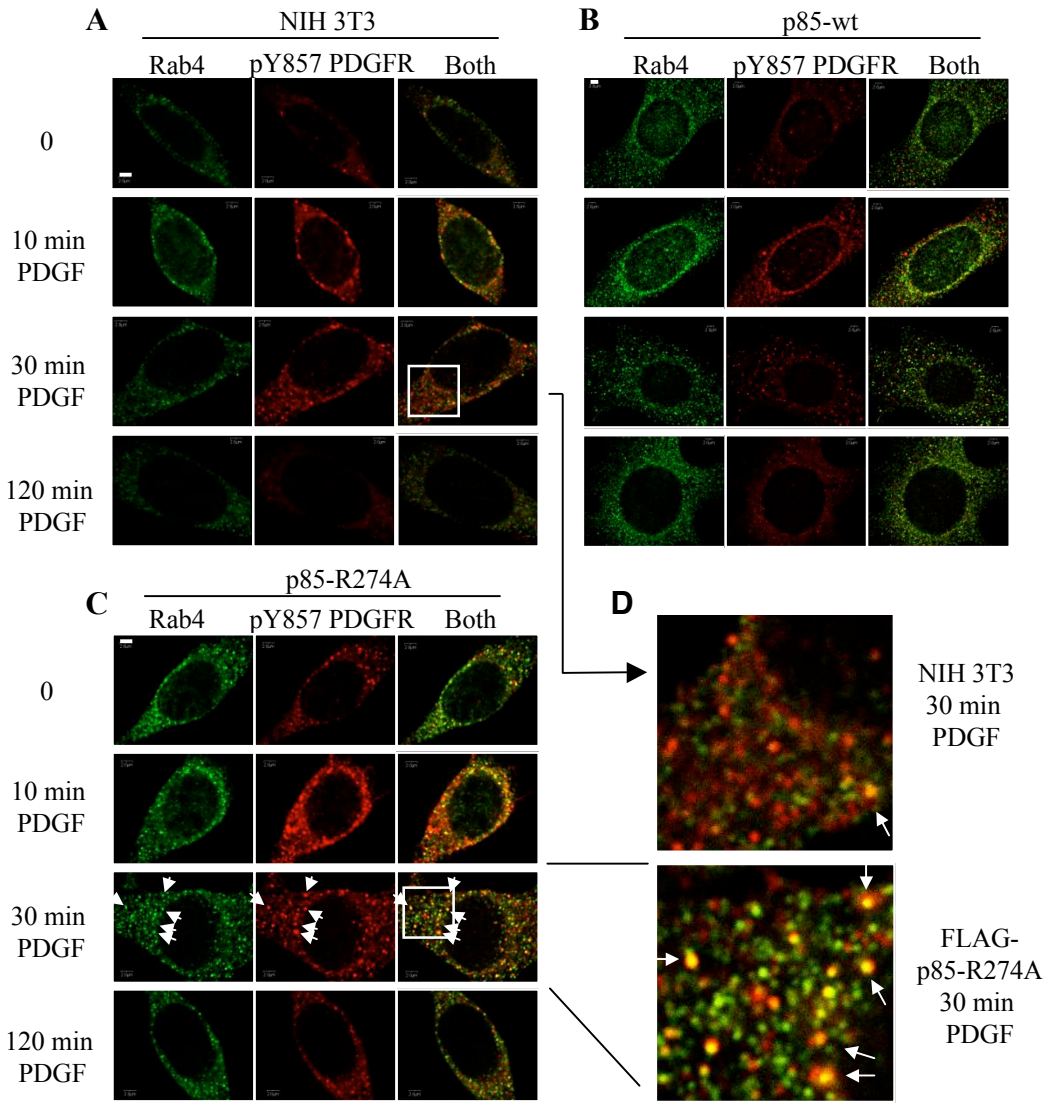

Fig. 4.14. Increased colocalization of activated PDGFR (pY857) in Rab4-positive vesicles from p85-R274A-expressing cells after 30 min of PDGF stimulation. Cells were treated as in Fig. 4.11 and probed to visualize the localization of Rab4 (green) and phosphorylated PDGFR (pY857; indicative of activated PDGFR) (red). Colocalization is observed as yellow (Both). (D) Selected boxed areas were enlarged for a more detailed view. Arrows indicate punctate colocalization more prevalent in p85R274A-expressing cells. Scale bar, 2 µm. Results are representative of three independent experiments performed by Andrea Hawrysh. These experiments were made possible by access to the confocal microscope by Dr. Mousseau, Dept. of Psychiatry.

regions in Rab5-positive compartments (Fig. 4.11) and also partially colocalized to the cell periphery in Rab4-positive compartments (Fig. 4.12). The PDGFR was found to localize more so in Rab4-positive vesicles than in Rab5 positive vesicles in cells expressing the p85-R274A mutant. The activated PDGFR (pY857) was found to colocalize with both Rab5-positive and Rab4-positive vesicles within p85-R274A expressing cells but not in control cells (Fig. 4.13 & 4.14). The ability of activated PDGFRs to localize in Rab4-positive recycling vesicles is unique to the p85-R274A expressing cells and suggests that receptors are not being dephosphorylated prior to recycling. These observations suggest expression of the p85-R274A mutant alters PDGFR trafficking through these Rab5 and Rab4 compartments. These results also suggest cells expressing the p85-R274A mutant perturbs the normal dephosphorylation kinetics of the PDGFR.

The PDGFR was both endocytosed and ubiquitinated in p85-R274A expressing cells suggesting that the lack of sorting to the lysosomal degradation pathway is not the result of defective uptake or post translational modifications. The mechanism of the decreased PDGFR degradation displayed by the p85-R274A expressing cells can be attributed to altered PDGFR trafficking between endosomal compartments and may also be linked to decreased PDGFR dephosphorylation.

5.0 DISCUSSION

5.1 Interaction of p85 with Rab5

The p85 subunit of PI3K stays associated with the PDGFR during receptor endocytosis (Kapeller *et al*., 1993). It was suggested that this protein may play a role in regulating PDGFR trafficking to a degradative pathway. Studies have shown that p85 binding sites on specific receptors are required for proper receptor down-regulation (Joly *et al*., 1994). Mutant PDGFRs unable to bind p85 were initially endocytosed as normal but were constitutively recycled and not degraded (Joly *et al*., 1995). Previous studies have shown p85 was able to interact and bind to Rab5, a G-protein which localizes to early and sorting endosomes and regulates the movement of vesicles containing activated PDGFR from the plasma membrane to sorting endosomes, only when associated with p110β (Christoforidis *et al*., 1999b). Chamberlain and colleagues have since shown a direct interaction between p85 and Rab5 (Chamberlain *et al*., 2004). The p85 protein contains a BH domain also known as the BCR-homology domain. It is a conserved 200 residue segment within the protein which normally encodes for GAP activity toward select G-proteins. Originally the p85 protein was thought to have no catalytic activity but recently has been shown to elicit *in vitro* GAP activity towards Rab5, Rab4, Cdc42, Rac1, and to a lesser extent Rab6 but not Rab11 (Chamberlain *et al*., 2004). Typically GAP proteins only bind to G-proteins in the active GTP bound conformation but periodically some GAP proteins, BNIP-2 and RhoGAP, are able to bind to both the inactive GDP-bound and active GTP-bound forms (Low *et al*., 1999; Self and Hall, 1995). The p85-wt protein was found to bind to both inactive and active conformations of Rab5, whereas some mutant p85 proteins were found to bind to the inactive or active conformations, but not both (Chamberlain *et al*., 2004). The first objective of this thesis was to characterize the function of the p85:Rab5 interaction in cells by generating a p85 mutant unable to bind Rab5 by focusing on which domains of p85 were needed for Rab5 binding.

Several mutant p85 proteins containing different p85 domains expressed alone or in combination with other domains were made. GST pull-down experiments were performed to assay the binding interactions between p85 and Rab5. The interaction between p85 and Rab5 was identified to be within the BH domain of the p85 protein, the proposed G-protein binding

site. Mutant proteins missing the BH domain, however, were still able to bind to Rab5 suggesting there are other domain(s) of p85 involved in Rab5 binding which still need to be elucidated. Some mutant p85 proteins were also selective in their binding and preferred to bind to Rab5 in either its GDP-bound or its GTP-bound conformation. Although future experiments, which go beyond the scope of this project, are still needed to fully understand the p85 determinants that dictate the binding specificity for Rab5 in the inactive and active conformations, the sequential 'hand-off' model for how p85 interacts with Rab5 during PDGFR endocytosis suggests that p85 could act as a GDF by binding to Rab5-GDP, as well as a Rab5 GAP.

GDF proteins typically interact with GDP-bound G-proteins. GDFs help to recruit Rab proteins to specific membranes by displacing inhibitory GDI proteins. A three-step GDF function model was proposed where a prenylated-Rab-GDI complex was presented to a GDF for its membrane recruitment (Pfeffer and Aivazian, 2004). In this model, it was proposed that the Rab-GDI complex would first weakly bind to the GDF protein at the target membrane. Secondly, the GDF would release the GDI and bind the prenylated Rab protein. Third, the prenylated Rab protein would be able to insert itself into the target membrane. It seemed the delivery of Rab proteins to their sites of function was selective on the basis of GDF localization and further specified by specific Rab5-GTP post-GDF effector protein interactions (e.g. EEA1).

According to the sequential 'hand-off' model, the p85 protein could potentially help to recruit Rab5 in its inactive GDP-bound conformation to the early endosome. The p85 protein could function as a GDF using the above three-step GDF function model (Fig. 5.1). Previous GDFs, the neurotrophin receptor p75 and prenylated Rab acceptor-1 protein, have been shown to directly associate with membranes through their transmembrane domains (Pfeffer and Aivazian, 2004). Although p85 does not directly interact with endosomal membranes like other GDFs, it does stay associated with the activated PDGFR at the plasma membrane and during endocytosis. The prenylated-Rab-GDI complex could be presented to p85 at the endosomal membrane during PDGFR endocytosis while p85 is complexed with the PDGFR. The p85 protein has been shown to interact with Rab5 in its GDP bound conformation and

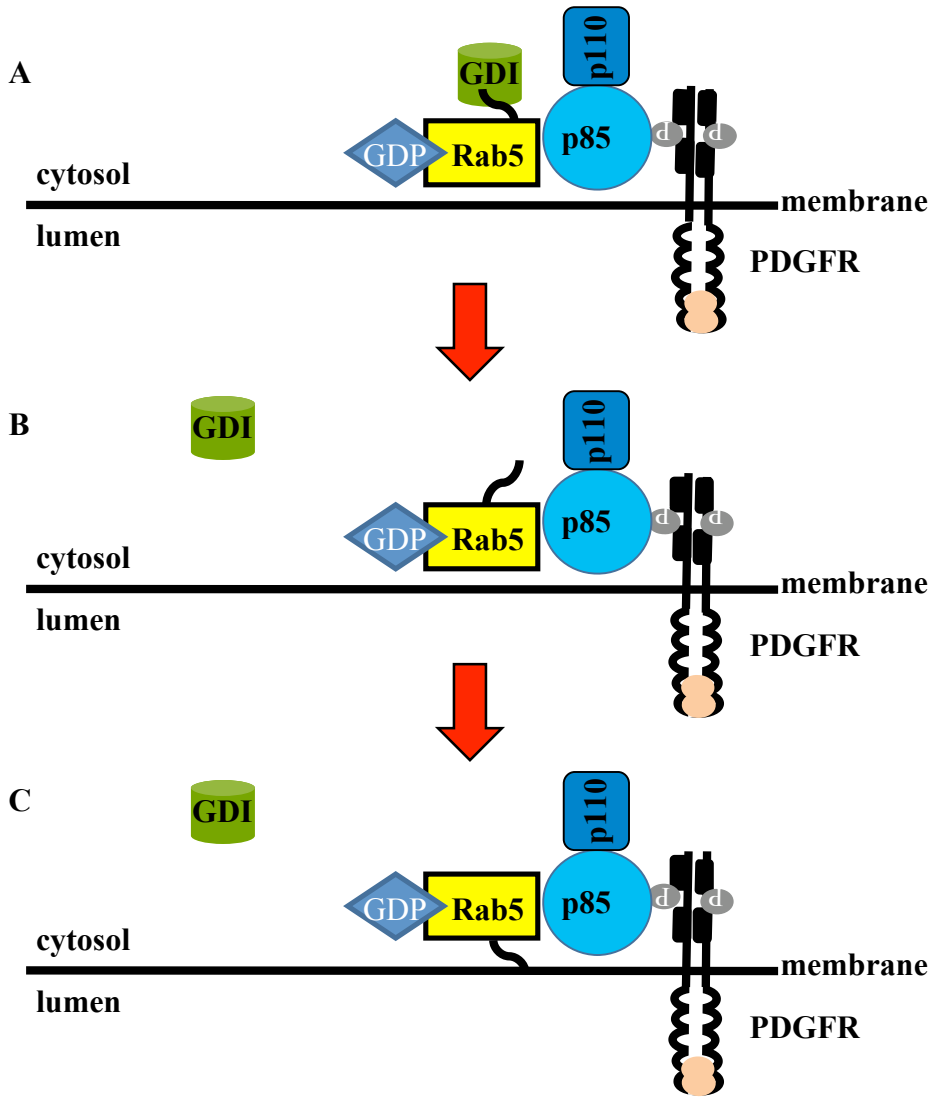

Fig. 5.1 Model of p85 GDF function. A) The prenylated-Rab-GDI complex is presented to p85 at the endosomal membrane during PDGFR endocytosis while p85 is complexed with the PDGFR. B) The p85 protein facilitates the release of the GDI and binds the prenylated Rab protein. C) The prenylated Rab protein inserts itself into the endosomal membrane where it could then exchange GDP to GTP.

could facilitate the release of the GDI and bind the prenylated Rab protein. Lastly, the prenylated Rab protein would be able to insert itself into the endosomal membrane, where it could then exchange Rab5-GDP to Rab5-GTP, perhaps via the PDGFR-associated Rin1 GEF protein (Barbieri *et al*., 2003) to facilitate membrane fusion events during endocytosis.

It has also been shown by Chamberlain and colleagues that p85 has GAP activity towards select Rab proteins (Chamberlain *et al*., 2004), however the *in vitro* GAP activity displayed by the p85 protein was dependent upon much higher p85 protein concentrations (μM) than what is typically seen by most GAP proteins (nM concentrations). The sequential "hand-off" model proposes both p85 and p110β bind Rab5-GTP and the formation of this trimeric complex allows the release of p85 from the receptor with a corresponding increase in RabGAP activity. This could suggest that the GAP activity of the p85 protein is further regulated by the associated p110 protein (Fig. 5.2). Typically GAPs provide a catalytic arginine finger and stabilize the flexible switch I and switch II regions of the G-proteins in their active GTP-bound state. In some instances, these two functions are carried out by more than one protein and the combined contribution of these proteins is necessary for maximal GAP activity. This appears to be the case for the ADP-ribosylation factor (Arf) and ArfGAP. The GAP activity of ArfGAP is increased 10-1000 fold by the presence of a coatomer protein or phospholipids (Goldberg, 1999); (Szafer *et al*., 2000). This is also the case for RanGAP where the GAP activity is influenced by Ran binding proteins (Seewald *et al*., 2002; Seewald *et al*., 2003). Since p85 possess an important R274 residue, this likely corresponds to the arginine finger and it may be that p110 binds to Rab5-GTP and stabilizes the switch regions to accelerate the GTPase activity of Rab5.

We hypothesize that p85 acts both as a GDF and a GAP towards Rab5 and potentially to other Rab proteins such as Rab4. Further studies will need to be conducted to fully understand the p85:Rab5 interaction in cells and to further investigate p85 interactions with other Rab proteins.

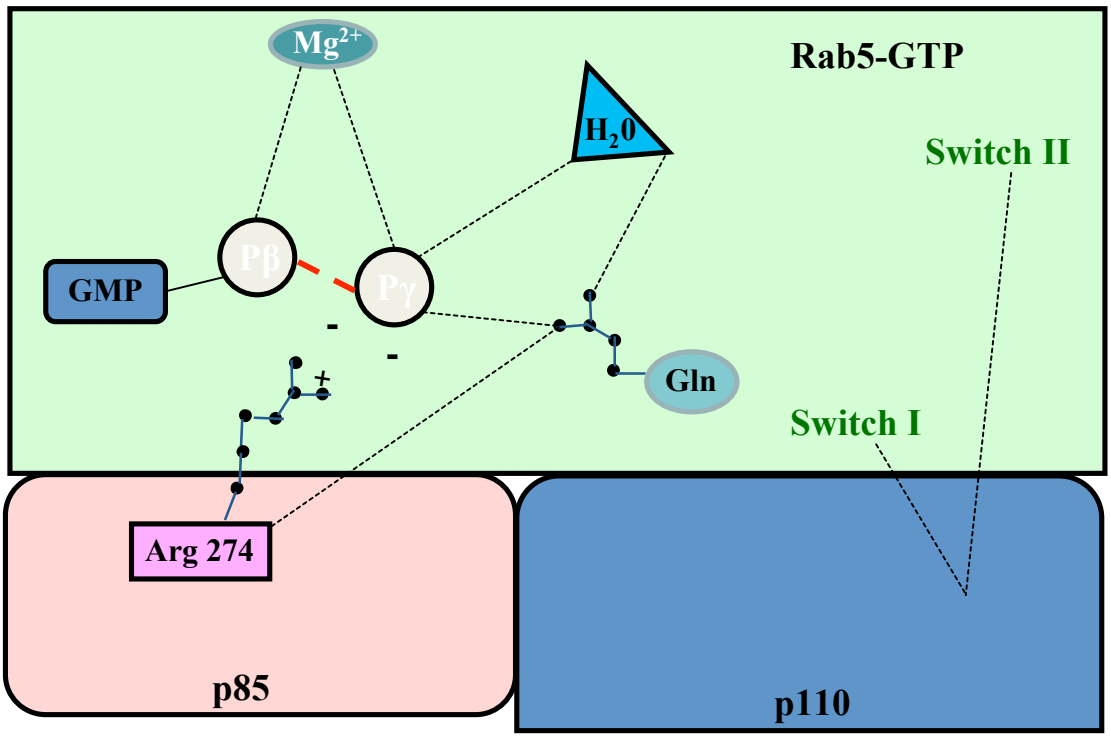

Fig. 5.2. The p85:p110 interaction with Rab5-GTP may stimulate the GTPase activity of Rab5. The GAP activity of the p85 protein may be further regulated by the association of the p110 protein. The p85 protein possess an important R274 residue which likely corresponds to the catalytic arginine finger of GAP proteins and it may be that p110 binds to Rab5-GTP and stabilizes the switch regions to accelerate the GTPase activity of Rab5.

5.1.1 Future work to determine the mechanism of Rab regulation by p85

The sequential 'hand-off' model for how p85 interacts with Rab5 during PDGFR endocytosis suggests that p85 could act as a GDF and a GAP towards Rab5. It suggests the additional binding of p110β to p85:Rab5-GTP increases the p85 RabGAP activity to facilitate GTP hydrolysis. A series of experiments have been proposed by our laboratory to help us better understand the role of p85 in Rab protein regulation.

To begin, we would like to better understand the p85:Rab5 interaction. There are two ways we are planning to do this: i) by measuring the binding affinities and GAP activities of p85:Rab5 complexes, and ii) by determining the crystal structure of the p85:Rab5 complex. Measuring the binding affinity constant, the "on" rate, and the "off" rate for several p85:Rab complexes, including Rab5, will be made possible using the BIACORE system located in the Structural Sciences Center at the University of Saskatchewan. A sensor chip will be made with chemically attached anti-GST antibodies. GST-Rab5-S34N and GST-Rab5-Q79L along with GDP + Mg^{2+} and GTP + Mg^{2+}, respectively, will be immobilized onto separate chips and purified p85 proteins will be allowed to flow over the chips where the binding affinities will be measured. We expect to see intermediate affinities between both p85:Rab5-GTP and p85:Rab5-GDP with the highest binding affinity seen between p85:p110β:Rab5-GTP. To determine the p85 structure/function relationship, in collaboration with Dr. Louis Delbaere (Canada Research Chair, Dept. of Biochemistry, University of Saskatchewan), the crystal structure of p85 complexes with phosphopeptide (to mimic the phosphorylated PDGFR), Rab5-S34N, Rab5-Q79L, Rab4-S27N and Rab4-Q72L will be determined. Information concerning the structure of these protein complexes will allow us to determine the residues important for binding, as well as the mechanism of Rab5 and Rab4 GTPase stimulation by p85.

To test the possible GDF function of p85 in Rab5 membrane recruitment, we will generate a p85-BH domain mutant which is unable to bind to Rab5 to determine if this mutant can disrupt Rab5 membrane recruitment and PDGFR trafficking. Mutagenesis experiments will be used to target residues responsible for Rab5 binding (as determined by the crystal structure) and pull-down experiments will be used to determine Rab5 binding or lack of binding. If p85 is a GDF, cells expressing this p85-BH mutant unable to bind Rab5 would be

defective in PDGFR endocytosis, resulting in PDGFR accumulation at the plasma membrane and increased downstream signalling, and Rab protein accumulation in the cytosol, unable to become membrane bound.

Finally, to investigate if p110β has an effect on p85 RabGAP activity, as suggested by our "hand-off" model, we will perform a series of GAP assays titrating different concentrations of p85:p110β with Rab5 and Rab4. We will compare these results with those from control GAP assays using only purified p85 protein. Our model predicts the p85:p110β will be able to increase the GTPase activity of both Rab5 and Rab4 at lower concentrations of purified p85:p110β added as compared to control p85 alone. To emulate the phosphorylated PDGFR, we will also perform GAP assays with phosphopeptide and control peptide to induce the PDGFR-bound conformation of p85 to see what effect this has on GAP activity. Our model suggests the GAP activity of p85 is increased when the trimeric p85:p110β:Rab-GTP complex is released from the PDGFR, therefore assays performed in the presence of phosphopeptide may show reduced GAP activity for both the p85:p110β complex and p85 alone.

Taken together, these experiments will allow us to better understand how Rab5 and Rab4 regulate PDGFR activation state, downstream signalling and trafficking through the endocytic pathway during PDGFR endocytosis. These experiments will also help us to understand the role of p85 binding and GAP activity within these complex processes. We will be able to improve our understanding of the sequence of events which co-ordinate and regulate the activities responsible for normal PDGFR trafficking within cells.

5.2 Model as to the mechanism of defective PDGFR degradation in cells expressing the p85-R274A mutant

The PDGFR is one of many growth factor receptors responsible for controlling numerous cellular processes such as proliferation, differentiation, and cell survival (Schlessinger, 2000). A process known as endocytosis is responsible for the down-regulation of this growth factor receptor. If there is a defect in this down-regulation pathway, there is defective PDGFR degradation and the PDGFR continues to signal for much longer periods of

time than what is normally allowed. This prolonged signalling can result in excess cell growth and cellular survival leading to cancerous properties. The p85-R274A mutant contains a point mutation within its BH domain rendering it inactive for *in vitro* GAP activity towards Rab proteins (Chamberlain *et al*., 2004). NIH 3T3 cells expressing this p85 mutant have increased and prolonged PDGFR activation as well as decreased PDGFR degradation. Recent evidence shows cells stably expressing p85-R274A can form tumors in nude mice (Chamberlain *et al*., 2008). In response to PDGF stimulation, the p85-R274A mutation did not alter its ability to bind to and regulate p110-PI3K activity (Chamberlain *et al*., 2004) thereby suggesting the effects of this mutant are independent of PI3K activity. The second objective of this thesis was to determine the mechanism of defective PDGFR degradation in cells expressing the p85-R274A mutant. In the case of the p85-R274A expressing cells, there were three aspects of receptor down-regulation that were studied to determine the mechanism of defective PDGFR degradation. These aspects were: i) PDGFR ubiquitination, ii) PDGFR endocytosis and iii) PDGFR trafficking.

The first aspect studied was whether or not the PDGFR was ubiquitinated. Studies have shown the PDGFR is monoubiquitinated and this signal is sufficient for endocytosis and degradation (Haglund *et al*., 2003). The monoubiquitination signal is involved in PDGFR trafficking for lysosomal sorting steps, thereby preventing receptor recycling (Marmor and Yarden, 2004). Studies have shown defects in the ubiquitination process decrease RTK internalization and sorting, resulting in oncogenesis (Peschard and Park, 2003). PDGFR IPs were performed after PDGF stimulation and the IP samples were probed for ubiquitin, along with other proteins involved in the ubiquitination process. Results confirmed that the PDGFR was indeed ubiquitinated and the defective PDGFR degradation was not due to a lack of degradative sorting signals (Fig. 4.8).

Next PDGFR endocytosis was studied to determine if the PDGFR was being internalized or accumulating at the plasma membrane. Studies have shown aberrant RTK internalization or overexpression of receptors at the plasma membrane lead to oncogenesis and gene amplification, increased gene expression, and defects in receptor trafficking and degradation can result in RTK overexpression (Dikic and Giordano, 2003; Peschard and Park,

2003; Thien and Langdon, 2001). Biotin was used to label the PDGFR on the cell surface. The cells were induced to endocytose the PDGFR by PDGF stimulation and the internalized biotin-labelled PDGFR was isolated from cell lysates. These experiments clearly showed that the PDGFR was being internalized in cells expressing the p85-R274A mutant (Fig. 4.10B).

The PDGFR was both ubiquitinated and endocytosed by the cell suggesting the PDGFR should have been degraded normally, providing there were no defects in PDGFR trafficking from the plasma membrane to the lysosome. Therefore PDGFR trafficking was studied using immunofluorescence experiments. The p85-BH domain contains *in vitro* GAP activity towards Rab5 and Rab4, proteins which regulate the entry of vesicles to the early endosome and the exit of vesicles back to the plasma membrane via recycling endosomes respectively. This suggests the possibility that expression of this mutant may deregulate Rab5 and Rab4 function and disturb Rab-mediated PDGFR trafficking. Immunofluorescence experiments looked at the colocalization of Rab5 and Rab4 with either the PDGFR or pY857 PDGFR.

A model as to the mechanism of defective PDGFR degradation in cells expressing the p85-R274A mutant was proposed from the results obtained (Fig. 5.3 and Fig. 5.4). Results (Fig. 4.11-4.14) suggest reduced PDGFR-associated-p85-R274A-encoded RabGAP activity initially resulted in increased Rab5-GTP-driven membrane fusion and rapid PDGFR endocytosis as well as increased Rab4-GTP-driven membrane fusion and rapid PDGFR recycling back to the plasma membrane (Fig. 5.3). The lack of GAP activity of the p85-R274A mutant was unable to contribute to and accelerate Rab5 and Rab4 GTP hydrolysis and over time this could result in Rab protein sequestration on intracellular membranes (Fig. 5.4). The Rab5-GTP protein accumulated on perinuclear early/sorting endosomal membranes and the Rab4-GTP protein accumulated on peripheral vesicles which may correspond to recycling endosomes. The net result was blocked PDGFR trafficking, which prevented normal PDGFR dephosphorylation and degradation, attributed to a lack of sufficient cytosolic Rab5-GDP and Rab4-GDP required to associate with new membranes and facilitate additional vesicle fusion events.

The effects seen by cells expressing the p85-R274A mutant seem to be specific for the

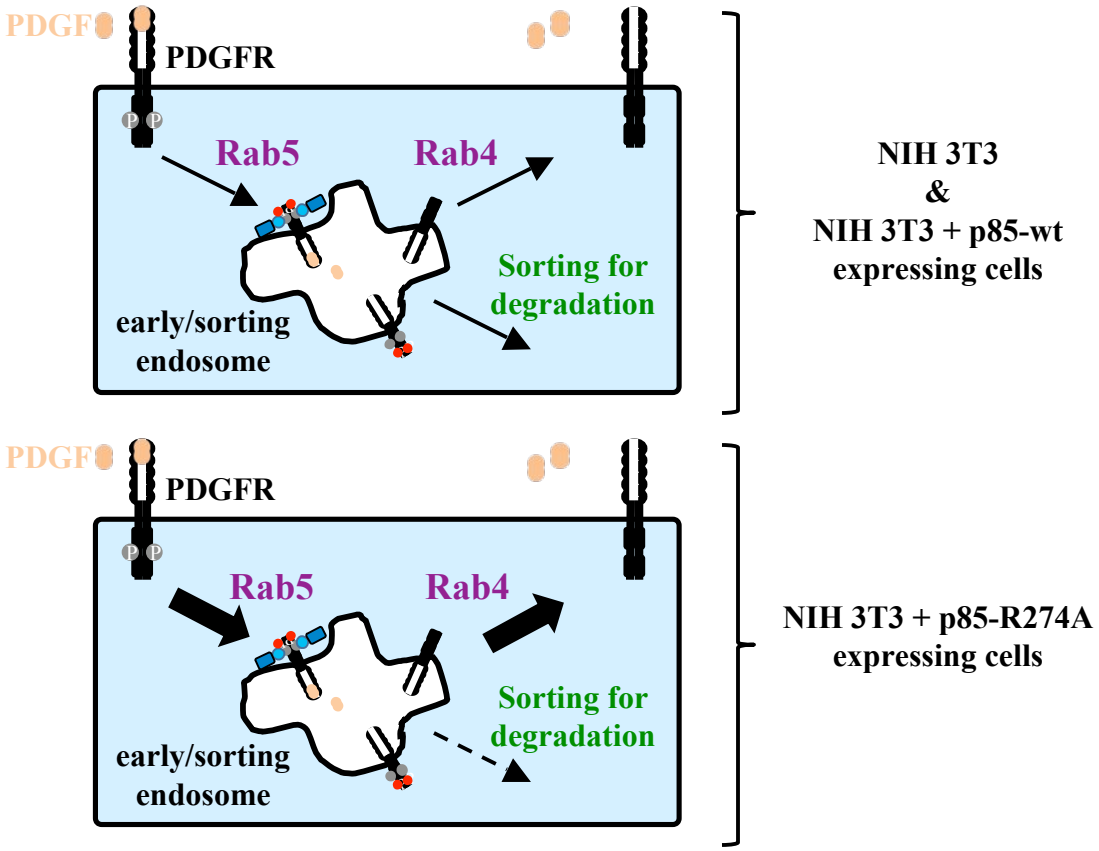

Fig. 5.3. Cells expressing the p85-R274A mutant show increased rates of PDGFR endocytosis and recycling. Reduced PDGFR-associated-p85-R274A-encoded RabGAP activity initially results in increased Rab5-GTP-driven membrane fusion and rapid PDGFR endocytosis as well as increased Rab4-GTP-driven membrane fusion and rapid PDGFR recycling back to the plasma membrane as compared to control cells.

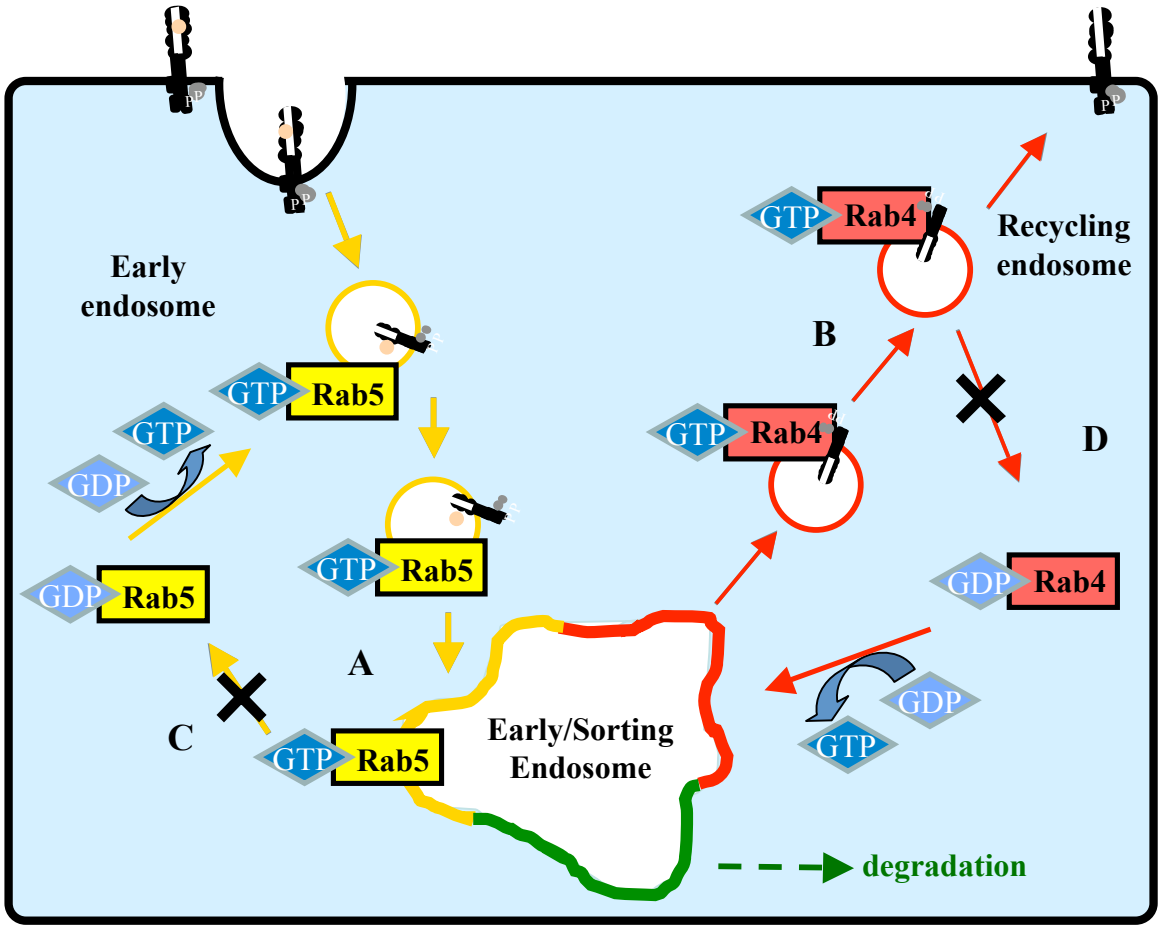

Fig. 5.4. Model as to the mechanism of defective PDGFR degradation in cells expressing the p85-R274A mutant. Reduced PDGFR-associated-p85-R274A-encoded RabGAP activity initially resulted in increased Rab5-GTP-driven membrane fusion and rapid PDGFR endocytosis and increased Rab4-GTP-driven membrane fusion and rapid PDGFR recycling back to the plasma membrane. Over time the lack of GAP activity of the p85-R274A mutant is unable to contribute to and accelerate Rab5 or Rab4 GTP hydrolysis leading to Rab protein sequestration on intracellular membranes. A) The Rab5-GTP protein accumulates on perinuclear early/sorting endosomal membranes and B) the Rab4-GTP protein accumulates on peripheral recycling endosomal membranes. This results in C) a lack of sufficient cytosolic Rab5-GDP and D) a lack of cytosolic Rab4-GDP required to associate with new membranes and facilitate additional vesicle fusion events.

p85 subunit of PI3K. PDGFRs lacking p85 binding sites are able to internalize but are constitutively recycled rather than degraded (Joly *et al*., 1994), while PDGFR with mutated binding sites for other signalling proteins (RasGAP and PLCγ1) are degraded as normal. It is possible that that there is a decrease of PI3K lipid products which are known to play critical roles in membrane fusion events. The lack of lipid products could prevent vesicle fusion events; however, there are several PI3K families responsible for generating these lipid products and it is unknown if vesicle fusion events would be blocked in these cells as well. Our model predicts that the lack of p85:Rab5 associations and decreased RabGAP activity would block PDGFR degradation. Our model predicts cells would have an increased rate of internalization and recycling. As shown previously, the decreased time the receptor stays in the early sorting endosome, reduces the chance for it to be targeted to the degradative pathway (Mayor *et al*., 1993). This lack of receptor degradation seems to be independent of normal PI3K activity, as expression of a p110α mutant defective for PI3K catalytic activity did not prevent EGFR endocytosis or degradation (Chen and Wang, 2001). The effects seem to be specific for the p85 subunit and contribute to the increasing knowledge and evidence of this protein having regulatory functions beside those involving p110α.

5.2.1 Future experiments to characterize the mechanism of receptor trafficking using p85-R274A expressing cells

Our model as to the mechanism of defective PDGFR degradation in cells expressing the p85-R274A mutant suggests Rab5 and Rab4 are sequestered on endosomal membranes. Because of this sequestration, PDGFRs are not properly trafficked through the endocytic pathway and are retained inside cells longer and are not degraded as quickly. Our lab will use complimentary biochemical and cell biology methods to test and monitor PDGFR trafficking.

Rabaptin5 is a protein which selectively binds the active GTP-bound conformations of Rab5 and Rab4. GST-Rabaptin5 pull-down experiments will be used to measure cellular levels of Rab5-GTP and Rab4-GTP from cell lysates after 0 and 30 min PDGF stimulation. Our model predicts cells expressing p85-R274A will have higher levels of Rab5-GTP and Rab4-

GTP after 30 min of PDGF stimulation due to Rab protein sequestered on endosomal membranes.

Subcellular fractionation experiments will be used to determine the membrane versus cytoplasmic location of Rab5 and Rab4 after PDGF stimulation. Cell lysates will be fractionated into membrane and cytosolic fractions, and intracellular organelle fractions. According to our model, an abundance of Rab5 and Rab4 should be found in the membrane fraction, the intracellular fraction, and found on early endosome (Rab5) and recycling endosomal (Rab4) organelle fractions in cells expressing the p85-R274A cells.

Lastly, we will use confocal microscopy and fluorescence recovery after photobleaching (FRAP) experiments to define the type of endosomal compartments perturbed in p85-R274A expressing cells. FRAP experiments, done in collaboration with Dr. Heidi McBride (Ottawa Heart Institute), will be used to track cyan fluorescent protein (CFP)-Rab5 and CFP-Rab4 membrane recovery rates after photobleaching the membrane-associated Rab protein on a vesicle in live cells. Our model predicts that when we express abundant CFP-Rab protein to provide a large cytoplasmic pool, cells expressing p85-R274A will show enhanced rates of fluorescence recovery after photobleaching because the CFP-Rab proteins will be moving from the cytoplasm to the vesicle membrane but will be trapped on the membrane in the GTP-bound form. In contrast, in control cells there will be less fluorescence recovery after photobleaching because the CFP-Rab proteins will be able to cycle off the membrane normally.

These experiments will allow us to identify where key proteins within the endocytosis pathway are located. In cell expressing the p85-R274A mutant, these experiments will allow us to determine the point(s) in the endocytosis pathway which is being disrupted and how the Rab proteins and p85 are responsible for this disruption. We will gain a better understanding of the events which dictate normal PDGFR trafficking within cells by first understanding the events responsible for disrupting it.

6.0 CONCLUSIONS

We have shown p85 may be responsible for regulating PDGFR endocytosis by contributing to the recruitment and deactivation of Rab proteins. The p85 protein is able to interact with Rab5 through its BH domain and may act as a GDF to help target Rab5 to the appropriate endosomal membrane where it would become activated to facilitate membrane fusion events during receptor endocytosis. The p85 RabGAP activity is also responsible for deactivating Rab5 by accelerating Rab5 GTPase activity resulting in Rab5 inactivation and decreased vesicle fusion events during receptor endocytosis. A p85-R274A mutant defective for RabGAP activity clearly alters PDGFR trafficking during receptor endocytosis and cells expressing this mutant display increased PDGFR activation and decreased degradation. We have proposed a model for this defective trafficking where the net result was blocked PDGFR trafficking, which prevented normal PDGFR dephosphorylation and degradation, attributed to a lack of sufficient cytosolic Rab5-GDP and Rab4-GDP required to associate with new membranes and facilitate additional vesicle fusion events. This model helps to explain why cells expressing the p85-R274A mutant form tumors in nude mice. The lack of lysosomal targeting, allows the receptor to be sequestered in cells but still have the ability to signal as the receptor would not be targeted to the MVB were signalling is abolished.

As the overlap between the molecular mechanisms of endocytosis and signalling becomes evident, more work is needed to untangle the regulatory networks and shed light on how the processes influence each other and cellular proliferation (Bache *et al*., 2004). It is becoming clear that the downregulation of RTKs by endocytosis and lysosomal sorting represents a key mechanism for signal termination. The experimental results outlined in this thesis give us a better understanding of a small part of this process and the proteins which are involved. Further exploration into this process is needed to fully understand its complexity and to understand how to manipulate this process for therapeutic intervention.

7.0 REFERENCES

Alvarez, R.H., Kantarjian, H.M., and Cortes, J.E. (2006). Biology of platelet-derived growth factor and its involvement in disease. Mayo Clin Proc *81*, 1241-1257.

Amerik, A.Y., Nowak, J., Swaminathan, S., and Hochstrasser, M. (2000). The Doa4 deubiquitinating enzyme is functionally linked to the vacuolar protein-sorting and endocytic pathways. Mol Biol Cell *11*, 3365-3380.

Anderson, K.E., Coadwell, J., Stephens, L.R., and Hawkins, P.T. (1998). Translocation of PDK-1 to the plasma membrane is important in allowing PDK-1 to activate protein kinase B. Curr Biol *8*, 684-691.

Andjelkovic, M., Alessi, D.R., Meier, R., Fernandez, A., Lamb, N.J., Frech, M., Cron, P., Cohen, P., Lucocq, J.M., and Hemmings, B.A. (1997). Role of translocation in the activation and function of protein kinase B. J Biol Chem *272*, 31515-31524.

Armstrong, J. (2000). How do Rab proteins function in membrane traffic? Int J Biochem Cell Biol *32*, 303-307.

Avruch, J., Khokhlatchev, A., Kyriakis, J.M., Luo, Z., Tzivion, G., Vavvas, D., and Zhang, X.F. (2001). Ras activation of the Raf kinase: tyrosine kinase recruitment of the MAP kinase cascade. Recent Prog Horm Res *56*, 127-155.

Bache, K.G., Slagsvold, T., and Stenmark, H. (2004). Defective downregulation of receptor tyrosine kinases in cancer. Embo J *23*, 2707-2712.

Barbieri, M.A., Kong, C., Chen, P.I., Horazdovsky, B.F., and Stahl, P.D. (2003). The SRC homology 2 domain of Rin1 mediates its binding to the epidermal growth factor receptor and regulates receptor endocytosis. J Biol Chem *278*, 32027-32036.

Blume-Jensen, P., and Hunter, T. (2001). Oncogenic kinase signalling. Nature *411*, 355-365.

Bokoch, G.M., Vlahos, C.J., Wang, Y., Knaus, U.G., and Traynor-Kaplan, A.E. (1996). Rac GTPase interacts specifically with phosphatidylinositol 3-kinase. Biochem J *315*, 775-779.

Bornfeldt, K.E., Raines, E.W., Graves, L.M., Skinner, M.P., Krebs, E.G., and Ross, R. (1995). Platelet-derived growth factor. Distinct signal transduction pathways associated with migration versus proliferation. Ann N Y Acad Sci *766*, 416-430.

Brodsky, F.M., Chen, C.Y., Knuehl, C., Towler, M.C., and Wakeham, D.E. (2001). Biological basket weaving: formation and function of clathrin-coated vesicles. Annu Rev Cell Dev Biol *17*, 517-568.

Bucci, C., Parton, R.G., Mather, I.H., Stunnenberg, H., Simons, K., Hoflack, B., and Zerial, M. (1992). The small GTPase rab5 functions as a regulatory factor in the early endocytic pathway. Cell *70*, 715-728.

Carpenter, C.L., and Cantley, L.C. (1996). Phosphoinositide kinases. Curr Opin Cell Biol *8*, 153-158.

Chamberlain, M.D., Berry, T.R., Pastor, M.C., and Anderson, D.H. (2004). The p85alpha Subunit of Phosphatidylinositol 3'-Kinase Binds to and Stimulates the GTPase Activity of Rab Proteins. J Biol Chem *279*, 48607-48614.

Chamberlain, M.D., Chan, T., Oberg, J.C., Hawrysh, A.D., James, K.M., Saxena, A., Xiang, J., and Anderson, D.H. (2008). Disrupted RabGAP function of the p85 subunit of phosphatidylinositol 3-kinase results in cell transformation. J Biol Chem *283*, 15861-15868.

Chen, X., and Wang, Z. (2001). Regulation of intracellular trafficking of the EGF receptor by Rab5 in the absence of phosphatidylinositol 3-kinase activity. EMBO Rep *2*, 68-74.

Christoforidis, S., McBride, H.M., Burgoyne, R.D., and Zerial, M. (1999a). The Rab5 effector EEA1 is a core component of endosome docking. Nature *397*, 621-625.

Christoforidis, S., Miaczynska, M., Ashman, K., Wilm, M., Zhao, L., Yip, S.C., Waterfield, M.D., Backer, J.M., and Zerial, M. (1999b). Phosphatidylinositol-3-OH kinases are Rab5 effectors. Nat Cell Biol *1*, 249-252.

Clabecq, A., Henry, J.P., and Darchen, F. (2000). Biochemical characterization of Rab3-GTPase-activating protein reveals a mechanism similar to that of Ras-GAP. J Biol Chem *275*, 31786-31791.

Claesson-Welsh, L. (1994a). Platelet-derived growth factor receptor signals. J Biol Chem *269*, 32023-32026.

Claesson-Welsh, L. (1994b). Signal transduction by the PDGF receptors. Prog Growth Factor Res *5*, 37-54.

Clague, M.J., and Urbe, S. (2001). The interface of receptor trafficking and signalling. J Cell Sci *114*, 3075-3081.

Collins, B.M., McCoy, A.J., Kent, H.M., Evans, P.R., and Owen, D.J. (2002). Molecular architecture and functional model of the endocytic AP2 complex. Cell *109*, 523-535.

Conner, S.D., and Schmid, S.L. (2003). Regulated portals of entry into the cell. Nature *422*, 37-44.

Datta, S.R., Katsov, A., Hu, L., Petros, A., Fesik, S.W., Yaffe, M.B., and Greenberg, M.E. (2000). 14-3-3 proteins and survival kinases cooperate to inactivate BAD by BH3 domain phosphorylation. Mol Cell *6*, 41-51.

De Camilli, P., Emr, S.D., McPherson, P.S., and Novick, P. (1996). Phosphoinositides as regulators in membrane traffic. Science *271*, 1533-1539.

Dikic, I., and Giordano, S. (2003). Negative receptor signalling. Curr Opin Cell Biol *15*, 128-135.

Engelman, J.A., Luo, J., and Cantley, L.C. (2006). The evolution of phosphatidylinositol 3-kinases as regulators of growth and metabolism. Nat Rev Genet *7*, 606-619.

Fang, Y., Johnson, L.M., Mahon, E.S., and Anderson, D.H. (2002). Two Phosphorylation-Independent Sites on the p85 SH2 Domains Bind A-Raf Kinase. Biochem Biophys Res Commun *290*, 1267-1274.

Freedman, T.S., Sondermann, H., Friedland, G.D., Kortemme, T., Bar-Sagi, D., Marqusee, S., and Kuriyan, J. (2006). A Ras-induced conformational switch in the Ras activator Son of sevenless. Proc Natl Acad Sci U S A *103*, 16692-16697.

Gavi, S., Shumay, E., Wang, H.Y., and Malbon, C.C. (2006). G-protein-coupled receptors and tyrosine kinases: crossroads in cell signaling and regulation. Trends Endocrinol Metab *17*, 48-54.

Goldberg, J. (1999). Structural and functional analysis of the ARF1-ARFGAP complex reveals a role for coatomer in GTP hydrolysis. Cell *96*, 893-902.

Haglund, K., Sigismund, S., Polo, S., Szymkiewicz, I., Di Fiore, P.P., and Dikic, I. (2003). Multiple monoubiquitination of RTKs is sufficient for their endocytosis and degradation. Nat Cell Biol *5*, 461-466.

Hanahan, D. (1983). Studies on transformation of Escherichia coli with plasmids. J Mol Biol *166*, 557-580.

Harpur, A.G., Layton, M.J., Das, P., Bottomley, M.J., Panayotou, G., Driscoll, P.C., and Waterfield, M.D. (1999). Intermolecular interactions of the p85alpha regulatory subunit of phosphatidylinositol 3-kinase. J Biol Chem *274*, 12323-12332.

Heidaran, M.A., Pierce, J.H., Jensen, R.A., Matsui, T., and Aaronson, S.A. (1990). Chimeric alpha- and beta-platelet-derived growth factor (PDGF) receptors define three immunoglobulin-like domains of the alpha-PDGF receptor that determine PDGF-AA binding specificity. J Biol Chem *265*, 18741-18744.

Heldin, C.H., Ostman, A., and Ronnstrand, L. (1998). Signal transduction via platelet-derived growth factor receptors. Biochim Biophys Acta *1378*, F79-113.

Heldin, C.H., Wasteson, A., and Westermark, B. (1985). Platelet-derived growth factor. Mol Cell Endocrinol *39*, 169-187.

Heldin, C.H., and Westermark, B. (1999). Mechanism of action and in vivo role of platelet-derived growth factor. Physiol Rev *79*, 1283-1316.

Heldin, N.E., Gustavsson, B., Claesson-Welsh, L., Hammacher, A., Mark, J., Heldin, C.H., and Westermark, B. (1988). Aberrant expression of receptors for platelet-derived growth factor in an anaplastic thyroid carcinoma cell line. Proc Natl Acad Sci U S A *85*, 9302-9306.

Hershko, A., and Ciechanover, A. (1998). The ubiquitin system. Annu Rev Biochem *67*, 425-479.

Huber, S., and Scheidig, A. (2005). High resolution crystal structure of human Rab4a in its active and inactive conformations. FEBS Lett. *579*, 2821-2829.

Ignatiuk, A., Quickfall, J.P., Hawrysh, A.D., Chamberlain, M.D., and Anderson, D.H. (2006). The Smaller Isoforms of Ankyrin 3 Bind to the p85 Subunit of Phosphatidylinositol 3'-Kinase and Enhance Platelet-derived Growth Factor Receptor Down-regulation. J Biol Chem *281*, 5956-5964.

Jiang, Y.H., and Beaudet, A.L. (2004). Human disorders of ubiquitination and proteasomal degradation. Curr Opin Pediatr *16*, 419-426.

Joly, M., Kazlauskas, A., and Corvera, S. (1995). Phosphatidylinositol 3-kinase activity is required at a postendocytic step in platelet-derived growth factor receptor trafficking. J Biol Chem *270*, 13225-13230.

Joly, M., Kazlauskas, A., Fay, F.S., and Corvera, S. (1994). Disruption of PDGF receptor trafficking by mutation of its PI-3 kinase binding sites. Science *263*, 684-687.

Kapeller, R., Chakrabarti, R., Cantley, L., Fay, F., and Corvera, S. (1993). Internalization of activated platelet-derived growth factor receptor- phosphatidylinositol-3' kinase complexes: potential interactions with the microtubule cytoskeleton. Mol Cell Biol *13*, 6052-6063.

Katso, R., Okkenhaug, K., Ahmadi, K., White, S., Timms, J., and Waterfield, M.D. (2001). Cellular function of phosphoinositide 3-kinases: implications for development, homeostasis, and cancer. Annu Rev Cell Dev Biol *17*, 615-675.

Katzmann, D.J., Odorizzi, G., and Emr, S.D. (2002). Receptor downregulation and multivesicular-body sorting. Nat Rev Mol Cell Biol *3*, 893-905.

King, T.R., Fang, Y., Mahon, E.S., and Anderson, D.H. (2000). Using a Phage Display Library to Identify Basic Residues in A-Raf Required to Mediate Binding to the Src Homology 2 Domains of the p85 Subunit of Phosphatidylinositol 3'-Kinase. J Biol Chem *275*, 36450-36456.

Kirchhausen, T. (2000). Clathrin. Annu Rev Biochem *69*, 699-727.

Klippel, A., Escobedo, J.A., Hu, Q., and Williams, L.T. (1993). A region of the 85-kilodalton (kDa) subunit of phosphatidylinositol 3- kinase binds the 110-kDa catalytic subunit in vivo. Mol Cell Biol *13*, 5560-5566.

Laemmli, U.K. (1970). Cleavage of structural proteins during the assembly of the head of bacteriophage T4. Nature *227*, 680-685.

LaRochelle, W.J., Jeffers, M., McDonald, W.F., Chillakuru, R.A., Giese, N.A., Lokker, N.A., Sullivan, C., Boldog, F.L., Yang, M., Vernet, C.*, et al.* (2001). PDGF-D, a new protease-activated growth factor. Nat Cell Biol *3*, 517-521.

Levkowitz, G., Waterman, H., Zamir, E., Kam, Z., Oved, S., Langdon, W.Y., Beguinot, L., Geiger, B., and Yarden, Y. (1998). c-Cbl/Sli-1 regulates endocytic sorting and ubiquitination of the epidermal growth factor receptor. Genes Dev *12*, 3663-3674.

Li, X., Ponten, A., Aase, K., Karlsson, L., Abramsson, A., Uutela, M., Backstrom, G., Hellstrom, M., Bostrom, H., Li, H.*, et al.* (2000). PDGF-C is a new protease-activated ligand for the PDGF alpha-receptor. Nat Cell Biol *2*, 302-309.

Linder, B.L., Chernoff, A., Kaplan, K.L., and Goodman, D.S. (1979). Release of platelet-derived growth factor from human platelets by arachidonic acid. Proc Natl Acad Sci U S A *76*, 4107-4111.

Liu, K., and Li, G. (1998). Catalytic domain of the p120 Ras GAP binds to Rab5 and stimulates its GTPase activity. J Biol Chem *273*, 10087-10090.

Low, B.C., Lim, Y.P., Lim, J., Wong, E.S., and Guy, G.R. (1999). Tyrosine phosphorylation of the Bcl-2-associated protein BNIP-2 by fibroblast growth factor receptor-1 prevents its binding to Cdc42GAP and Cdc42. J Biol Chem *274*, 33123-33130.

Mahon, E.S., Hawrysh, A.D., Chagpar, R.B., Johnson, L.M., and Anderson, D.H. (2005). A-Raf associates with and regulates platelet-derived growth factor receptor signalling. Cell Signal *17*, 857-868.

Manning, B.D., and Cantley, L.C. (2007). AKT/PKB signaling: navigating downstream. Cell *129*, 1261-1274.

Margarit, S.M., Sondermann, H., Hall, B.E., Nagar, B., Hoelz, A., Pirruccello, M., Bar-Sagi, D., and Kuriyan, J. (2003). Structural evidence for feedback activation by Ras.GTP of the Ras-specific nucleotide exchange factor SOS. Cell *112*, 685-695.

Marmor, M.D., and Yarden, Y. (2004). Role of protein ubiquitylation in regulating endocytosis of receptor tyrosine kinases. Oncogene *23*, 2057-2070.

Mayor, S., Presley, J.F., and Maxfield, F.R. (1993). Sorting of membrane components from endosomes and subsequent recycling to the cell surface occurs by a bulk flow process. J Cell Biol *121*, 1257-1269.

McKay, M.M., and Morrison, D.K. (2007). Integrating signals from RTKs to ERK/MAPK. Oncogene *26*, 3113-3121.

Mills, I.G., Jones, A.T., and Clague, M.J. (1998). Involvement of the endosomal autoantigen EEA1 in homotypic fusion of early endosomes. Curr Biol *8*, 881-884.

Mills, I.G., Jones, A.T., and Clague, M.J. (1999). Regulation of endosome fusion. Mol Membr Biol *16*, 73-79.

Miyake, S., Lupher, M.L., Jr., Druker, B., and Band, H. (1998). The tyrosine kinase regulator Cbl enhances the ubiquitination and degradation of the platelet-derived growth factor receptor alpha. Proc Natl Acad Sci U S A *95*, 7927-7932.

Mohrmann, K., and van der Sluijs, P. (1999). Regulation of membrane transport through the endocytic pathway by rabGTPases. Mol Membr Biol *16*, 81-87.

Musacchio, A., Cantley, L.C., and Harrison, S.C. (1996). Crystal structure of the breakpoint cluster region-homology domain from phosphoinositide 3-kinase p85 alpha subunit. Proc Natl Acad Sci U S A *93*, 14373-14378.

Payne, D.M., Rossomando, A.J., Martino, P., Erickson, A.K., Her, J.H., Shabanowitz, J., Hunt, D.F., Weber, M.J., and Sturgill, T.W. (1991). Identification of the regulatory phosphorylation sites in pp42/mitogen-activated protein kinase (MAP kinase). EMBO J *10*, 885-892.

Pereira-Leal, J.B., and Seabra, M.C. (2000). The mammalian Rab family of small GTPases: definition of family and subfamily sequence motifs suggests a mechanism for functional specificity in the Ras superfamily. J Mol Biol *301*, 1077-1087.

Peschard, P., and Park, M. (2003). Escape from Cbl-mediated downregulation: a recurrent theme for oncogenic deregulation of receptor tyrosine kinases. Cancer Cell *3*, 519-523.

Pfeffer, S., and Aivazian, D. (2004). Targeting Rab GTPases to distinct membrane compartments. Nat Rev Mol Cell Biol *5*, 886-896.

Raiborg, C., Rusten, T.E., and Stenmark, H. (2003). Protein sorting into multivesicular endosomes. Curr Opin Cell Biol *15*, 446-455.

Rubino, M., Miaczynska, M., Lippe, R., and Zerial, M. (2000). Selective membrane recruitment of EEA1 suggests a role in directional transport of clathrin-coated vesicles to early endosomes. J Biol Chem *275*, 3745-3748.

Scheffzek, K., Ahmadian, M., and Wittinghofer, A. (1998). GTPase-activating proteins: helping hands to complement an active site. Trends Biochem. Sci. *23*, 257-262.

Schlessinger, J. (2000). Cell signaling by receptor tyrosine kinases. Cell *103*, 211-225.

Seabra, M.C., Goldstein, J.L., Sudhof, T.C., and Brown, M.S. (1992). Rab geranylgeranyl transferase. A multisubunit enzyme that prenylates GTP-binding proteins terminating in Cys-X-Cys or Cys-Cys. J Biol Chem *267*, 14497-14503.

Seewald, M.J., Korner, C., Wittinghofer, A., and Vetter, I.R. (2002). RanGAP mediates GTP hydrolysis without an arginine finger. Nature *415*, 662-666.

Seewald, M.J., Kraemer, A., Farkasovsky, M., Korner, C., Wittinghofer, A., and Vetter, I.R. (2003). Biochemical characterization of the Ran-RanBP1-RanGAP system: are RanBP proteins and the acidic tail of RanGAP required for the Ran-RanGAP GTPase reaction? Mol Cell Biol *23*, 8124-8136.

Self, A.J., and Hall, A. (1995). Measurement of intrinsic nucleotide exchange and GTP hydrolysis rates. Methods Enzymol *256*, 67-76.

Shih, A.H., and Holland, E.C. (2006). Platelet-derived growth factor (PDGF) and glial tumorigenesis. Cancer Lett *232*, 139-147.

Simonsen, A., Lippe, R., Christoforidis, S., Gaullier, J.M., Brech, A., Callaghan, J., Toh, B.H., Murphy, C., Zerial, M., and Stenmark, H. (1998). EEA1 links PI(3)K function to Rab5 regulation of endosome fusion [see comments]. Nature *394*, 494-498.

Somsel Rodman, J., and Wandinger-Ness, A. (2000). Rab GTPases coordinate endocytosis. J Cell Sci *113 Pt 2*, 183-192.

Sondermann, H., Soisson, S.M., Boykevisch, S., Yang, S.S., Bar-Sagi, D., and Kuriyan, J. (2004). Structural analysis of autoinhibition in the Ras activator Son of sevenless. Cell *119*, 393-405.

Song, B.D., and Schmid, S.L. (2003). A molecular motor or a regulator? Dynamin's in a class of its own. Biochemistry *42*, 1369-1376.

Song, G., Ouyang, G., and Bao, S. (2005). The activation of Akt/PKB signaling pathway and cell survival. J Cell Mol Med *9*, 59-71.

Sprang, S.R. (1997). G proteins, effectors and GAPs: structure and mechanism. Curr Opin Struct Biol *7*, 849-856.

Stenmark, H., and Olkkonen, V.M. (2001). The Rab GTPase family. Genome Biol *2*, REVIEWS3007.3001-3007.3007.

Stenmark, H., Valencia, A., Martinez, O., Ullrich, O., Goud, B., and Zerial, M. (1994). Distinct structural elements of rab5 define its functional specificity. Embo J *13*, 575-583.

Szafer, E., Pick, E., Rotman, M., Zuck, S., Huber, I., and Cassel, D. (2000). Role of coatomer and phospholipids in GTPase-activating protein-dependent hydrolysis of GTP by ADP-ribosylation factor-1. J Biol Chem *275*, 23615-23619.

Tallquist, M., and Kazlauskas, A. (2004). PDGF signaling in cells and mice. Cytokine Growth Factor Rev *15*, 205-213.

Teis, D., and Huber, L.A. (2003). The odd couple: signal transduction and endocytosis. Cell Mol Life Sci *60*, 2020-2033.

Thien, C.B., and Langdon, W.Y. (2001). Cbl: many adaptations to regulate protein tyrosine kinases. Nat Rev Mol Cell Biol *2*, 294-307.

Tsygankov, A.Y., Teckchandani, A.M., Feshchenko, E.A., and Swaminathan, G. (2001). Beyond the RING: CBL proteins as multivalent adapters. Oncogene *20*, 6382-6402.

Tuvim, M.J., Adachi, R., Hoffenberg, S., and Dickey, B.F. (2001). Traffic control: Rab GTPases and the regulation of interorganellar transport. News Physiol Sci *16*, 56-61.

Ullrich, O., Horiuchi, H., Bucci, C., and Zerial, M. (1994). Membrane association of Rab5 mediated by GDP-dissociation inhibitor and accompanied by GDP/GTP exchange [see comments]. Nature *368*, 157-160.

Urbe, S. (2005). Ubiquitin and endocytic protein sorting. Essays Biochem *41*, 81-98.

Wang, Y., Pennock, S.D., Chen, X., Kazlauskas, A., and Wang, Z. (2004). Platelet-derived growth factor receptor-mediated signal transduction from endosomes. J Biol Chem *279*, 8038-8046.

Yu, J., Zhang, Y., McIlroy, J., Rordorf-Nikolic, T., Orr, G.A., and Backer, J.M. (1998). Regulation of the p85/p110 phosphatidylinositol 3'-kinase: stabilization and inhibition of the p110alpha catalytic subunit by the p85 regulatory subunit. Mol Cell Biol *18*, 1379-1387.

Zheng, C.F., and Guan, K.L. (1994). Activation of MEK family kinases requires phosphorylation of two conserved Ser/Thr residues. EMBO J *13*, 1123-1131.